

EFFECTS OF STEP CHANGES IN FEED CONCENTRATION
AND INCOMPLETE MIXING OF ANION AND CATION
RESIN ON THE PERFORMANCE OF
MIXED-BED ION EXCHANGE

By

BYEONG IL NOH

Bachelor of Science
Hanyang University
Seoul, Korea
1984

Master of Science
Oklahoma State University
Stillwater, Oklahoma
1988

Submitted to the Faculty of the
Graduate College of the
Oklahoma State University
in partial fulfillment of
the requirements for
the degree of
DOCTOR OF PHILOSOPHY
July, 1992

19920 N779e

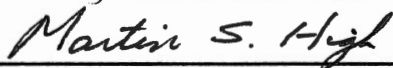
Thesis
19920
N779e

EFFECTS OF STEP CHANGES IN FEED CONCENTRATION
AND INCOMPLETE MIXING OF ANION AND CATION
RESIN ON THE PERFORMANCE OF
MIXED-BED ION EXCHANGE

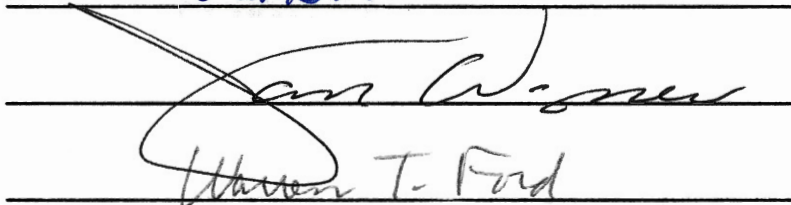
Thesis Approved:



Thesis Adviser








Dean of the Graduate College

PREFACE

The primary objective of this work is to collect experimental data to evaluate the effects of variable feed concentration and incomplete mixing of anion and cation resin on the performance of mixed-bed ion exchange.

To make feed concentration variable, step changes in feed concentration were arbitrarily introduced into the experimental column. For the incompletely mixed bed, only anion resin was loaded in about the upper 20 % of the column and more cation resin in the lower portion. Downflow was used for the experiments. Feed concentrations of $2.0E-4$ - $5.0E-5$ M NaCl were used. The superficial velocity was about 0.132 cm/s for the variable feed concentration experiments and 2.5 cm/s for the incomplete mixing of resins experiments. The effluent from the column was collected periodically and analyzed using on-line/off-line ion chromatography. Water samples from the Tulsa Riverside Power Plant were analyzed to obtain on-line operating data from a full scale condensate polisher.

The breakthrough curves of chloride and sodium, plotted as the ratio of the effluent to influent concentration versus run times in hour, gave some detailed results about the effects of step changes in feed concentration and

incomplete mixing of resins. The experimental data will provide a valuable data base for understanding the performance of mixed-bed ion exchange at ultralow concentrations. The data can also be used to simulate mathematical models, which describe the performance of mixed-bed ion exchange at ultralow concentrations, under various conditions such as major cooling water leakage and incompletely mixed beds observed in full-scale industrial units.

The results of the experiments for both cases were used to evaluate Haub and Foutch's (1986a, b) hydrogen cycle model, which has the ability to predict the performance of industrial mixed beds. When the experimental data were compared with the model prediction, the results showed that the model predicted satisfactorily mixed-bed ion-exchange behavior with proper property data and resin capacity. The model shows that the nonionic mass transfer coefficients and resin capacity affect the general shape of breakthrough curves. The mass transfer coefficients of Carberry (1960) used for the model are larger than the actual values observed during experiments. To match the model prediction to the experimental data, the coefficient was reduced by 30 % for sodium and 40 % for chloride. The resin capacity was also decreased from the values supplied by the resin manufacturer by 10 % for cation and 30 % for anion resin.

ACKNOWLEDGMENTS

I wish to express sincere appreciation to my major advisor, Dr. Gary L. Foutch for his intelligent guidance, inspiration and invaluable aid throughout my graduate program. Further advice and criticism from the advisory committee members, Dr. Jan Wagner, Dr. Martin S. High, Dr. Alan Tree, and Dr. Warren T. Ford were also very helpful throughout the study.

A note of thanks is given to Dr. Dariel W. King, Dr. Steve Wang, Mr. Dave Jones, and Mr. Charles L. Baker for their help in conducting the experiments and analysis.

My parents encouraged and supported me all the way and helped me keep my goal constantly in sight. Thanks go to them for their undivided time in the final stages of the project. Special gratitude and appreciation are expressed to my wife. She provided moral support and was a real believer in my abilities. I'd like to say thanks to all Korean students in Stillwater for their sacrifice and endeavor.

Financial assistance from the School of Chemical Engineering at Oklahoma State University, the National Science Foundation, and Public Service of Oklahoma for the completion of this study are gratefully appreciated.

TABLE OF CONTENTS

Chapter	Page
I. INTRODUCTION	1
II. LITERATURE REVIEW	5
Condensate Polishing	5
Mixed-Bed Ion Exchange	11
Exchange Resins.	12
Modeling	18
Ionic Diffusion Coefficient.	23
Nonionic Mass Transfer Coefficient	25
III. EXPERIMENTAL APPARATUS AND PROCEDURES	30
Experimental Apparatus	30
Experimental Columns	33
Ion Exchange Resins.	34
Ion Chromatography	34
Auxiliary Facilities	38
Experimental Procedures.	40
Variable Feed Concentration.	44
Incomplete Mixing of Resins.	45
IV. EXPERIMENTAL RESULTS	48
Variable Feed Concentration.	49
Incompletely Mixed Bed	66
Analysis of Water Samples From PSO	78
V. DISCUSSIONS OF RESULTS	85
Accuracy and Reporducibility	86
Mathematical Model	88

Chapter	Page
Computer Model	91
Main and Subroutines	91
Numerical Techniques	94
Parametric Studies	96
Modification of Programming Method103
Variable Feed Concentration.105
Model Prediction For The System.106
System Parameters.114
Incompletely Mixed Bed119
Model Prediction For The System.120
Effects of System Parameters130
On-Line Operating Data From PSO.141
VI. CONCLUSIONS AND RECOMMENDATIONS.147
BIBLIOGRAPHY152
APPENDIXES160
APPENDIX A - EXPERIMENTAL PROCEDURES.	161
APPENDIX B - ERROR ANALYSIS.168
APPENDIX C - EXPERIMENTAL DATA180

LIST OF TABLES

Table	Page
I. Deep Bed Condensate Polisher Functions.	7
II. Actual Regeneration Data.	12
III. A Summary of The Correlation Equations For The Mass Transfer Coefficients.	28
IV. Physical Properties of Dowex Resin.	35
V. Characteristics of Chemicals Used for IC.	38
VI. List of Auxiliary Facilities.	41
VII. Experimental Conditions for Variable Feed Concentration Experiment.	50
VIII. Experimental Conditions for Incompletely Mixed Bed Experiments	67
IX. Operating Condtions of a Condensate Polisher at Tulsa Riverside Plant.	80
X. Model Input Parameters.	93
XI. A Sample Calculation For The Mass Transfer Coefficients At Low Reynolds Number118
XII. A Sample Calculation For The Mass Transfer Coefficients At Moderate Reynolds Number.131
XIII. Physical Properties of New Dowex Resins142
XIV. Accuracy of Ion Chromatography Analysis169
XV. Numerical Data of Variable Feed Concentration Experiments180
XVI. Numerical Data of The Incomplete Mixing of Resins Experiments.195
XVII. pH Data199

LIST OF FIGURES

Figure	Page
1. Flow Diagram for Experimental Column.	31
2. Flow Diagram for Water Purification Column.	32
3. Feed Concentration Profiles for Constant and Variable Feed Concentration Experiments with One Peak.	52
4. The Effect of One Peak in Feed Concentration on Chloride Breakthrough Curve	53
5. Semilog Plot of Experimental Data for the Effect of One Peak in Feed Solution on Chloride Curve	54
6. The Effect of One Peak in Feed Concentration on Sodium Breakthrough Curve	55
7. Semilog Plot of Experimental Data for the Effect of One Peak in Feed Solution on Sodium Curve	56
8. Feed Concentration Profiles for Constant and Variable Feed Concentration Experiments with Two Peaks	60
9. The Effect of Two Peaks in Feed Concentration on Chloride Breakthrough Curve	61
10. Semilog Plot of Experimental Data for the Effect of Two Peaks in Feed Solution on Chloride Curve.	62
11. The Effect of Two Peaks in Feed Concentration on Sodium Breakthrough Curve.	64
12. Semilog Plot of Experimental Data for the Effect of Two Peaks in Feed Solution on Sodium Curve.	65
13. The Effect of Incomplete Mixing of Resins on Chloride Breakthrough Curve with $FCR = 0.5$	69
14. The Effect of Incomplete Mixing of Resins on Sodium Breakthrough Curve with $FCR = 0.5$	70

Figure	Page
15. Comparison of pH in Incompletely and Completely Mixed Bed with FCR = 0.5.	73
16. The Effect of Incomplete Mixing of Resins on Chloride Breakthrough Curve with FCR = 0.6. . . .	75
17. The Effect of Incomplete Mixing of Resins on Sodium Breakthrough Curve with FCR = 0.6.	76
18. Comparison of pH in Incompletely and Completely Mixed Bed with FCR = 0.6.	79
19. Influent and Effluent Profiles of a Condensate Polisher with Old Resins at the Tulsa Riverside Power Plant	81
20. Influent and Effluent Profiles of a Condensate Polisher with New Resins at the Tulsa Riverside Power Plant	82
21. The Effect of Dimensionless Distance Increment on the Chloride Breakthrough Curve(TAU=0.01). . . .	99
22. The Effect of Dimensionless Distance Increment on the Sodium Breakthrough Curve(TAU=0.01). . . .	100
23. The Effect of Dimensionless Time Increment on the Chloride Breakthrough Curve (XI=0.005).	101
24. The Effect of Dimensionless Time Increment on the Sodium Breakthrough Curve (XI=0.005).	102
25. Experimental Data and Model Prediction for the Effect of One Peak in Feed Solution on Chloride Curve. .	107
26. Experimental Data and Model Prediction for the Effect of One Peak in Feed Solutin on Sodium Curve . .	108
27. Experimental Data and Model Prediction for The Effect of Two Peaks in Feed Solution on Chloride Curve .	109
28. Experimental Data and Model Prediction for The Effect of Two Peaks in Feed Solution on Sodium Curve .	110
29. Semilog Plot of Expermental Data and Model Prediction for the Effect of Two Peaks in Feed Solution on Chloride Curve.	111

Figure	Page
30. Semilog Plot of Experimental Data and Model Prediction for the Effect of Two Peaks in Feed Solution on Sodium Curve.112
31. Experimental Data and Model Prediction for the Effect of Incomplete Mixing of Resins on Chloride Breakthrough Curve with FCR=0.5122
32. Experimental Data and Model Prediction for the Effect of Incomplete Mixing of Resins on Sodium Breakthrough Curve with FCR=0.5123
33. Experimental Data and Model Prediction for the Effect of Incomplete Mixing of Resins on Chloride Breakthrough Curve with FCR=0.6126
34. Experimental Data and Model Prediction for the Effect of Incomplete Mixing of Resins on Sodium Breakthrough Curve with FCR=0.5127
35. Model Prediction for Effect of Incomplete Mixing of Resins on Mixed-Bed Ion Exchange (FCR=0.6). . .	.129
36. Experimental Data and Model Prediction with the Modified Mass Transfer Coefficients134
37. Effect of Anion Resin Capacity on Chloride Breakthrough ($Q_c=2.0$ meq/cu.cm)136
38. Effect of Anion Resin Capacity on Sodium Breakthrough ($Q_c=2.0$ meq/cu.cm)137
39. Experimental Data and Model Prediction for Complete and Incomplete Mixing of Resins with Modified ITC and Resin Capacity (FCR=0.5).139
40. Experimental Data and Model Prediction for Complete and Incomplete Mixing of Resins with Modified ITC and Resin Capacity (FCR=0.6).140
41. Calibration Curve of Chloride (Method File : ANION6.MET)170
42. Calibration Curve of Sodium (Method File : CATION6.MET).171
43. pH Calibration Curve.173

Figure	Page
44. Reproducibility of Variable Feed Concentration Experiments (Runs R128 and R211).175
45. Reproducibility of Incomplete Mixing of Resins Experiments (Runs R1201 and R116)176
46. The Result of Analysis of Fresh Anion Resin Using Laser Raman Spectroscopy.177
47. The Result of Analysis of Used Anion Resin Using Laser Raman Spectroscopy.178

NOMENCLATURE

a_s	specific surface area, cm^2 area / cm^3 resin
C_i	concentration of species i , meq/cm^3
d_{pi}	particle diameter of resin i , cm
D_i	diffusion coefficient of species i , cm^2/s
D_e	effective liquid phase diffusivity, cm^2/s
f_c	cation resin volumn / total resin volumn
F	Faraday's constant, coulombs / mole
J_i	ionic flux of species i , $\text{meq}/\text{s cm}^2$
k_i	nonionic liquid phase mass transfer coefficient of species i , cm/s
Q_i	total resin exchange capacity of resin i , meq/ml
r	radial distance
R	universal gas constant
R_i	ratio of electrolyte to nonelectrolyte mass transfer coefficient of species i
t	time, s
X_i'	equivalent fraction of species i based on the column feed concentration, C_i / C_i^f
y_i	equivalent fraction of species i in resin phase
Z	distance from column inlet, cm

Greek Letters

ϵ	bed void fraction
μ_s	superficial liquid velocity, cm/s
ξ_i	dimensionless distance based on property of resin i
τ_i	dimensionless time based on property of resin i
ϕ	electric potential, ergs/coulomb

Superscripts

*	interfacial equilibrium condition
f	column feed condition
o	bulk phase condition

Subscript

a	anion exchange parameter, chloride ion
c	cation exchange parameter, sodium ion
i	species i

CHAPTER I

INTRODUCTION

Ion exchange is defined as a reversible exchange of like charged ions between a liquid and a water-insoluble solid without substantial changes in the structure of the solid. It was first recognized as a physical-chemical phenomena in the middle of nineteenth century (Kunin, 1960). The utilization of the ion exchange process on a commercial scale started at the turn of the twentieth century, stemmed from the application of both natural and synthetic silicates to water softening (Dowex, 1958). The recent appearance of high-capacity and durable ion exchangers has stimulated much interest in ion exchange, resulting in a number of applications in widely divergent fields.

A typical mixed-bed unit used to produce ultrapure water, of which conductance is less than 0.055 $\mu\text{S}/\text{cm}$ at 25 $^{\circ}\text{C}$ (Grammont et al., 1986), consists of a strong-acid cation resin in the hydrogen form and a strong-base anion resin in the hydroxide form (Helfferich, 1965). A cation in the ionic solution is exchanged for a hydrogen ion on the cation resin and an anion is exchanged for a hydroxide ion on the anion resin at the same time. The exchanged hydrogen ion then reacts with the hydroxide ion to produce pure water.

This neutralization reaction makes the exchange process fast and irreversible (Kunin and McGarvey, 1951).

Mixed-bed ion exchange provides a convenient and economical method to produce ultrapure water, and is thus applicable to many significant industries which need ultrapure water. Nuclear and coal fired electrical power plants are the major industrial user of ultrapure water and utilize mixed-bed ion exchange for condensate polishing and makeup water purification. They use ultrapure water to avoid erosion and corrosion problems in the steam cycle. Electronic and instrument industries require ion exchange to make pure water for process rinsing. The chemical industry needs pure water for the production of ammonia. The pulp, paper, and petroleum industries also need pure water for the operation of high pressure boilers. Presently, use of mixed-bed ion exchange for the above applications, and, in particular, for the treatment of low level solids water requires realistic estimates of mixed-bed performance. However, the fundamental theories and detailed modeling of the ion exchange process are far behind the current technical applications. Thus, mathematical models and laboratory work are imperative to develop an understanding of the process.

Haub and Foutch (1986a, b) have developed a theoretical hydrogen cycle model to describe mixed-bed ion exchange at ultralow ionic concentrations. Their model considers the dissociation of water, cation-resin fraction, exchange

rates, resin capacities, resin particle sizes, reversibility of exchange, and bulk/film neutralization. Divekar et al. (1987) have developed Haub and Foutch's model further to include the effect of temperature on the performance of mixed-bed ion exchange. Zecchini (1990) has extended the model to address amine form operation. Yoon (1990) and King (1991) have evaluated experimentally the model.

The major objective of the present study is to obtain experimental data under various conditions. The experiments were designed to collect the data for the cases of variable feed concentration and incompletely mixed beds observed in large scale industrial plants. The experiments were conducted with inlet concentration ranges of 2×10^{-4} to 5×10^{-5} meq/ml and different flow rates of 0.132 to 7.0 cm/sec. The cation-resin fraction of 0.375 to 0.610 was used. On-line and/or off-line sample collection and data acquisition systems were used to obtain the experimental data. A Dionex Ion Chromatograph Model 4500i increases significantly the laboratory on-line detection limits lower than one part per billion (PPB) for sodium and chloride. The data obtained in this work can be used to evaluate the accuracy of mixed-bed ion exchange models at ultralow concentration. A study for the effect of flow rate on mixed bed performance is possible using the data.

With the cooperation of Public Service of Oklahoma, on-line operating data from a full scale condensate polisher was obtained by analyzing water samples from the Tulsa

Riverside Power Plant. The influent and effluent data of the polisher were used to investigate the degradation of the cation resin in terms of nonionic mass transfer coefficients and resin capacity.

The computer programming method to solve the model of Haub and Foutch (1986a, b) was modified to allow for variable input data in order to simulate the variable feed concentration and variable cation-resin fraction along a bed. The performance of the model was evaluated by comparing the model prediction to the experimental data. The deviations between the data and the predicted values were discussed using the different mass transfer coefficients from the correlation equations of Carberry (1960) and Kataoka et al. (1972) and different cation and anion-resin capacity from the resin manufacturer.

CHAPTER II

LITERATURE REVIEW

Basic definitions, principles, and applications of ion exchange have been well documented by Helfferich (1962, 1966), Kunin (1960), Grimshaw and Harland (1975), and Naden and Streat (1984). Discussion on the kinetic theories describing ion exchange rates used in the column models is also presented in these references. Haub (1984), Yoon (1990), and Zecchini (1990) reviewed extensively the ion exchange literature on mixed-bed ion exchange processes: fundamentals, rate laws, column models, and mixed-bed modeling. Only the materials pertinent to this work will be briefly reviewed in this chapter.

Condensate Polishing

The largest market for ultrapure water is the steam cycle of nuclear and coal fired power plants that use mixed-bed ion exchange for condensate polishing and makeup water purification (Slejko, 1990). Condensate polishing is associated with a steam/water circuit where a continuous operating full-flow mixed-bed unit is utilized downstream from a condensation system (Crits, 1981). The condensate becomes contaminated by corrosion products, mostly in the form of precipitated metal oxides, from the power generating

system. The ionic contamination of the condensate is minimal during normal operation. This situation can change suddenly in the cases of occasional condenser tube leaks and rapid flow rate change due to power transients (O'Sullivan, 1987; Tittle, 1987). Sodium and chloride ions have been identified as major corrodents of steam generator tubes and support structures. Dissolved oxygen, sulfate and corrosion products of copper and iron are other important constituents known as steam generator corrodents (Rios and Maddagiri, 1985). These materials must be removed to allow steam generators to achieve their original design life.

Recirculating steam cycle applications have to be replaced in less than 10 years in some cases because of corroded tubes and support structures (Rios and Maddagiri, 1985).

In a subcritical drum boiler, these contaminants will accumulate in the boiler water and can be controlled by use of blowdown and/or chemical additions. In supercritical units, however, the problem of contaminants has to be corrected prior to water entering into the boiler, since there is no steam drum and boiler water cycle to aid in contaminant control (Crits, 1984). This is accomplished with a condensate polisher in the system. The condensate polisher performs two functions: filtration and deionization. It removes both the oxidation products within the system, and the suspended and dissolved materials that may enter from an external source. In essence, this system polishes the condensate during normal operation and reduces

the contaminant levels during periods of high contaminant in-leakage, allowing the needed time for correction. The outlines of the functions of a high-rate deep-bed condensate polisher are listed in Table I.

TABLE I
DEEP BED CONDENSATE POLISHER FUNCTIONS
(Crits, 1984)

-
- Continuously removing "on-line corrosion products" as well as removing the increased amounts of crud during initial startup and during restarts.
 - Continuously removing silica and other volatiles to avoid turbine fouling or steam contamination.
 - Reducing blowdown from pressurized water reactor or drum-type units.
 - Removing any substance, dissolved salts, when makeup water demineralizers are not functioning properly, or when condensers are leaking.
 - Removing CO₂ from air in leakage to the condenser.
 - To allow an orderly shutdown or time for making condenser isolations during major condenser leakage.
-

In addition to the polishing system, chemicals aid in obtaining the desired feedwater quality. Ammonia is added to increase the feedwater pH to the range 9.3 - 9.6 in the absence of copper alloy, and 8.8 - 9.2 in systems where copper alloys are present (Sawochka, 1988). These ranges are based primarily on laboratory and plant data obtained on

systems using ammonia for pH control. Hydrazine is added as an oxygen scavenger. As an alternative to ammonia, morpholine has been used for pH control at several pressurized water reactor (PWR) stations to reduce corrosion rates below those observed with ammonia/hydrazine control (Sawochka, 1988).

A criterion for an alternative amine to ammonia is greater affinity for water than for steam in a two-phase system (Sawochka, 1988). This is characterized by a reduced steam-to-liquid distribution coefficient defined as the ratio of additive concentration in the steam phase to its concentration (non-ionized) in the liquid phase. As the coefficient decreases, more additive is present in the liquid phase in two-phase regions such as extraction lines, heater shells, and condensers. This raises the pH of the liquid phase, which reduces corrosion rates. The coefficient for morpholine is significantly lower than for ammonia, leading to a much higher fraction going to the liquid phase in two-phase regions (Cobble and Turner, 1985).

Another criterion for an alternative amine is the ionization constant of the additive in the liquid phase (Zecchini, 1990). The constant indicates the extent of ionization when dissolved in water. Ammonia is a stronger base than morpholine below 200 °C. The lower ionization constant of morpholine thus requires large amounts of morpholine in water for a given pH. This results in rapid exhaustion of cation resins and decreases the polisher

capacity, leading to a greater tendency for ionic leakage (Sawochka, 1988a). Therefore, plants using condensate polishers require a balance between reduced corrosion product transport and increased ionic pH in two-phase regions of the cycle.

To produce high quality water, the cation and anion resins need to be regenerated to hydrogen and hydroxide form, respectively (H/OH cycle). However, operation in this mode continually removes the ammonia or other amine added to the boiler feed water as a pH control agent and, thus, reduces the cation resin capacity for sodium. It has been common practice to provide excess cation resin to anion resin in most condensate purification plants to compensate for the reduced cation resin capacity for sodium. To have an appropriate plant size needed for these large volumes of cation resin, some plants have been operated with cation resin in the ammonium (NH_4/OH cycle) or other amine cycle instead of the hydrogen cycle. With the resins operated in this mode, ammonia is not removed by the cation resin. As a result, in the absence of condenser leaks, long periods of service, in excess of fifty days, are possible (Sadler et al., 1983). But, the ammonia cycle introduces other problems due to the unfavorable equilibrium for the exchange of sodium over ammonia (Ball et al, 1984).

Mixed-bed ion exchange for deionizing aqueous solutions was initially designed for a flow rate of about five gal/min/sq.ft (Caddel and Moison, 1954). With improved ion

exchange resins and mixed-bed deionization techniques, the flow rate can be increased to as high as 100 gal/min/sq.ft without loss of a resin efficiency (Caddel and Moison, 1954). However, when resins age, exchange kinetics is not as rapid and leakages occur prematurely. Experience has shown that resins at 50 gal/min/sq.ft (3.4 cm/sec) often become fouled or "aged" within a few years and begin to show low exchange capacity, particularly during condenser leakages (Wirth, 1980; Crits, 1981). At 50 gal/min/sq.ft, the average life of plant resins has been about five years. With careful operation, a 50 gal/min/sq.ft service flow rate for condensate polishing appears to be quite satisfactory (Crits, 1981).

An overall cation-to-anion resin ratio of 2:1 has been used successfully in typical power plants for many years with good crud removal capability. However, several installations with the ratio in high pH fossil applications have experienced premature chloride breakthrough prior to the normal ammonia endpoint (Crits, 1981). In this case, more anion resin is advisable, such as 1:1.5. The use of a volumetric ratio of 1:1 would be satisfactory for neutral pH systems (Crits, 1981).

The condensate polisher will become exhausted after a period of service and will require reconditioning. The reconditioning process, which includes cleaning and the regeneration of the resin bed, is usually accomplished in a two-tank external regeneration system (Tittle, 1987): a

cation separation-regeneration column and an anion regeneration column. This off-line operation minimizes the risk of feedwater contamination with regenerant chemicals. Anion regeneration is carried out using NaOH and cation regeneration uses either H_2SO_4 or HCl (Dowex, 1958). An example of typical regeneration data is shown in Table II.

Even though no pretreatment bed was recommended by Crits (1981), several polishing plants were designed and built with mixed beds preceded by filters, cation units, magnetic filters, two beds, or precoat filters (Rios and Maddagiri, 1985; Tittle, 1987). These pretreatment systems reduce sodium and other leakages due to traces of regenerants inadvertently left on the resins and ammonia from high pH condensers. Thus, they offer some protection of the resins and reduce the frequency of mixed-bed regenerations.

Mixed-bed Ion Exchange

Ion exchange can be defined as a reversible exchange of ions between a solid and a liquid in which there is no substantial change in the structure of the solid. A typical mixed-bed ion exchange unit used to produce ultrapure water consists of a strong-acid cation resin in the hydrogen form and a strong-base anion resin in the hydroxide form. The exchanged hydrogen ions in the cation resin react chemically with the exchanged hydroxide ions in the anion resin to produce water (Helfferich, 1965; Rao and Gupta, 1982).

TABLE II
ACTUAL REGENERATION DATA
(Crits, 1984)

Regeneration	
Seprex (NH ₄)	
No. steps	50
Time, hours	10
Cation	
Cation resin	4 m ³
Regenerant dosage	
99 % H ₂ SO ₄ /m ³	240 kg/m ³
99 % H ₂ SO ₄ /reg.	979 kg
93 % H ₂ SO ₄ /reg.	499 l
Anion	
Anion resin	2 m ³
Regenerant dosage (Seprex)	
99 % NaOH/m ³	352 kg/m ³
99 % NaOH/reg.	712 kg
25 % NaOH/reg.	2237 l

Exchange Resins

An ion exchange resin particle is usually a water-insoluble, elastic, and three-dimensional hydrocarbon network, to which a large number of ionizable groups are attached. The most ideal hydrocarbon network is that formed by the copolymerization of styrene and divinylbenzene (Kunin, 1958). This structure gives a maximum resistance to oxidation, reduction, mechanical wear and breakage, and is insoluble in common solvents. It can take up ions of positive (cation resin) or negative charge (anion resin) from an electrolyte solution and release other ions of the same charge into the solution in an equivalent amount. According to the characteristics of the functional groups, these ion exchange resins are classified as four fundamental types (Kunin, 1958): strongly-acidic and weakly-acidic cation resins and strongly-basic and weakly-basic anion resins. There are a lot of references about the characteristic properties of ion-exchange resins (Kunin, 1958; Helfferich, 1962; Inczedy, 1966; Goldring, 1966; Reichenberg, 1966; Wheaton and Hatch, 1969). A comprehensive literature review on the structures, preparation, and properties of resins has been completed by Haub (1984).

The quantitative performance of an ion exchange resin can be expressed in terms of total capacity, which is defined as the number of ionic or potentially ionic sites per unit

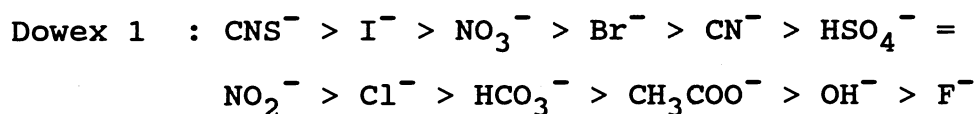
weight of resin dried at 105 °C (dry weight total capacity), or volume of swollen resin settled in water (wet volume total capacity) (Dowex, 1958). The total capacities of strongly acidic and strongly basic resins are nearly identical with the values of the capacity calculated from the sulphur or nitrogen content as determined by a suitable analytical method (Jackson and Bolto, 1990). Typically, the total capacities of strongly acidic and basic resin are determined by acid-base titration, and those of weakly acidic and weakly basic resins are determined by neutralizing capacity measurements (Dowex, 1958; Inczedy, 1966).

The net number of ionic sites which are utilized in a given volume of resin in a given cycle is known as the operating (break-through) capacity of the resin in that particular cycle. While the total capacity is constant and characteristic of a particular resin, the operating capacity depends on several factors. Caddell and Moison (1954) showed that increasing the flow rate from 5 to 100 gal/min/sq.ft with a fixed level of influent concentration produced high purity water without loss of resin capacity expressed in terms of the ions retained by the resins and that raising the influent concentration from 3 to 192 ppm almost doubled the ion exchange capacity of the mixed-bed. Harries and Ray (1984) believed that variations in resin particle size affect the overall exchange rate of mixed-bed, hence ionic leakage and operational capacity. Hsu and

Pigford (1991) studied the equilibrium properties and the mass transfer rates in an amphoteric, thermally regenerable resin, Amberlite XD-2 and confirmed that the equilibrium resin capacity for sodium chloride adsorption is strongly affected by temperature, solute concentration and pH of the aqueous solution.

Selectivity of a resin is defined as the degree of preference of the resin for one ion with respect to another, even if the ions are present in equivalent quantities. Selectivity is dependent on the nature of the counterion, the nature of the functional group, the degree of resin saturation, resin crosslinkage, total solution concentration, and external forces such as temperature (Bonner and Pruett, 1959a,b; Wheaton and Hatch, 1969; Soldaton and Bichkova, 1984; Triay and Rundberg, 1987). As the degree of cross-linking increases and the solution concentration decreases, selectivity of resins increases (Myers and Boyd, 1956). Ions with higher valence, smaller equivalent volume, lower free energy of hydration, and greater polarizability are more strongly adsorbed from dilute solutions (Helfferich, 1962; Reichenberg, 1966; Inczedy, 1966). The order of adsorption strengths on the strongly acidic cation resin and strongly basic anion resin are as follows (Dowex, 1958).

Dowex 50 : $Ba^{++} > Sr^{++} > Ca^{++} > Mg^{++} > Be^{++} > Ag^+ > Tl^+$
 $> Cs^+ > Rb^+ > NH_4^+ > K^+ > Na^+ > H^+ > Li^+$



For Dowex 2, OH^- falls between Cl^- and HCO_3^- . The order can vary according to resin loading and polymer crosslinking. This phenomenon is known as affinity reversal or selectivity reversal and is particularly widespread for systems with hydrogen as a counterion (Reichenberg, 1966).

Numerous theoretical models which relate selectivity to their controlling parameters have been developed based on fundamental thermodynamics (Gregor, 1948; Harris and Rice, 1956; Myers and Boyd, 1956; Kraus and Raridon, 1959). Reichenberg (1966) reviewed and discussed these models in details. The simplest and most widely used model is that of Gregor (1948), who applied the concept of hydrated ionic radius to selectivity and addressed resin crosslinking effects. This model, however, fails to address selectivity reversals. Diamond and Whitney (1966) discussed variations in resin selectivity from dilute (0.001 M) to concentrated aqueous solutions. They treated the resin phase as a concentrated electrolyte solution and considered the effects of differences in the water-water, ion-water, and ion-ion interactions in each phase on the ionic species. They suggested a hydrophobic effect where the aqueous phase prefers the ion with the greatest hydration. Harries (1986) proposed that hydration controls the basic affinity order and matrix swelling affects the relative order as a function

of resin crosslinking. He also suggested that the ion charge density and the nature of fixed groups influence the order.

Selectivity coefficient is a relationship of the component activities in the resin and liquid phases. Frequently, it is expressed in terms of concentrations in both phases, giving the selectivity coefficient as a function of resin composition and total solution concentration (Reichenberg, 1956). Ion exchange is generally an exothermic process and, hence, temperature affects adversely the selectivity coefficient. Kraus and Raridon (1959) showed a method for expressing the temperature dependency of the selectivity coefficient using the Debye-Hukel theory of electrolytes. Bonner and Pruett (1959a,b) determined experimentally parameters included in Kraus and Raridon's expression. Divekar et al. (1987) developed equations for the selectivity coefficients as functions of temperature to study the effects of temperature on the performance of mixed-bed ion exchange. They used experimental data reported on 16 % DVB Dowex exchanger for the cation resin selectivity coefficient. However, only one data point, which is typical for Type II anion exchange resin, was used to generate the equation for the anion resin selectivity coefficient due to the lack of anion data. They believed that with increasing temperature, the selectivity coefficient changes to a much smaller extent than the other parameters and that this change is overridden for the mixed-

bed ion exchange performance by the ionization constant and the ionic diffusion coefficients.

Modeling

Mixed-bed ion exchange is conceived as the simultaneous exchange of cations and anions by an intimate mixture of cation and anion exchange resins in the hydrogen and hydroxide forms, respectively. The purpose of mixing cation and anion resins is to obtain a neutralization reaction which would make the exchange process fast and irreversible (Kunin and McGarvey, 1951). Haub (1984), Yoon (1990), and Zecchini (1990) have completed systematic literature reviews of ion exchange equilibria, rate controlling step, and kinetic models which are required for modeling process of mixed-bed ion exchange.

Ion-exchange rates are determined by mass transfer steps, more specifically, mutual diffusion of counterions inside the 'Nernst' liquid film adhering to the resin particle, and/or mutual diffusion of counterions inside the resin particle itself. Boyd et al. (1947) were among the earliest research workers who established that ion exchange rates are determined by a diffusion process: particle or film diffusion. They believed, through a cation exchange kinetic study, that the exchange process is controlled by liquid-film diffusion at solution concentrations less than 0.01 M. This was verified by several experiments (Kuo and David, 1963; Turner and Snowdon, 1968a; Gomez-Vaillard and

Kershenbaum, 1981). An early study on the kinetics of mixed-bed deionization shows that the exchange rate is controlled by film diffusion which assumes ionic diffusion through a very thin liquid film surrounding a resin particle (Frisch and Kunin, 1960).

Diffusion processes in ion-exchange systems have been described by Fick's Law models. Schlogle and Helfferich (1957) showed that for mutual diffusion ions of dissimilar mobilities, the effect of electrical-potential gradient must also be considered along with the concentration gradient, and that the Nernst-Planck equation describes correctly such ion exchange mass transfer steps. Thereafter, the Nernst-Planck equation has been used for analyzing the kinetics in ion exchange. It has been confirmed experimentally that the Nernst-Planck equation can reasonably be applied to express the rate equation in film diffusion control (Copeland and Marchello, 1969; Glaski and Dranoff, 1963; Kataoka et al., 1968, 1973; Smith and Dranoff, 1964; Turner and Snowdon, 1968a, b; Rao and David, 1964; Bajpai et al., 1974).

Longitudinal diffusion, or axial diffusion, is diffusion in the interstitial solution parallel to the column axis. To account for this effect in a modeling process, the column material balance must include changes in content by diffusion into and out of the layer under consideration. The term resulting from axial diffusion in the material balance contains the flow rate in the denominator and is disregarded for most purposes (Helfferich, 1962). Cooney

(1991) suggested methods for computing concentration profiles and breakthrough curves in fixed bed adsorbers for cases of zero and non-zero axial dispersion. He showed that the ratio of mass transfer resistance to the axial dispersion coefficient serves as an indicator of whether or not axial dispersion effects are important. Axial dispersion has a greater effect on the film diffusion controlled case than the particle diffusion controlled case (Cooney, 1991) and is not ignored when the particle size and/or flow rate is substantially lower than usual (Helfferich, 1962; Cooney, 1991).

Haub and Foutch (1986a) derived the ionic flux equations for mixed-bed ion exchange at ultralow solution concentration, based on the Nernst-Planck theory with the static-film hydrodynamic model and nonionic mass-transfer coefficient correlations which were proposed by Carberry (1960) and Kataoka et al. (1972) for pack beds. Previous models considered mixed-bed ion exchange as a single salt removing process and used only one resin phase, or equilibrium calculations to describe the process (Frisch and Kunin, 1960). Haub (1984) believed that the unit is not single salt removing and that the diffusion limited nature of ion exchange must be considered. The model derived by Haub and Foutch (1986a) considers cation resin fraction, exchange rates, exchange capacities, particle sizes, reversibility of exchange, water dissociation, and neutralization reaction within the film and bulk liquid

phases. Thus, the model is capable of simulating certain column parameters and exchange conditions which are not considered in existing mixed-bed ion exchange models. The assumptions used for modeling process are well described in their paper (Haub and Foutch, 1986a). Later, this model was developed to include the influence of operating temperature (Divekar et al., 1987) and tested to determine the effective numerical limits for the program input parameters (Hu, 1986; Moon, 1987). Zecchini (1990) has recently extended the model to address non-neutral and multi-component systems. The model developed by Zecchini especially considers the solution pH and the simulation of the H-OH cycle until the amine break with a third reactive ion. Haub and Foutch's (1986a,b) mathematical model is evaluated using the experimental data obtained in this work.

Hu (1986) evaluated Haub and Foutch's model using actual data from Arkansas Nuclear Power plant located near Russellville, Arkansas. The model appeared to predict a much lower effluent quality than the actual data. Hu believed that two possibilities causing the discrepancy in the model performance are; the computer model simulates idealized conditions which do not account for the influent upsurges, or fluctuating influent concentration, often encountered in plant operation; or the actual data are often below the lowest detectable impurity limits of the instrument employed at the power plant.

Yoon (1990) investigated the effect of cation and anion resins ratio on mixed-bed ion exchange performance at ultralow concentration using the model derived by Haub and Foutch (1986a, b). According to his results, the model predicts the correct trends for breakthrough curves of sodium and chloride for various cation resin fractions. However, much deviation of the predicted values by the model from actual experimental data was found. He suggested a new set of the single-ionic diffusivities and a correlation equation as a function of ionic solution to produce reasonable curve fit.

Recently, King (1991) studied the effects of temperature and amines on the performance of mixed-bed ion exchange column for ultralow concentrations of sodium and chloride. He performed experiments at two temperatures: 25 °C and 40 °C, and with two amines, morpholine and ammonia. The experimental data were compared with the predicted values by Zecchini's (1990) model. King showed that the sodium breakthrough curve depends slightly on temperature while the dependency of the chloride breakthrough curve on temperature is substantial. This results may be due to the relatively high selectivity coefficient for chloride compared to sodium. King believed that the selectivity coefficient for chloride is much more sensitive in temperature.

Ionic Diffusion Coefficient

The liquid-side diffusion coefficients of ions in water have been reported by many investigators in the literature (Robinson and Stokes, 1960; Passiniemi, 1983; Harries and Ray, 1984; Petruzzelli, et al., 1987) and were used to describe the mixed-bed ion exchange system (Harries and Ray, 1984; Haub and Foutch, 1986b). However, there exist differences in those reported ionic diffusivities and especially for hydrogen, the difference is more than four times (Yoon, 1990). Graham and Dranoff (1982) believed that the variation of the ionic diffusivity in the resin phase can be of the order of two to three.

Helfferich (1965) developed a mathematical model for ion-exchange processes accompanied by strong neutralization reactions. His model supported the use of a constant effective diffusivity for a mixed bed. Tittle (1981) also used a constant system diffusivity in flux equations for modeling the mixed bed. The ionic diffusivities, however, are believed to be strongly dependent on the type of other ions in the solution, solution concentration, solution pH, and temperature (Graham and Dranoff, 1982; Harries, 1988; Divekar et al., 1987). Harries (1988) showed that the ionic diffusion coefficient for sodium increases in alkaline solutions and that for chloride increases in acidic solutions. He also studied the effect of cation resin size on anion exchange rate and showed that a relatively small

increase of particle size caused a significant reduction in anion exchange kinetics due to the pH changes within the bed.

Yoon (1990) developed a linear correlation equation of the diffusion coefficients as a function of ionic concentration using his mixed-bed ion exchange data collected in a 10^{-4} M NaCl solution. His correlation equation gives approximately an order of magnitude lower coefficients than those of Robinson and Stokes (1960). He used the correlation equation to best fit his experimental data to the predicted values by Haub and Foutch's (1986a, b) model.

With the assumption of no tendency for the fluid to slip at the surface of the diffusing particle, Wilke (1949) has developed an empirical correlation for a rigid sphere moving in creeping flow based on the hydrodynamical diffusion theory. Wilke and Chang (1955) improved Wilke's correlation for diffusion coefficients in dilute solutions. The hydrodynamical theory has been developed from the Nernst-Einstein equation, which states that the diffusivity of a single particle or solute molecule through a stationary medium is given as a function of the mobility of the particle and temperature (Daniels and Alberty, 1979). The simple hydrodynamic approach gives expressions for the diffusion coefficient for spherical molecules in dilute solution and also for the coefficient of self-diffusion

(Bird, et al., 1960). Wilke's correlation is good within $\pm 10\%$ for dilute solutions of nondissociating solutes.

Non-ionic Mass Transfer Coefficient.

Non-ionic mass transfer coefficient is the classical method to describe the driving potential between interphases or intraphases. Carberry (1960) proposed a theoretical equation for mass transfer in a packed bed of spherical particles by applying the simplified boundary layer model for a flat plate to the fixed bed under the assumption that the boundary layer develops and collapses over a distance approximately equal to one particle diameter. However, in the low Reynolds number (Re) region, Carberry's equation has been reported to deviate from experimental data (Kataoka et al., 1972). Kataoka et al. (1972) derived a theoretical mass transfer equation by applying the hydraulic radius model to laminar flow in a packed bed. They assumed that the void parts in the packed column can be regarded as a bundle of tubes and that mass transfer between packing material surfaces and flowing liquids in the packed bed is similar to mass transfer between the inner tube surface and flowing liquid with steady laminar velocity profile in the assembly of tubes. They suggested that Carberry's equation can be applied for $Re > 100$ and their equation fits at $Re < 10$. In the range $10 < Re < 100$, the difference between predicted results using these two models is probably within the limits of precision of most of the experimental data.

Haub and Foutch (1986a) used Carberry's equation for particle Reynolds numbers greater than 20 and Kataoka's equation for less than 20.

At very low Reynolds numbers ($Re < 1$), theoretical models and experimental results show decreased mass transfer coefficients. These low values of the mass transfer coefficients are believed to be due to micro-nonuniformity in flow distribution (Zabrodsky, 1965a, b). Nelson and Galloway (1975) presented a theory of mass transfer in dense systems of particles. Rowe (1975) modified this theory and pointed out that the theory could only be tested if experimental data in liquid fluidized beds at very low Reynolds numbers were available. Koloini et al. (1977) studied mass transfer coefficients between fluidized ion exchange resins and dilute solutions of hydrochloric and benzoic acids in the range of low Reynolds numbers. They reported much lower values of mass transfer coefficients than previously measured. Rahman and Streat (1981) obtained mass transfer correlation for fluidized, fixed, and distended beds in the range $2 < Re < 25$. They reported that at low voidage of 0.55 - 0.60, the rate of mass transfer is reduced inferring that a fluidized bed tends to maintain an ordered axial structure.

Recently, Zarraa (1992) investigated mass transfer during the removal of cupric ions from dilute copper sulphate solution in a fluidized bed of ion exchange resin at low Reynolds numbers. He reported through parametric

studies that the mass transfer coefficients increase with increasing superficial liquid velocity and decrease with increasing particle diameter, bed height, and copper sulphate concentration. The correlation equation for the mass transfer coefficients is given in terms of the Sherwood number, the modified Reynolds number, the Schmidt number, and the scale factors which are the ratios of particle diameter to bed diameter and to bed height. This equation is valid in the range $0.23 < Re < 2.27$.

The mass transfer coefficient also depends on film thickness, and pH in liquid phase. Harries and Ray (1984) showed that the mass transfer coefficient of chloride exchange is a function of influent concentration. The mass transfer coefficient is lower for the lower influent concentration because the film thickness increases as the influent concentration decreases. Harries (1988) believed that the mass transfer coefficient of chloride is high at low pH and low at high pH, and that for sodium is high at high pH and low at low pH. Yoon (1990) suggested a correlation of the mass transfer coefficient for packed beds, where the constant from the correlation of Kataoka, et al. (1972) is given as a function of the cation resin fraction for ultralow influent concentrations. Table III shows a summary list of the various correlation equations for the nonionic mass transfer coefficients.

TABLE III

A SUMMARY OF THE CORRELATION EQUATIONS FOR
THE MASS TRANSFER COEFFICIENTS

. Carberry (1960)

$$k = 1.15 \frac{V_s}{\epsilon} (Sc)^{-\frac{2}{3}} (Re_1)^{-\frac{1}{2}}$$

. Kataoka et al. (1972)

$$k = 1.85 \frac{V_s}{\epsilon} \left[\frac{\epsilon}{1 - \epsilon} \right]^{\frac{1}{3}} (Sc)^{-\frac{2}{3}} (Re_2)^{\frac{2}{3}}$$

. Rowe (1975)

$$Sh = \frac{2\xi + \left[\frac{2\xi(1-\epsilon)}{\{1-(1-\epsilon)^{1/3}\}^2} - 2 \right] \tanh(\xi)}{\frac{\xi}{1-(1-\epsilon)^{1/2}} - \tanh(\xi)}$$

$$\text{where } \xi = \left[\frac{1}{(1-\epsilon)^{1/3}} - 1 \right] \frac{\alpha}{2} (Sc)^{\frac{1}{3}} (Re)^{\frac{1}{2}}$$

. Rahman and Streat (1981)

$$Sh = \frac{0.86}{\epsilon} (Sc)^{\frac{1}{3}} (Re)^{\frac{1}{2}}$$

TABLE III (Continued)

. Yoon (1990)

$$k = A \frac{V_s}{\epsilon} (Sc)^{-\frac{2}{3}} (Rem_2)^{-\frac{1}{2}}$$

where $A = 0.454 - 0.168 \log(\text{FCR})$ for cation
 $A = 0.364 + 0.028 (\text{FCR})$ for anion

. Zarraa (1992)

$$Sh = 0.85 Rem_1^{0.54} Sc^{0.33} \left[\frac{dp}{d} \right]^{-0.75} \left[\frac{dp}{L} \right]^{0.41}$$

Where $Rem_1 = (dp V_s \rho) / (\epsilon \mu)$
 $Rem_2 = (dp V_s \rho) / \{(1-\epsilon) \mu\}$
 $Sc = \mu / (\rho D)$
 $Sh = (k_L dp) / D$
 $V_s =$ superficial velocity
 $\epsilon =$ bed void fraction
 $dp =$ particle diameter
 $d =$ bed diameter
 $L =$ bed height
 $D =$ ionic diffusion coefficient
 $\rho =$ density
 $\mu =$ viscosity
 $\text{FCR} =$ cation-to-anion resin ratio

CHAPTER III

EXPERIMENTAL APPARATUS AND PROCEDURES

Experimental Apparatus

The experimental system was first designed and used by a former investigator at Oklahoma State University (King, 1991). The system was modified and updated to add an on-line pH monitoring device for the present study. Figure 1 shows the schematic diagram of the mixed-bed ion exchange experimental column. The system is composed mainly of an experimental column, its accessories for feeding, heating, and measuring experimental parameters such as temperature, resistivity and pH, and an ion chromatograph for measuring effluent concentration. There are two different flow paths in the system; one is to feed a solution of the specific concentration to the experimental column, and the other is to provide high purity water for chemical and feed preparation. Figure 2 presents this supporting flow system with water purification columns. Two personal computers are used to support the operation of the system. One computer contains Labtech Notebook software and records resistivity and pH as functions of time. The other computer controls the ion chromatograph and is used for post processing of the data using Dionex software.

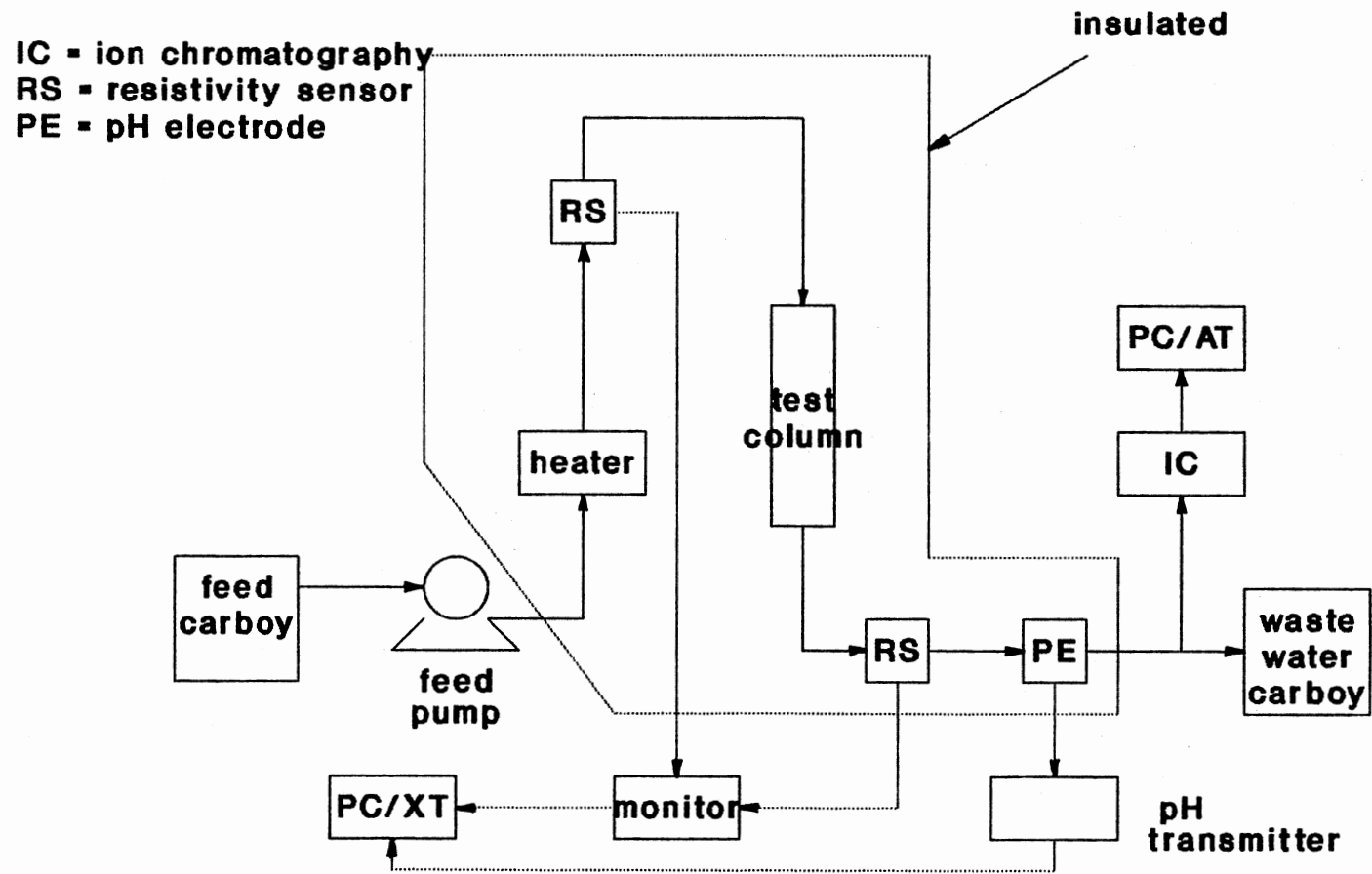


Figure 1. Flow Diagram for MBIE Experimental System

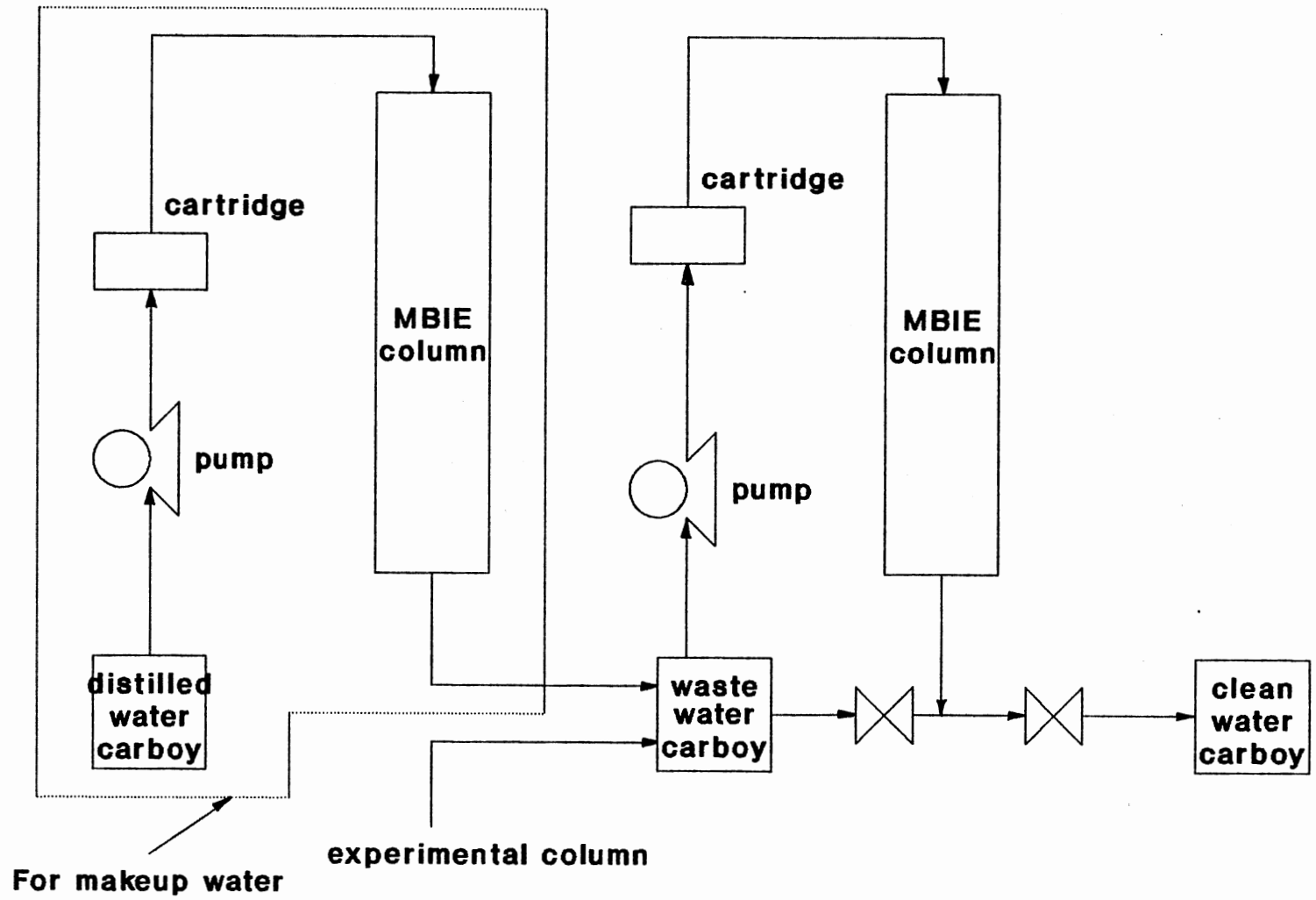


Figure 2. Flow Diagram for Water Purification System

Experimental Columns

The experimental columns used for this work were Pyrex glass prepared by the Materials Laboratory at Oklahoma State University. These columns were transparent to see the loaded resins. A fritted disk made from foam packing material was placed in the bottom of the column to keep the resin inside the column during the experimental runs. For the incompletely mixed-bed ion exchange experiments, another disk was placed between the unmixed and the mixed portions to prevent the resins from being mixed during the experimental runs.

The experimental columns have two different sizes: 1 inch ID x 18 inch length x 0.13 inch thickness (2.54 cm x 46 cm x 0.32 cm) and 0.728 inch ID x 8.66 inch length x 0.16 inch thickness (1.849 cm x 22 cm x 0.41 cm). The larger column was built and first used by the previous investigator (King, 1991). This column was used for the variable feed concentration experiments. The flow rates for the incompletely mixed-bed experiments were increased by 10 times compared to the variable feed concentration experiments to keep the superficial velocity in the range of 2.3 - 2.7 cm/sec. These flow rates resulted in significantly high pressure throughout the whole system. Therefore, the column had to be replaced with a smaller one to get the same superficial velocity with lower pressure

drop caused by the reasonable flow rate without any modification of the existing experimental system.

Ion Exchange Resins

Dowex resins provided by the Dow Chemical Company were used for this study. The physical properties of the resins are shown in Table IV. Each of these resins was rinsed with high purity water (18 Meg-ohm water) and stored in plastic containers until they were used to prepare experimental columns.

Ion Chromatograph

A Dionex Series 4500i Gradient Ion Chromatograph (IC) was used to analyze the on-line and/or off-line effluent ionic concentration of solutions from the experimental column. The IC is designed for single- or dual-system operation to analyze anion and cation concentrations independently or simultaneously. Each basic system includes a Gradient Pump, an Advanced High-Pressure Chromatography Module, a Conductivity Detector-II, an Advanced Computer Interface, an Eluant Degas Module, and enclosures with power strip and drawer slides. The Gradient Pump is a microprocessor-based eluant delivery system designed to pump mixtures of up to four solvents at precisely controlled flow rates. The Advanced High-Pressure Chromatography Module isolates a column, a micromembrane suppresser, and valves from thermal variations in the laboratory. The Conductivity

TABLE IV
PHYSICAL PROPERTIES OF DOWEX RESINS*

parameter	cation	anion
name	HGR-W2-H	SBR-P-C-OH
lot	MM891006-2	MM890113-IC
capacity (meq/ml)	2.18 (Na ⁺ form)	1.1 (Cl ⁻ form)
selectivity	Na-H 1.13	Cl-OH 22.0
void fraction	0.335-0.34	0.335-0.34
water retention capacity (%)	48.2	54.3
density (lb/ft ³)	50.0	41.0
diameter(cm)	0.08	0.06
appearance	light yellow to amber solid(bead)	white to dark amber solid(bead)
particle size distribution		
<u>mesh</u>	<u>%</u>	<u>%</u>
+16	1.2	0.2
+20	46.9	9.1
+25	45.1	-
+30	6.0	72.8
+35	-	14.2
+40	0.6	2.6
+45	-	0.8
+50	0.3	0.4
-50	0.0	0.0

* From the vendor

Detector-II is a microprocessor-based detection system for conductive ions. Electronic signal processing increases the signal-to-noise ratio, enhancing sensitivity and lowering detection limits. The detector automatically offsets up to 1600 μS of background conductivity and compensates for temperature-caused conductivity variations. The system operation was controlled remotely by the Dionex software through the Advanced Computer Interface. This IC increased the laboratory detection level to ionic concentrations of 0.2 ppb sodium and 0.3 ppb chloride.

The Dionex company provided AutoIon 450 Data System(AI-450) Chromatography Software installed on a personal computer. This program is a family of chromatography automation software which controls the IC; automatically collects, processes and reports data; and provides utilities that simplify interpretation of results. This software was updated during the period of this work and fully utilizes the features of Microsoft Windows version 3.0. King (1991) describes procedures for the post processing of the data using the AI-450 software, and interfacing with a spreadsheet and an auxiliary file manager in detail.

Eluant solutions for the IC were prepared from fully deionized water and reagent grade chemicals. For the anion eluant, a mixture of 1.8 mM sodium carbonate and 1.7 mM sodium bicarbonate was used. The cation eluant was mixture of 27.5 mM hydrochloric acid and 2.25 mM DL-2,3-diaminopropionic acid monohydrochloride. The flow rate for

anion eluant was 2.0 ml/min. and for cation eluant 1.0 ml/min. A 0.025 M sulfuric acid solution was used for the anion regenerant and 70 mM tetrabutylammonium hydroxide for the cation regenerant. The regenerant flow rates were 2.5 ml/min for anion and 5.0 ml/min for cation. Table V shows the characteristics and manufacturers of the chemicals used to prepare the eluants and regenerants for the IC. The details in the preparation of these solutions are given in Appendix A.

For storage and feeding the eluant solutions, four bottles were used: two for each ion eluant. Fifty percent eluant from one bottle was mixed with 50 % eluant from the other bottle at chemically inert solenoid valves. The outputs from the four proportioning valves were combined in the manifold and then directed through the Gradient Mixer to the pump. The eluant in each bottle had the final eluant composition. Alternatively, one of the two bottles could be filled with pure water and the other with double-concentrated eluant to produce the final eluant composition after passing the mixer.

Nitrogen and helium were used for degassing eluants and pressurizing the eluants and regenerant containers. Degassing prevents bubbles from foaming in the eluant selector valves and assures optimum operation of the pumps.

To determine the ion concentrations, either peak area or peak height could be used. In this study, peak area was measured to obtain quantitative results because peak area

TABLE V
CHARACTERISTICS OF CHEMICALS USED FOR IC

chemical	purity	manufacturer	comment
sodium carbonate	99 %	Fisher Sci.	anion eluant
sodium bicarbonate	99 %	Fisher Sci.	anion eluant
Hydrochloric Acid	36.5-38%	Fisher Sci.	cation eluant
DAP*	99 %	Fluka Chemie	cation eluant
Sulfuric Acid	95-98 %	Fisher Sci.	anion reg.
TBAOH*	55% aqueous solution	Southwestern Anal. Chemical Inc.	cation reg.

* DAP : DL-2,3-Diaminopropionic Acid Monohydrochloride
TBAOH : Tetrabutylammonium Hydroxide

measurement provided stability at low ion concentrations. Calibration curves in Appendix B show the relations between peak areas and ion concentrations for sodium and chloride.

Auxiliary Facility

As shown in Figure 2, two large mixed-bed ion exchange plexiglas columns were used in series to supply high purity

water for the chemicals and feed preparation. For make-up water, the city water was fed into the first column after being treated by distillation and a filter housing cartridge. The effluent of the experimental column was introduced through the second cartridge into the second column to produce high purity water. The water finally produced from the second column had good quality with a resistivity reading greater than 18.2 Meg-ohm-cm, the standard of pure water at 25°C.

Eight different-sized containers in the range of 10 - 50 liters were used to store the feed and effluent of the purification columns and the experimental column. These containers were low-density polyethylene with quick-action spigots and leak-tight caps. A piston pump was used to feed influent into the experimental column for the incompletely mixed-bed experiments and a metering pulse pump for the variable feed concentration experiments. For the flow path to the second purification column, two metering pulse pumps were used and their combined capacity was 33 liter/hr. Two resistivity and temperature sensors were used to measure on-line resistivity and temperature of the flow before (channel 1) and after (channel 2) the experimental column. They were connected to a monitor and an XT personal computer where the Labtech Notebook software was installed. The details of setup and control with the Labtech Notebook software are presented by King (1991). An electrode and a pH transmitter were used for the on-line pH monitoring system and were

connected to the XT personal computer through a DAS-8 Board. The original setup of the Labtech Notebook was modified to monitor and collect the on-line pH data in this study. The channel for the output signal to a fractional sample collector was removed because it was no longer in use. Instead, another channel was set up for analog input from the pH transmitter. A temperature controller and heating tapes were used to keep the system at constant temperatures. Plastic fittings and 1/4 inch plastic tubes were used for the flow path. A list of these auxiliary facility is given in Table VI.

Experimental Procedures

Because the feed concentration for these experiments is very low, special attention is given to removing the sources of water contamination. Pure water was prepared by passing new water from the distillation column, or the effluent of the experimental column, through high capacity mixed-bed ion exchange columns in series. Resistivity greater than 18.2 Meg-ohm-cm at room temperature was checked to make sure water quality.

Water produced by the purification system was collected in a 25 liter carboy which had been used only for pure water. As soon as pure water was made, it was used to prepare either the feed solution or the chemicals for the IC. A leaching problem from the carboy became significant after about 48 hours. Water stored in the carboy more than

TABLE VI
LIST OF AUXILIARY FACILITY

facility	unit	capacity	manufacturer
cartridge	2		Corning Mega-Pure
carboy	3	50 l	Nalge Comp.
	3	30 l	
	1	20 l	
	1	10 l	
piston pump	1	60 l/hr	Madden Corp.
pulse pump			
PD 31P	1	2.4 l/hr	Neptune
PHP44	1	18 l/hr	Omega Eng. Inc.
PHP82	1	15 l/hr	Omega Eng. Inc.
resistivity & temp. sensor	2		Signet Sci.
resistivity monitor	1		Signet Sci.
pH transmitter	1		Omega Eng. Inc.
pH electrode	1		Omega Eng. Inc.
DAS-8 Board	1		Metabyte Corp.
temp. controller	1		PowerStat
personal computer			
AT	1		PC Tech
XT	1		Excutive

12 hours was fed into the purification columns again to ensure water quality.

The resins provided by the manufacturer were rinsed with the high purity water from the purification columns and stored in plastic containers. For the experiments, specific wet volumes of cation and anion resin were taken from the resin containers and mixed. Then, the resins were placed in the experimental column carefully and checked to ensure complete mixing and uniform packing throughout the column cross-section. The column was filled with pure water fully, while being tipped to remove any air bubbles between the resin particles and promote uniform packing. A fritted disk, made from foam packing material with a screen made of stainless steel, was used to support the mixed-bed resins and to ensure uniform flow distribution. After assembling the system, pure water was fed into the column until the column was brought to the desired experimental conditions. The bed depth was then measured and recorded with the measured resin volumes on a Quattro Pro spreadsheet.

The feed solution was prepared by diluting a concentrated solution with pure water from the purification columns. The concentrated solution was obtained by dissolving the calculated amount of salt in a 1000 ml flask with pure water. After pipetting 10 ml of the concentrated solution to a 10 liter carboy and adding pure water, vigorous agitation was used, and complete mixing was checked by conductivity measurement. Then, the solution was added

to carboys for the feed solution. Only a specified carboy was used for a certain duty. If necessary, the makeup feed water was made and added to the feed carboys.

To maintain a constant temperature, the experimental line from the feed pump to the pH transmitter was insulated using heating tapes. The column was brought to the desired experimental temperature using a temperature controller and heating tape as pure water flowed through the system. Two temperature sensors were used; channel 1 and 2, so the entrance and exit temperatures of the column could be read on the monitor. After the system stabilized at the experimental conditions, the feed solution was introduced into the system and flowed from the top of the column to the bottom. When the feed solution reached the top portion of the column first, the resistivity at channel 1 would decrease. This point was considered as the starting point of the run. Flow rate was measured periodically at the end of the flow path using a graduated cylinder and a stop watch. For the variable feed concentration experiments, the flow rate was almost constant and accurate. For the incomplete mixing of resins experiments, the flow rate showed relatively high instability. The error of measuring the flow rates is analyzed in Appendix B.

Periodically, on-line resistivity and pH data were collected during the run and recorded on computer output files by the Labtech software. The pH transmitter originally offered a 4 to 20 mA DC output for 0 to 14 pH

with a constant voltage of 15 V. This current-output signal was converted into the voltage-output of 0 to 5 V by applying a resistance across the output at the transmitter. Thus, the voltage outputs from the transmitter were recorded with time and used to calculate the actual pH data using the calibration curves shown in Appendix B.

Water samples were collected periodically and analyzed using on-line or off-line procedure. For both on-line and off-line procedures, the samples were injected through the sampling pump which was controlled by the AI-450 software. The post-run processing of the chromatography data was performed by using utilities in the AI-450 program and Quattro Pro. The step-by-step procedures for the preparation and the operation of the experiments are shown in Appendix A. The following is a detailed description of the specific procedures for the variable feed concentration and the incomplete mixing of resins experiments.

Variable Feed Concentration

For the variable feed concentration experiments, step changes in feed concentration were arbitrarily introduced into the experimental column for several hours during the runs. The normal feed concentration was $2.0\text{E-}4$ M for early experiments. Later, the lower concentration of $1.0\text{E-}4$ M was used. The concentrations of the peaks were five to ten times higher than the normal feed concentration. A 30 liter carboy was used to store and feed the concentrated solution

for step changes in feed concentration. To introduce a peak in feed concentration into the column, the valve for the normal feed solution was switched to the concentrated solution. Then, the resistivity at channel 1 was checked. The starting point of the peak was determined when the resistivity started to decrease. To return the normal feed concentration, the valve was switched to the normal feed concentration. The point that the resistivity at channel 1 increased was the ending point of the peak.

For the variable feed solution experiments, an on-line procedure was utilized because of the long duration of the experimental run, resulting from a deep bed and low flow rate. This procedure could remove a possible source of contamination from a sample bottle. The IC was connected directly to the flow system and automatically collected and analyzed the effluent samples every one hour and recorded the results on computer files. All the sampling and analyzing procedures were controlled by the Dionex AI-450 program. The detailed operation procedure of the IC associated with the AI-450 software is given in Appendix A.

Incomplete Mixing of Resins

The incompletely mixed-bed experiments were initially performed with relatively high flow rate of about 12.0 ml/s, which had a superficial velocity much closer to the industrial conditions of 2.5 cm/s. The experimental system used for the variable feed concentration experiments was

also used without major changes. Some preliminary runs were made to determine the proper configuration of the system under new conditions. The preliminary runs were mainly to overcome the high pressure drop problem due to the high flow rate. The total length of the flow path was reduced as much as possible to decrease the pressure drop. The flow line from the IC to the system was also removed, and the sample analysis was completed with off-line procedure. The feed pump was replaced with a high capacity piston pump to maintain constant flow rates.

Even though the total flow path was reduced to about 60 % of the previous system, there were still stability problems due to the high flow rate. Also, this flow rate introduced a number of air bubbles into the column. The air bubbles might be the source of carbonate or bicarbonate, which affect the breakthrough curve of chloride strongly. After several preliminary runs, the experimental column was replaced by a smaller column of 1.85 cm diameter. The new column made it possible to decrease the flow rate significantly, while maintaining the same superficial velocity. The flow rate with the new column was about 7.0 ml/s. To perform a experimental run with this flow rate without interruption during the run, the flow rate for the water purification columns should also increase to provide enough pure water for the preparation of the feed solution. Thus, the purification system was modified to include a second feed pump. The combined capacity of two feed pumps

was 33.0 liter/hr. The quality of water was checked, and the increased flow rate was found not to affect the quality.

The experiments were conducted with lower feed concentration of $5.0E-5$ M and more cation resin than the variable feed concentration experiments. These conditions were close to industrial practice. Based on the flow rate and the resin capacity, the amount of each resin was decided to have an reasonable experimental duration. About 5.0 ml of each resin was used, and the maximum duration was about 13 hours. The bed depth was about 4.0 cm and caused initial leakage due to insufficient contact time between the solution and resin, but made it possible to conduct a run within a day.

To make an incompletely mixed bed, about half of the measured anion resin was mixed with the measured cation resin and placed in the bottom of the column. The rest of the anion resin was charged in the upper portion of the column. A fritted disk was placed between these two portions to prevent mixing of the resins during the runs.

Samples were collected periodically by hand using sample bottles. The bottles were rinsed at least three times using pure water from the purification columns before sampling and filled fully to remove air in the bottles. To avoid the leaching from the bottle itself, the samples were analyzed within at most 6 hours.

CHAPTER IV

EXPERIMENTAL RESULTS

The objectives of this study are to obtain experimental data and to evaluate the mathematical model of Haub and Foutch (1986a, b), which has the ability to predict the performance of industrial mixed bed ion exchange, under various conditions. As shown in the previous chapter, the experiments were designed to collect data for the cases of variable feed concentration and incomplete mixing of cation and anion resin observed typically in large scale industrial plants.

In this chapter, the experimental results are presented. Several experiments for both cases were carried out, including preliminary runs for proper system configuration. The effluent from the column was collected periodically and analyzed using on-line ion chromatography for the variable-feed concentration experiments, and off-line analysis for the incompletely-mixed bed experiments. The peak areas from the chromatograms were used to produce ionic concentration calibration curves. These calibration curves were obtained by analyzing standard solutions, and were dependent on a method file used for analysis. For the present work, two different method files were used to control the time events of ion chromatograph operation. Appendix B contains

the calibration curves for chloride and sodium obtained by using one of these two method files.

In general, the experimental data are plotted and presented in terms of concentration as a function of run time in hours. When plotted, the data showed smooth breakthrough curves, even though they tended to scatter at the early stage of each run, especially for the variable feed concentration experiments. Appendixes B and C present the accuracy of the experiments and the numerical data, respectively.

Variable Feed Concentration

A total of eight experimental runs was conducted to investigate the effects of the variable feed concentration on the performance of mixed-bed ion exchange. However, only five were selected for data analysis because the rest were preliminary runs. Table VII shows the experimental conditions of these runs. All experiments were carried out under similar flow rates and temperatures. Usually, a much longer time is required to reach the equilibrium concentration for cations than anions, provided the same amount of each resin is used. This is due to higher selectivity coefficients for anionic resin than cationic resin. For this study, less cation resin was used so that both ions reached equilibrium at nearly the same time, although these low cation-to-anion resin ratios are rarely used in industry. Based on the desired flow rates,

TABLE VII
EXPERIMENTAL CONDITIONS* FOR VARIABLE FEED
CONCENTRATION EXPERIMENTS

Run No.	Flow** Rate (ml/sec)	Cation Resin Fraction	Column Depth (cm)	Feed Conc. (eq/l)	Comments
R128	0.667	0.391	13.4	2.0E-4	. Duplicate of R211
R211	0.667	0.384	13.0	2.0E-4	. Constant feed conc.
R218	0.667	0.375	13.2	2.0E-4	. Feed conc. changed to 1.0E-3 for 4 hrs . Compared to R211
R326	0.665	0.377	14.3	1.0E-4	. Constant Feed conc.
R503	0.665	0.379	13.9	1.0E-4	. Feed conc. changed to 1.0E-3 for 5 hrs & 0.5E-3 for 4 hrs . Compared to R326

* All experiments were conducted under the same conditions of

- . Temperature = 25 °C
- . Column Diameter = 2.54 cm

** Superficial velocity = 0.132 cm/sec

appropriate column depth and feed concentration were determined to give reasonable experimental durations. The maximum duration of a run was about 250 hours. The results of Run R211 and its duplicated run, Run R128, were compared to evaluate the reproducibility of the experimental system. The comparison is shown in Appendix B.

For the variable feed concentration experiments, step changes in feed concentration were arbitrarily introduced in the experimental column during the runs. The effluent concentrations were measured by the on-line analytical process. These concentrations were plotted as the relative concentration versus run time. The relative concentration is peak area obtained from the chromatograms. The effluent profiles were then compared with those of the constant feed concentration experiments.

Run R211 had constant feed concentration and Run R218 had one peak in the feed concentration profile. The peak was introduced into the column 6 hours after starting the run and maintained for 4 hours. The feed concentration was then dropped to the initial concentration and kept constant for the rest of the run. Figure 3 shows the feed concentration profiles for Runs R211 and R218. Figures 4 to 7 show the comparison of either chloride or sodium breakthrough curves from both runs.

In Figure 4, the profile indicates that the chloride curve starts to rise after 70 - 80 hours for Run R211 and for Run R218 after 50 - 60 hours. Thus, introducing a peak

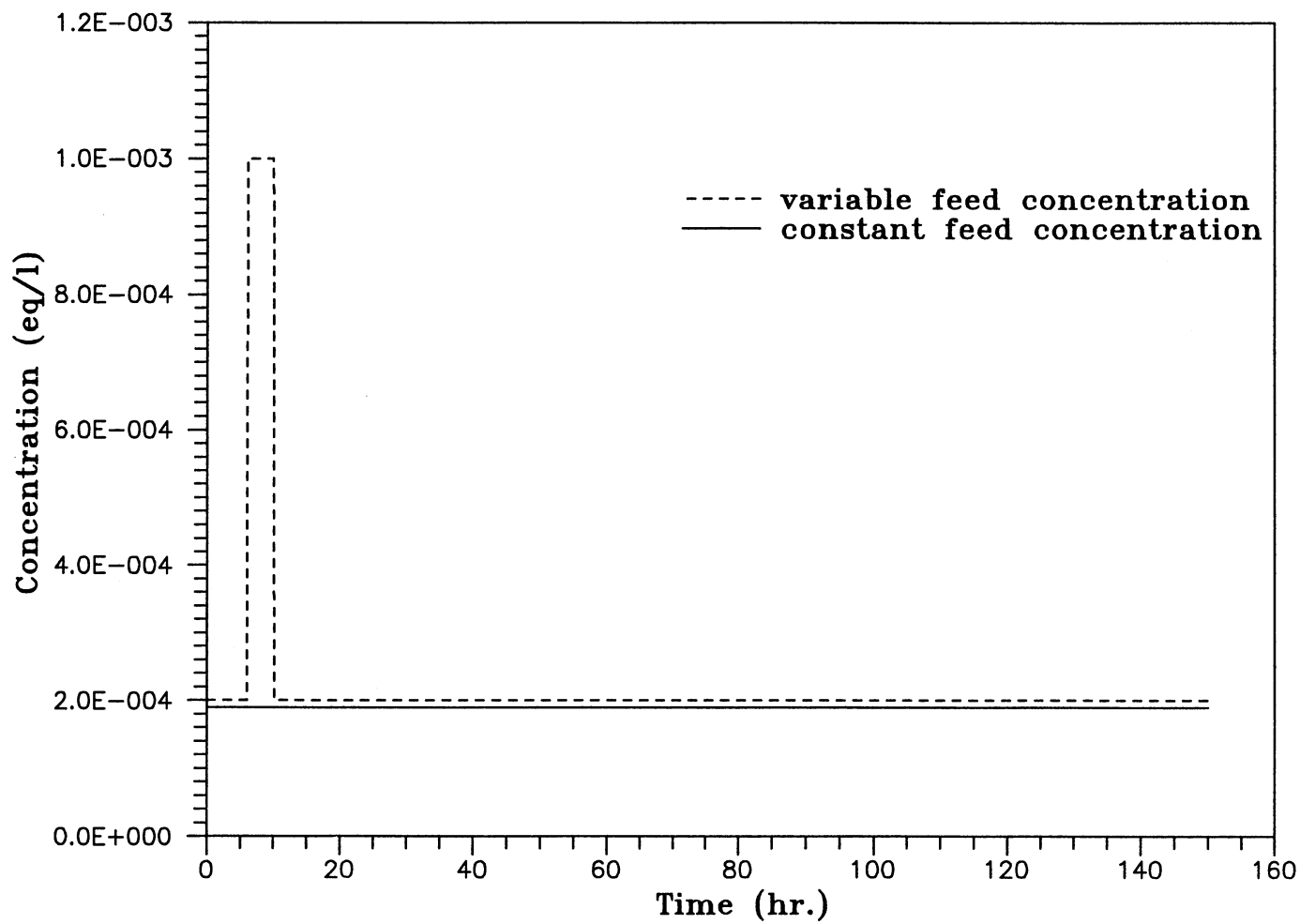


Figure 3. Feed Concentration Profiles for Constant and Variable Feed Concentration Experiments with One Peak

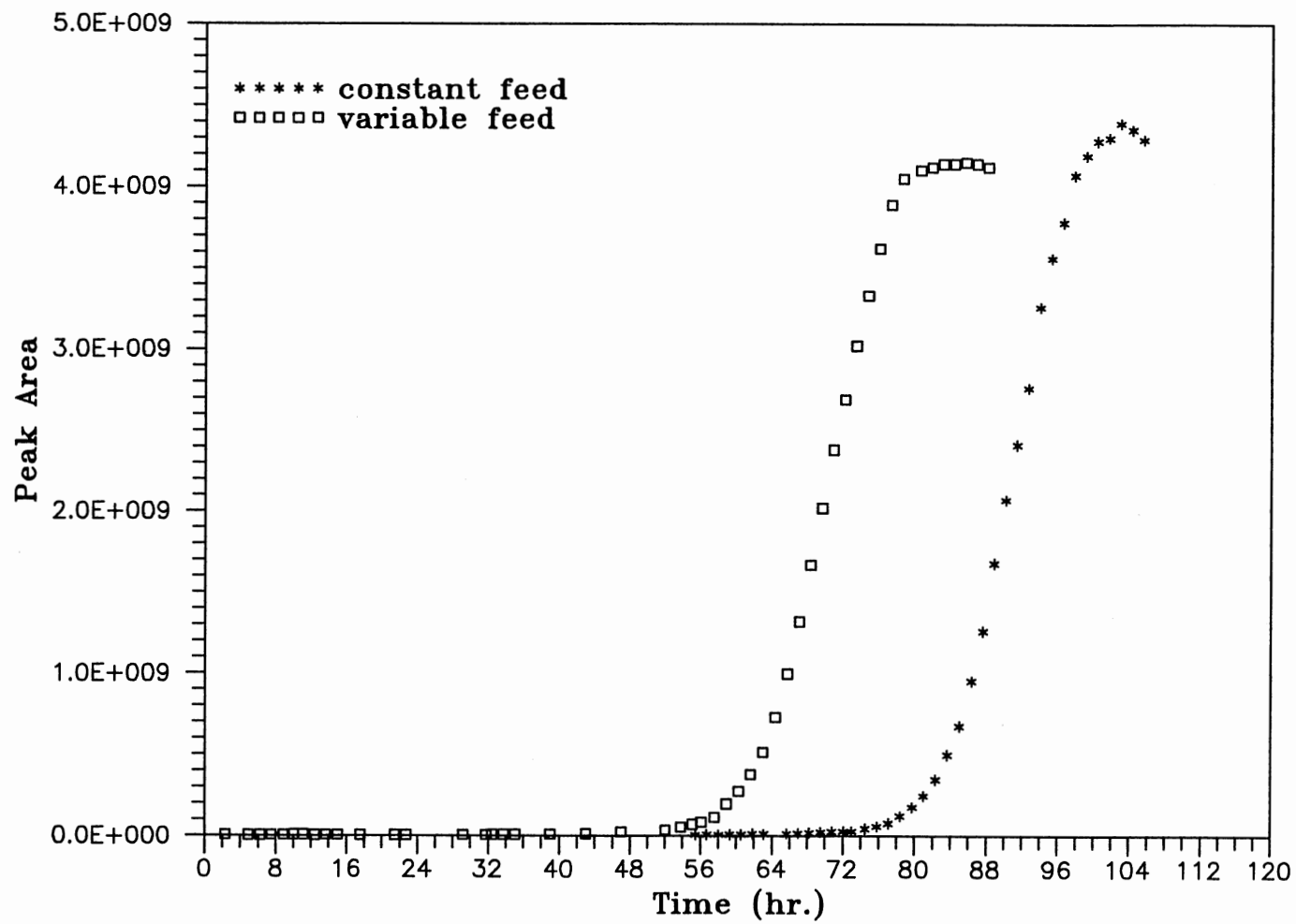


Figure 4. The Effect of One Peak in Feed Concentration on Chloride Breakthrough Curve

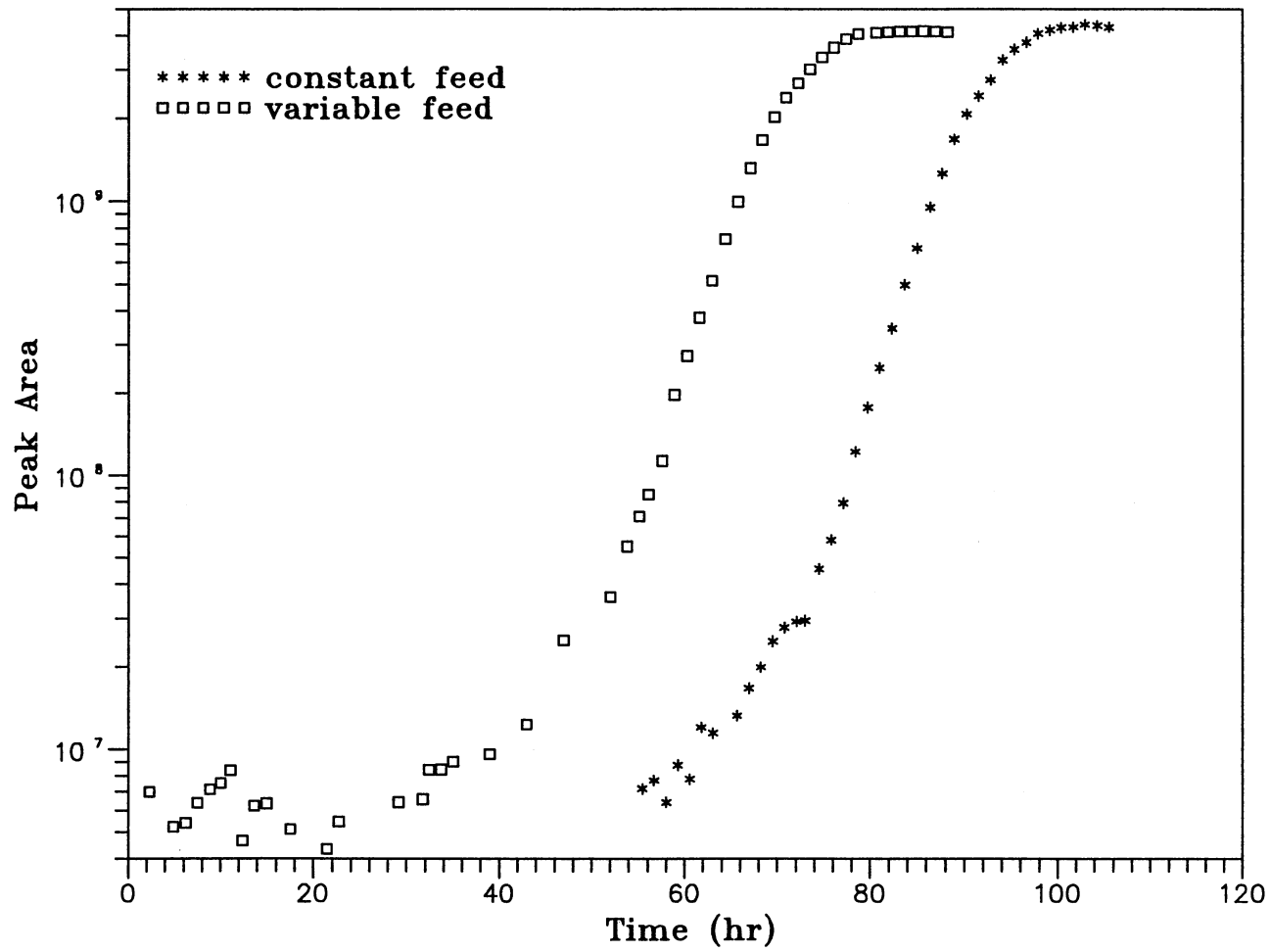


Figure 5. Semilog Plot of Experimental Data for the Effect of One Peak in Feed Solution on Chloride Curve

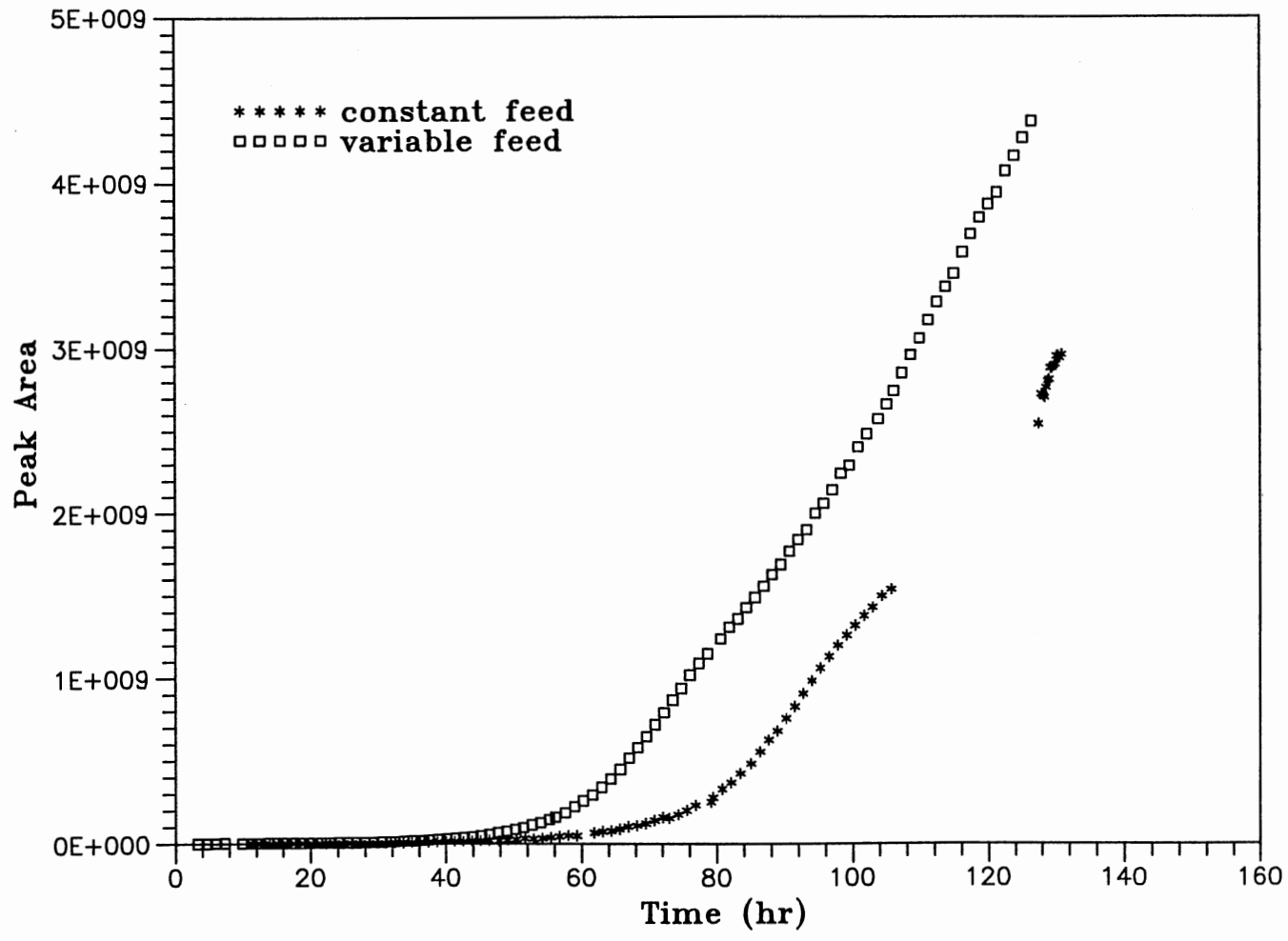


Figure 6. The Effect of One Peak in Feed Concentration on Sodium Breakthrough Curve

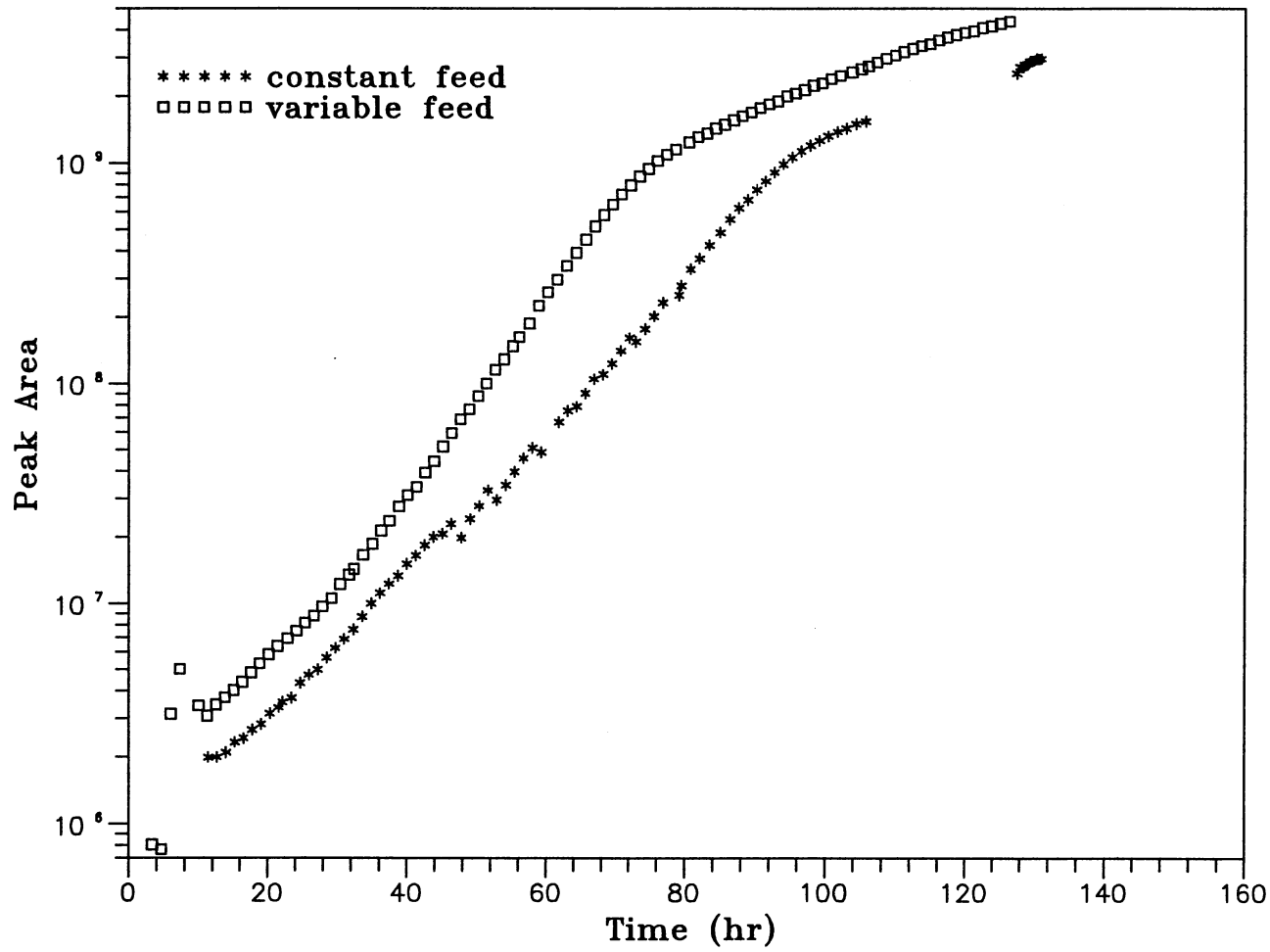


Figure 7. Semilog Plot of Experimental Data for the Effect of One Peak in Feed Solution on Sodium Curve

in the feed concentration results in faster breakthrough time for chloride, as we expect. It appears that the peak does not affect the shape of breakthrough curves. It may be interesting to calculate the total amount of chloride removed through both runs before the breakthrough time. For both runs, the flow rate was about 2.4 liter/hour (0.667 ml/sec) and the normal feed concentration was 7.11 ppm chloride. Assuming that there is no chloride leakage in the effluent until the breakthrough curves start to rise, a total amount of 1.195 - 1.366 g chloride was removed in 70 - 80 hours for Run R211. For Run R218, the normal concentration was changed to 35.5 ppm chloride and maintained for 4 hours. Totally, 1.194 - 1.365 g chloride was removed in 50 - 60 hours, which is close to that for Run R211. This fact may mean that if peak concentration and its duration are known, the chloride breakthrough time can be predicted.

Figure 5 contains the same data as Figure 4, plotted as log concentration versus run time. This semilog plot makes it possible to amplify and investigate the curves at the early run times. As shown in this figure, there is a low level of leakage after the peak is introduced. This might result from insufficient contact time between the solution and the resin. When the feed returns to the normal concentration, the leakage seems to disappear and the effluent concentration becomes the same as that of the constant feed concentration case.

Figures 6 and 7 show the effluent concentration profiles of sodium for Runs R211 and R218. The curves appear to have similar slopes to each other after breakthrough. The slopes are relatively broad compared to those for chloride. This is because the anion resin has a higher selectivity coefficient than the cation resin. Closer inspection of the curves indicates that the curve for Run R218 begins to rise between 30 - 40 hours. For Run R211, the breakthrough time is about 50 - 60 hours. The normal feed concentration was 4.61 ppm sodium and the flow rate was 2.4 liter/hour. With the assumption of sodium free effluent until the breakthrough, the close amounts of sodium are found to be removed through both runs (0.553 - 0.664 g for Run R211 and 0.509 - 0.619 for Run R218). Based on the results of these calculations, it seems to be possible to predict approximately the performance of an ion exchange bed after a sudden change in the constant feed concentration. Figure 7 shows that the effluent of Run R218 starts to have higher concentrations than that of Run R211 after the peak is introduced in the feed concentration. This was not found in chloride breakthrough curves (see Figure 5). This is probably due to the much higher selectivity coefficient of the anion resin.

Similarly, Runs R326 and R503 have constant feed concentration and two peaks in the feed concentration, respectively. The feed solution for these runs was less concentrated ($1.0E-4$ eq/l) than that for Runs R211 and R218

($2.0E-4$ eq/l). Figure 8 shows the feed concentration profiles of the runs. For Run R503, the feed concentration was maintained constant for the first 24 hours and increased rapidly to $1.0E-3$ eq/l. Five hours after the increase, the feed concentration dropped to the initial concentration and remained constant for 18 hours. Then, the feed introduced a second peak of $5.0E-4$ eq/l for 4 hours.

Figure 9 shows the effects of the peaks in the feed concentration on chloride breakthrough. As expected, the breakthrough curve is earlier for Run R503 than for Run R326. At first inspection, the two curves are further apart than those in the experiments with one peak in feed concentration (Runs R211 and R218). The figure indicates chloride breakthrough between 140 - 160 hours for Run R326 and between 80 - 100 hours for Run R503. For these runs, the flow rate was approximately 2.39 liter/hour (0.665 ml/sec) and the feed solution had a normal concentration of 1.78 ppm chloride. Based on these experimental conditions, the total amount of chloride removed until breakthrough is 0.596 - 0.68 g for Run R326 and 0.465 - 0.555 g for Run R503. Unlike the results of the one-peak experiments, much less chloride appears to be removed by introducing two peaks in feed concentration.

Figure 10 is a semilog plot of the data in Figure 9. The data for both runs show an instability at the early stage of the runs. The actual concentrations in this period are considered to be below parts per billion. Although both

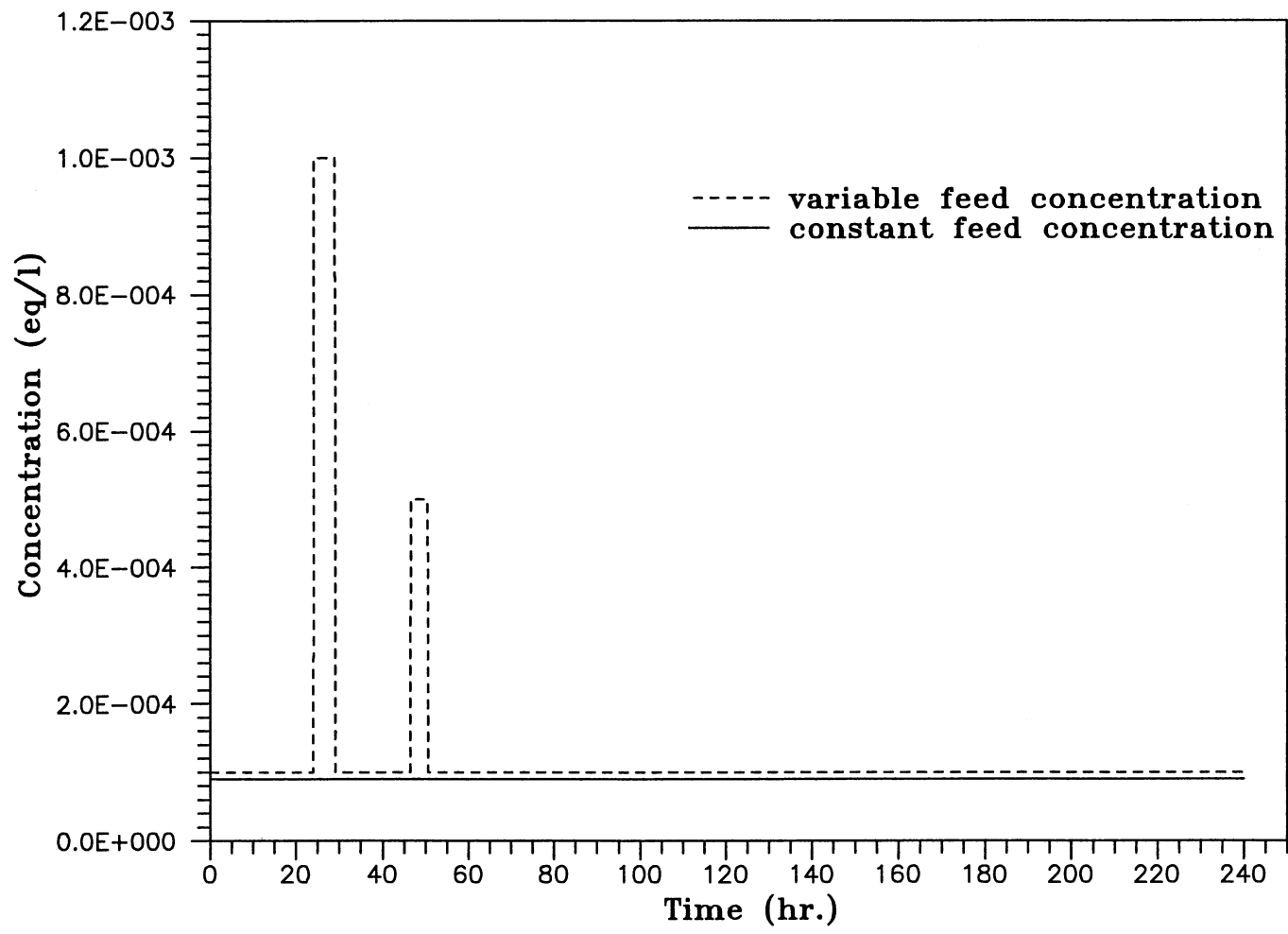


Figure 8. Feed Concentration Profiles for Constant and Variable Feed Concentration Experiments with Two Peaks

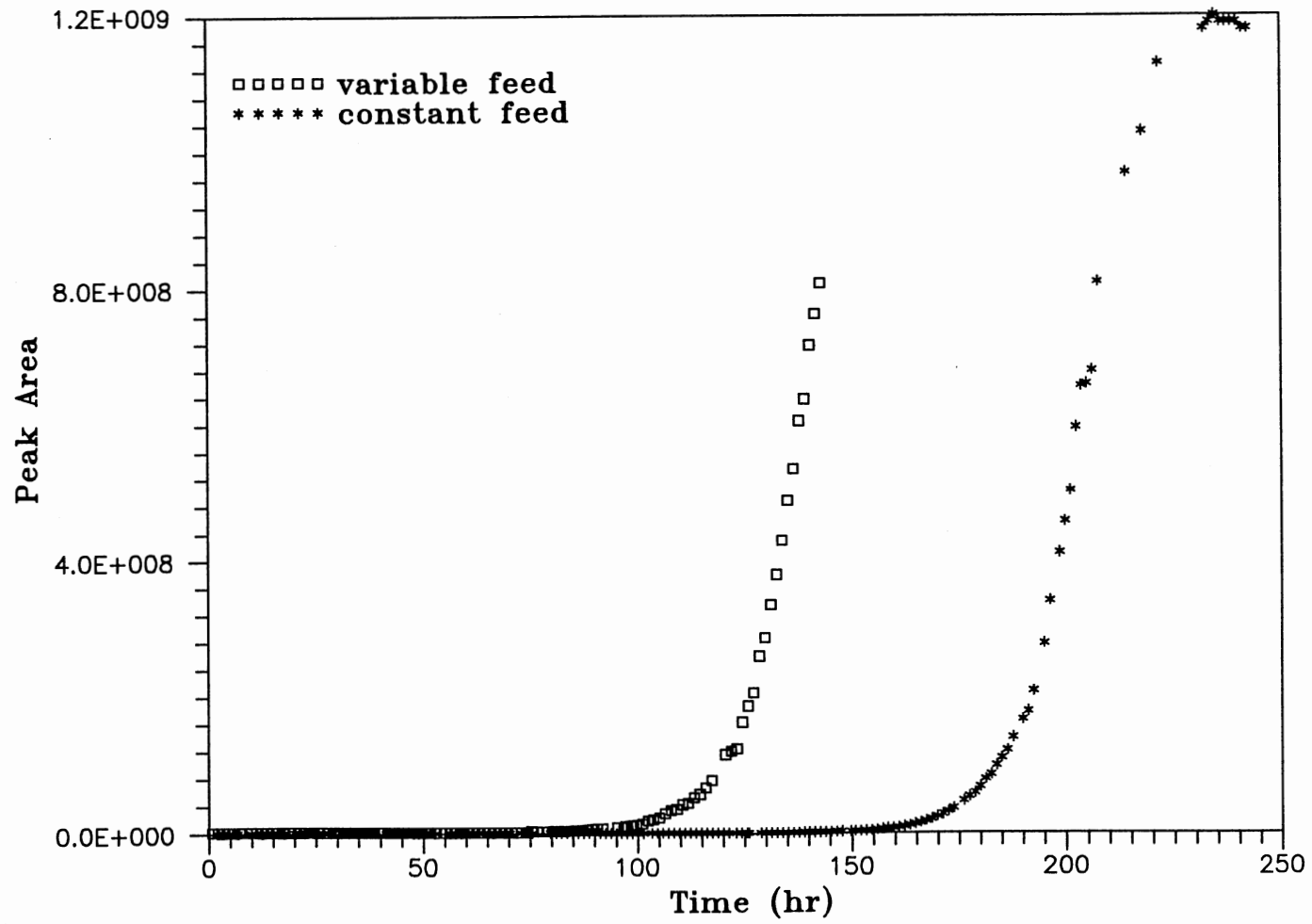


Figure 9. The Effect of Two Peaks in Feed Concentration on Chloride Breakthrough Curve

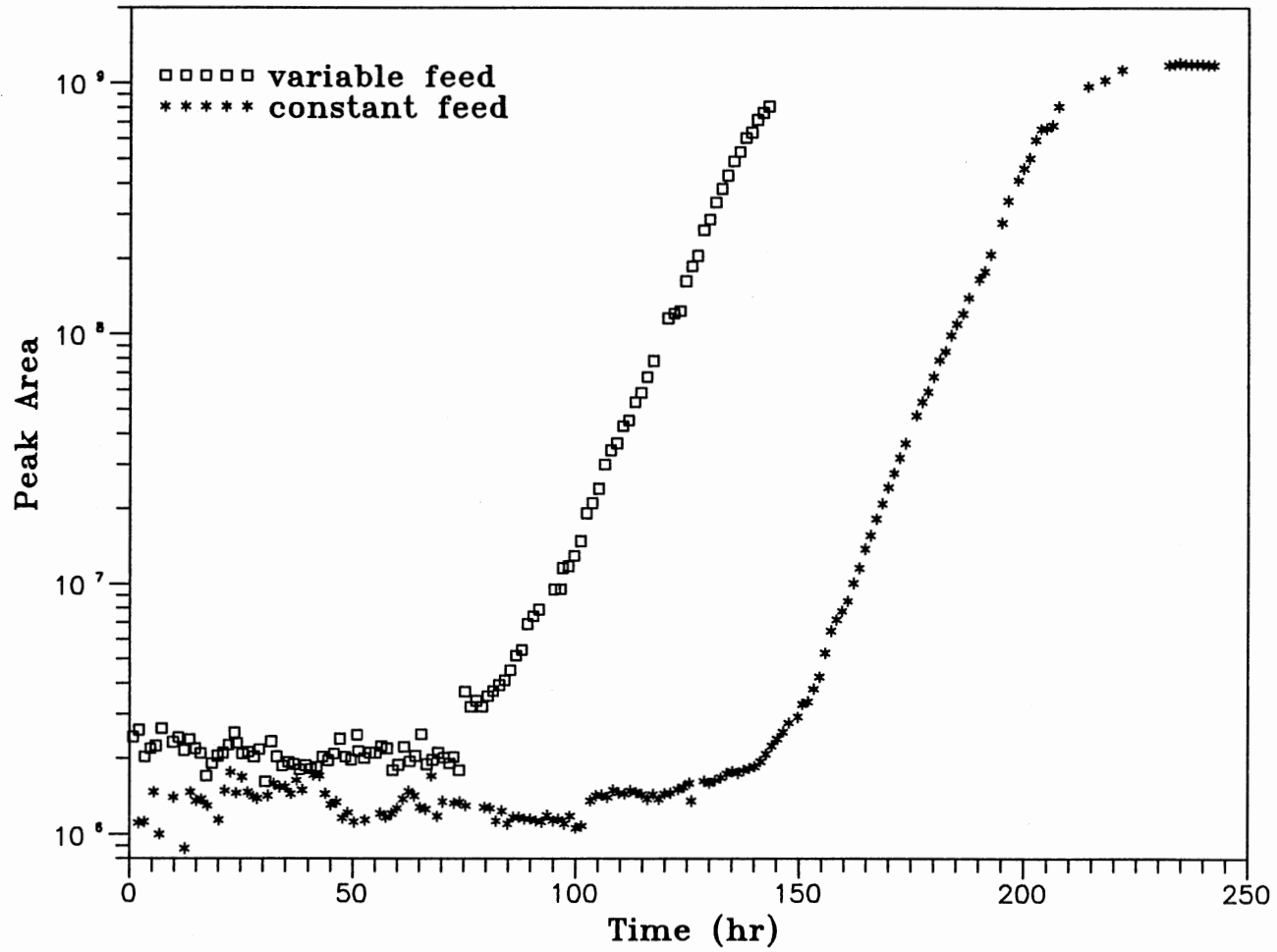


Figure 10. Semilog Plot of Experimental Data for the Effect of Two Peaks in Feed Solution on Chloride Curve

peak area and peak height for such low concentrations are hardly consistent, the peak area could be used to calculate ion concentrations due to a smaller standard deviation than that of the peak height. Also, the detection level of the ion chromatograph is illustrated in this figure. There is no difference in the effluent concentrations of both runs until the concentrations start to increase. This is the same phenomena as in the one-peak experiments.

Figures 11 and 12 show the comparisons of the effluent sodium concentrations of Runs R326 and R503 in a linear and a semilog plot, respectively. For sodium, the data show enough consistency to observe differences in the curves shapes. In Figure 11, two small peaks in the curve for Run R503 are detected where two peaks in feed concentration are introduced. Compared to the results of the one-peak experiments, the peaks in the breakthrough curve can be expected based on less concentrated feed solution than that for the one-peak experiments, with the same concentrations of the peaks in the feed profiles. These peaks result from the insufficient contact time between solution and the cation resin. The breakthrough time of Run R503 appears to be after the first peak is introduced into the column. This fact can be confirmed through Figure 12. It is, therefore, expected that much less sodium is removed until breakthrough when the two peaks are introduced in feed concentration than when feed concentration is constant.

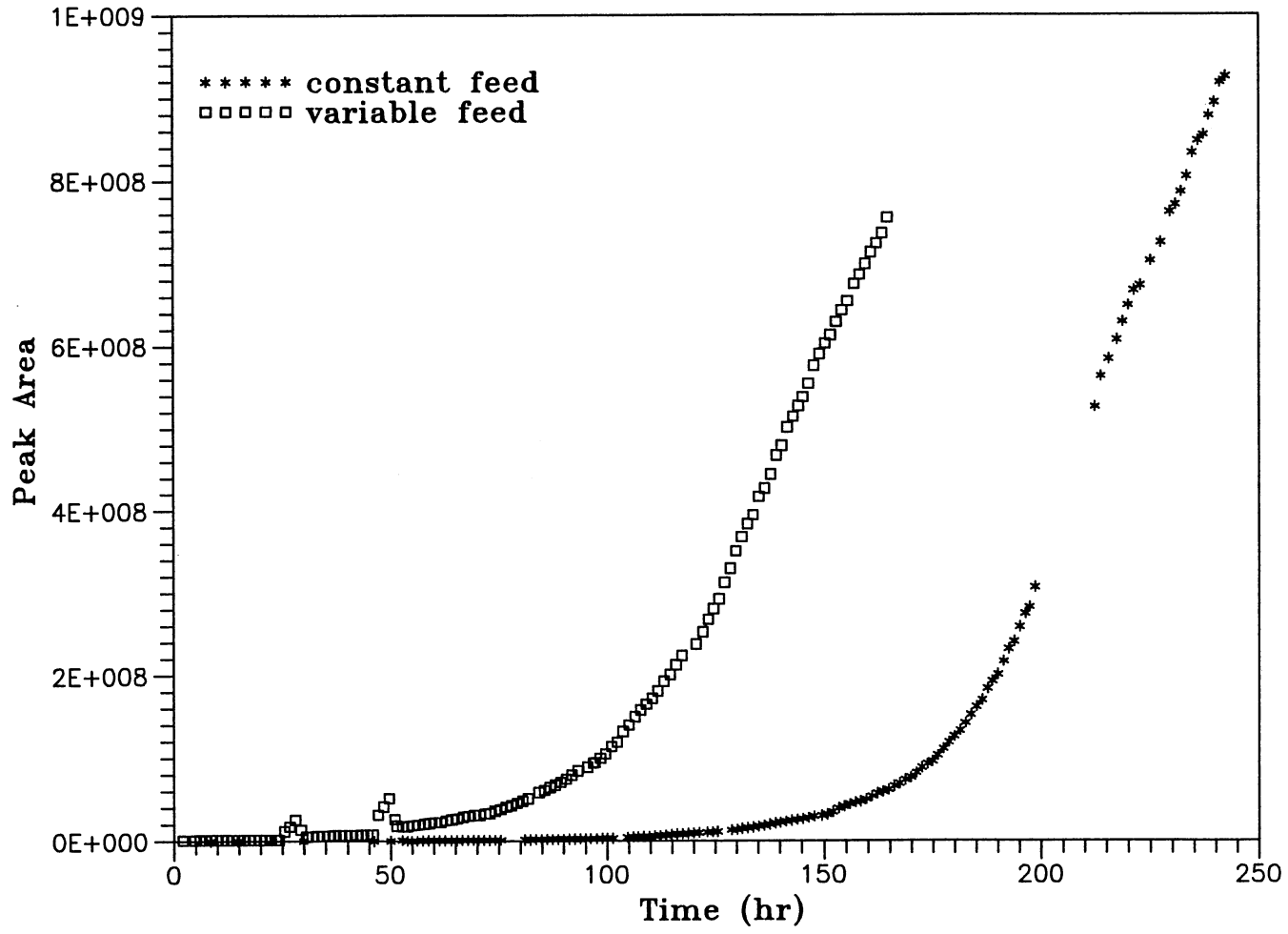


Figure 11. The Effect of Two Peaks in Feed Concentration on Sodium Breakthrough Curve

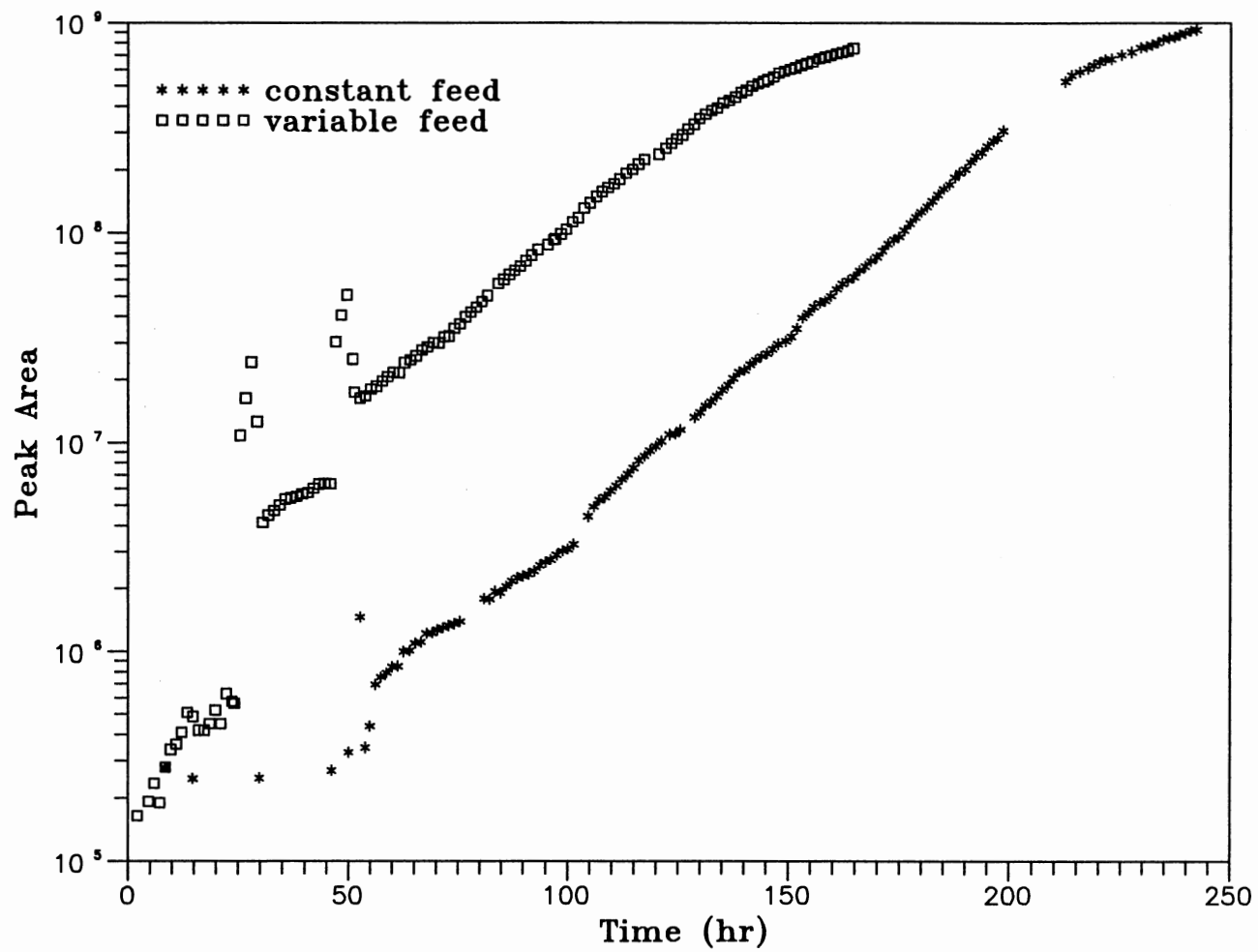


Figure 12. Semilog Plot of Experimental Data for the Effect of Two Peaks in Feed Solution on Sodium Curve

Incompletely-Mixed Bed

Ten experimental runs were performed to characterize general trends of breakthrough curves with incompletely mixed beds. For the experiments, relatively high flow rates were used to increase the superficial velocity closer to industrial conditions of about 2.5 cm/sec. These high flow rates caused high pressure drop throughout the experimental system. The system, which was also used for the variable feed concentration experiments, should thus be modified to reduce the pressure drop. Through several preliminary runs, the experimental column and the feed pump were replaced for an appropriate configuration of the system. The effluent samples were collected and analyzed using the off-line analytical procedure.

Table VIII shows the experimental conditions of the selected runs. All the experiments were conducted under the same conditions except for the ratio of cation resin to anion resin. Bed depth and feed concentration were determined to give a realistic experimental duration. The maximum duration of the runs was about 13 hours. Off-line samples were collected every 30 minutes and analyzed by IC. The results of the analysis were expressed in terms of C/C_0 as a function of run time in hours. C/C_0 is the ratio of the measured effluent concentration to the influent or feed concentration. The feed concentration, C_0 , was held constant for the experiments. On-line pH and resistivity

TABLE VIII
 EXPERIMENTAL CONDITIONS* FOR INCOMPLETELY
 MIXED BED EXPERIMENTS

Run No.	Flow Rate (ml/sec)	Temp. (°C)	Bed Depth (cm)	Cation Resin Fraction	Comments
R1201	6.92	21	4.1	0.505	. Complete mixing
R107	6.90	22	4.2	0.505	. Incomplete mixing . Unmixed top 21.4% . 0.638 FCR** in mixed portion . Compared to R1201
R116	6.93	21	4.1	0.506	. Duplicate of R1201
R213	7.00	21	4.2	0.610	. Complete mixing
R216	6.94	22	4.0	0.600	. Incomplete mixing . Unmixed top 20.0% . 0.732 FCR in mixed portion . Compared to R213

* All experiments were conducted under the same conditions of

- . Feed concentration = 5.0×10^{-5} eq/l
- . Column diameter = 1.849 cm

** FCR = Fraction of Cation Resin

data were collected every 30 minutes. To verify the general reproducibility of the experimental data, the results of Runs R1201 and R116 were compared and shown in Appendix B.

For Run R107, an incompletely mixed bed experiment, approximately 5 ml of each resin was taken and about half of the measured anion resin volume was mixed with the cation resin and placed in the lower portion of the column. The rest of the anion resin was placed in the upper portion of the column. This incompletely mixed portion was 21.4 % of the total bed depth. This would be considered as a realistic experimental condition because anion resin is likely to be rich in the top portion of industrial beds after regeneration procedure due to its lower density than cation resin. The effluent profile of this run was then compared with that of Run R1201, a completely-mixed bed experiment. The comparison of the results of these experiments is given in Figures 13 and 14.

Figures 13 and 14 indicate the effects of incomplete mixing of the resins on chloride and sodium breakthrough curves, respectively. In these figures, it can be seen that different levels of initial leakage of cation and anion appear in the effluent of the exchange process. These leakages might result from the insufficient contact between solution and the resins due to the high flow rate and the short bed depth. Compared to the anion effluent concentration, the cation effluent concentration shows

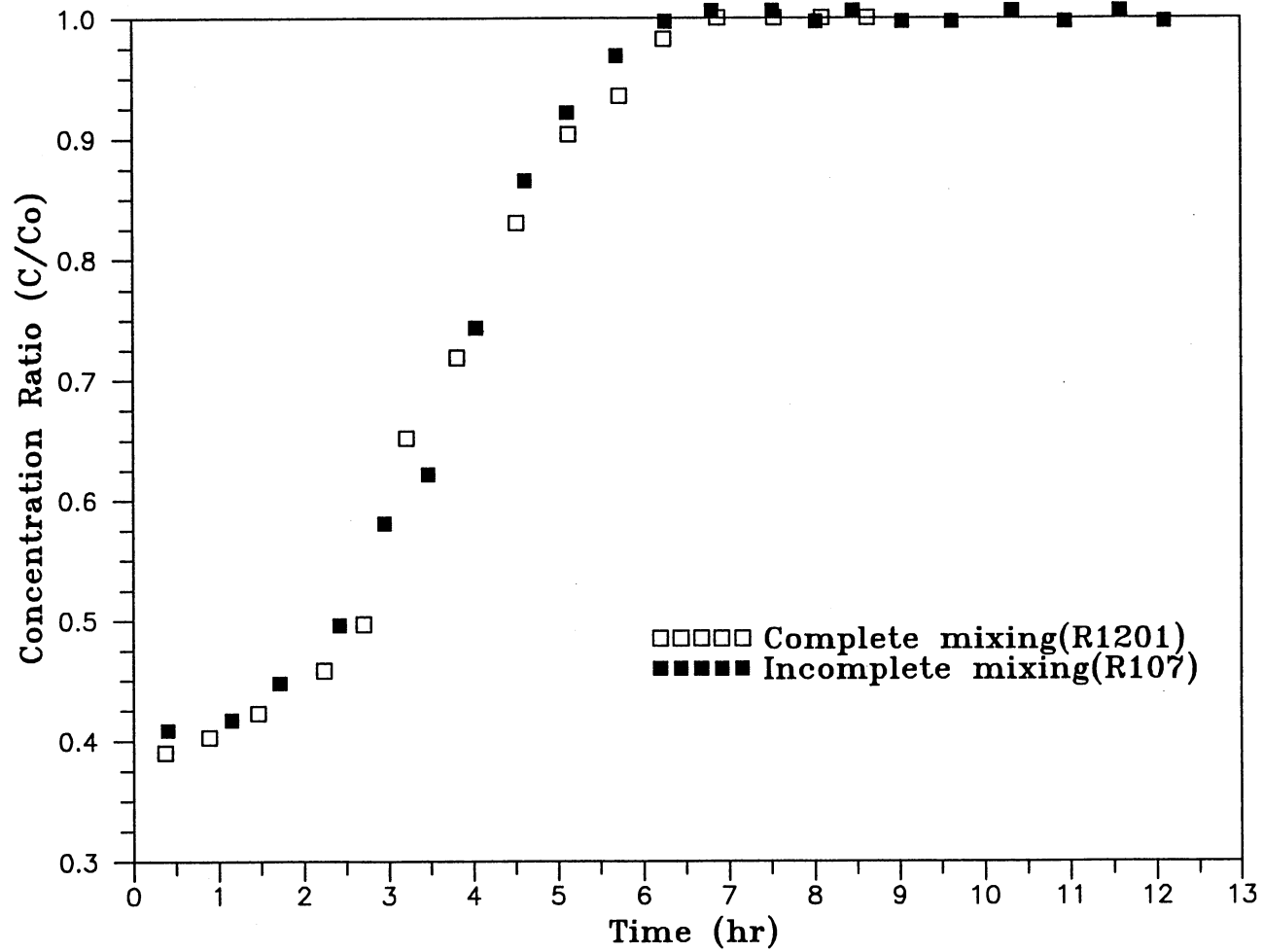


Figure 13. The Effect of Incomplete Mixing of Resins on Chloride Breakthrough Curve with FCR=0.5

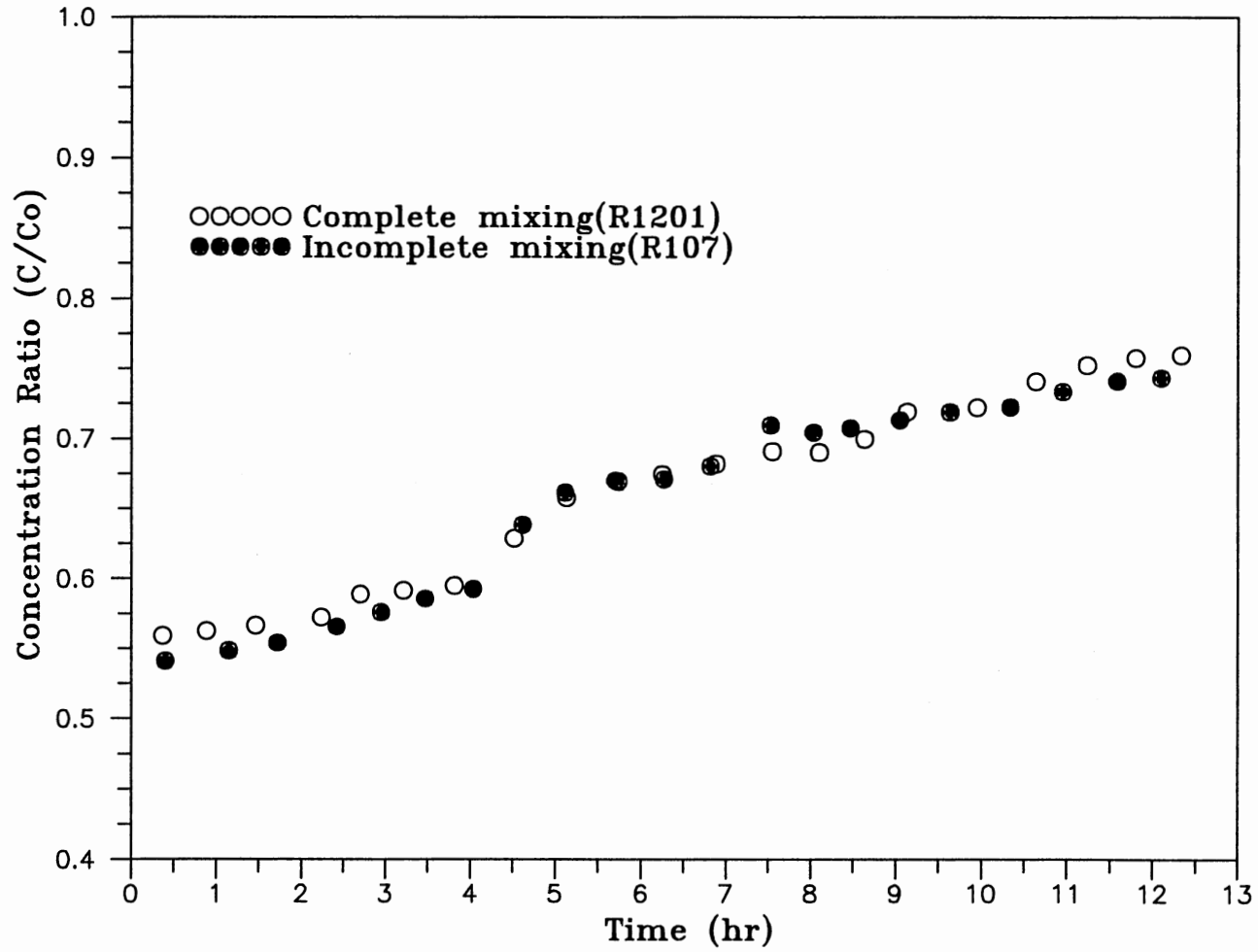


Figure 14. The Effect of Incomplete Mixing of Resins on Sodium Breakthrough Curve with FCR=0.5

higher levels of leakage and more gradual breakthrough curves. These would be due to the lower selectivity coefficient of the cation resin than the anion resin. It has been said that the higher the selectivity coefficient is, the steeper the breakthrough curve is and the more favorable the equilibrium (Helfferich, 1962a, b).

As shown in Figures 13 and 14, the comparison does not give as much difference between complete and incomplete mixing of the resins as expected. An interesting point is, however, that incomplete mixing has an effect on breakthrough curves of both ions only in the first 3 - 4 hours. A close investigation of those figures shows that incomplete mixing of the resins increases the sodium exchange rate slightly and decreases slightly the chloride exchange rate during the first 3 - 4 hours. These experimental results agree well with previous studies (Harries, 1988; Yoon, 1990). Harries (1988) showed that cation exchange was more favorable in an alkaline medium than a neutral or acidic medium because the mass transfer coefficient of sodium is higher in high pH, while the mass transfer coefficient of chloride is higher in low pH. In addition, Yoon (1990) evaluated the effect of the cation resin ratio on the performance of mixed-bed ion exchange and found that cation or anion exchange with a lower oppositely-charged resin ratio was affected adversely. He claimed that a change of the cation resin fraction would change the pH of the aqueous phase within the bed, resulting in the change of

the exchange rates of both ions. The experiment for the present work was performed with only anion resin in the upper portion and more cation resin in the lower portion of the column. Because the experiment utilized downflow, incomplete mixing of the resins will make anion and cation exchange occur in a more alkaline solution. This affects the mass transfer coefficients of sodium and chloride by the way Harries (1988) claimed and, eventually, results in an increased exchange rate of sodium and a decreased exchange rate of chloride. Figures 13 and 14 also indicate that this pH effect on the cation exchange rate disappears after the first 4 - 6 hours. This is because the mixed-bed acts like a cation single bed as active sites on the anion resin are exhausted and, therefore, neutralization reaction is only affected by the addition of new hydroxide ions.

Figure 15 gives pH profiles of Runs R2101 and R107. In this figure, it is known that incomplete mixing causes lower pH in the effluent than complete mixing. A possible interpretation of these pH profiles is that pH increases through the unmixed upper portion and decreases through the cation-resin-rich portion and finally becomes lower than that of complete mixing at the bottom of the bed. As pH decreases in the mixed portion, the cation exchange rate decreases and the anion exchange rate increases along with the bed depth. This might result in compensating effects on each exchange rate and thus slight differences in breakthrough curves of both ions.

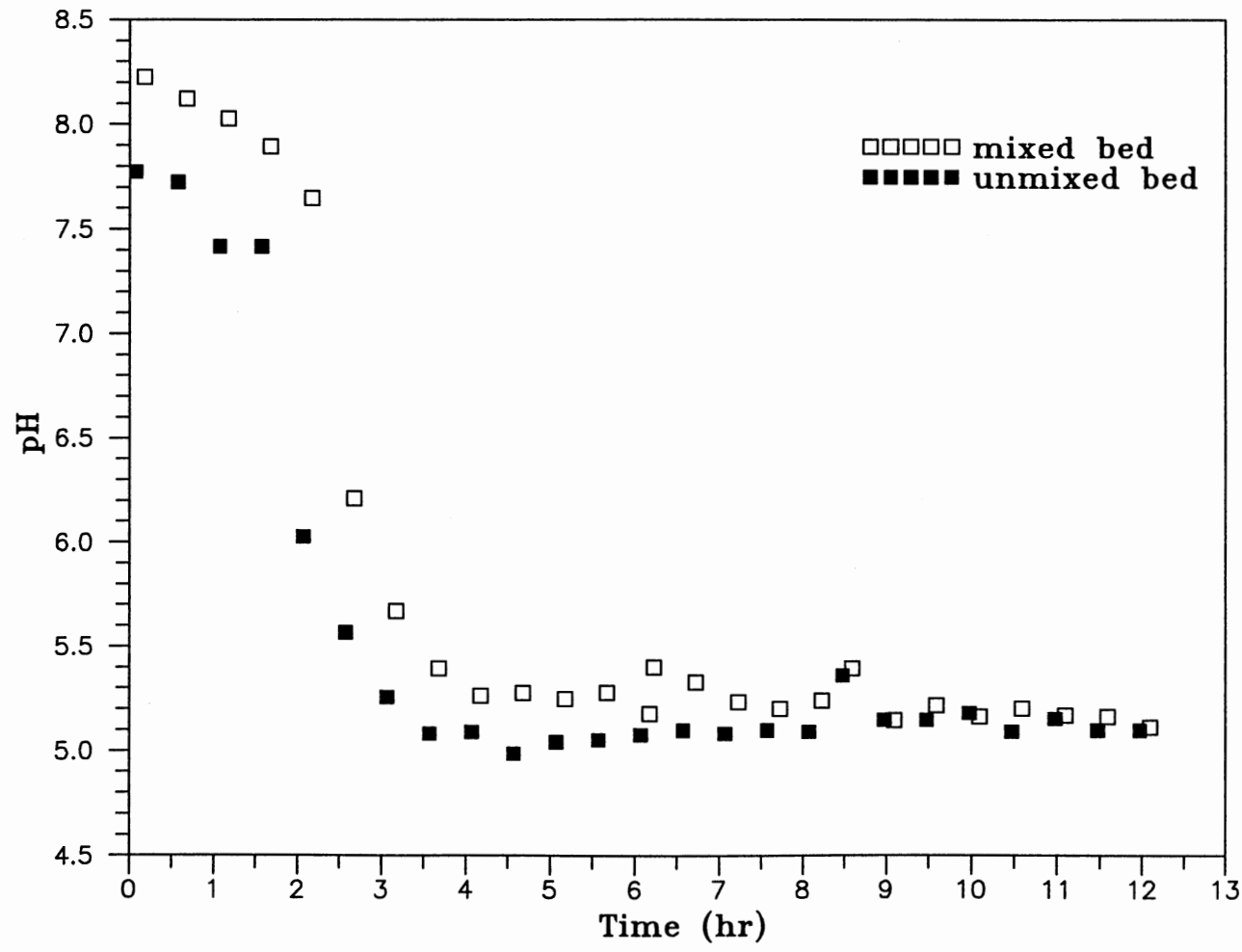


Figure 15. Comparison of pH in Incompletely and Completely Mixed Bed with FCR=0.5

Runs R213 and R216 were done with relatively large amount of cation resin in the column; the cation resin fraction was about 0.6 for both runs. The exact volumes of the cation resin were 6.4 ml for Run R213 and 6.0 ml for Run R216. About 4 ml of the anion resin was used for each run. The results of these experiments are presented in Figures 16 and 17. As expected, the cation effluent concentration shows lower initial leakage and the anion effluent concentration shows higher initial leakage than those of the previous experiments with the same volumes of the cation and anion resins. Harries (1988) found that the effect of pH is more substantial on the anion exchange than on the cation exchange. Thus, the slope change of the anion breakthrough curve is greater than that of the cation breakthrough curve when the resin fraction is changed. The experimental data obtained by Yoon (1990) showed the same trends as Harries (1988). He found that sodium breakthrough curves have small slope changes when the amount of anion resin is increased from 1.0 to 3.0 g with the fixed amount of cation resin 3.0 g, while chloride breakthrough curves show much increased slopes when the amount of cation resin is increased from 1.0 to 3.0 g with 3.0 g anion resin. In the present work, Figures 16 and 17 indicate much sharper slopes of chloride breakthrough curves and slightly decreased slopes of sodium breakthrough curves compared with those in Figures 13 and 14, which show the results of the experiments with about 5.0 ml of each resin. Figures 16 and 17 also show that the

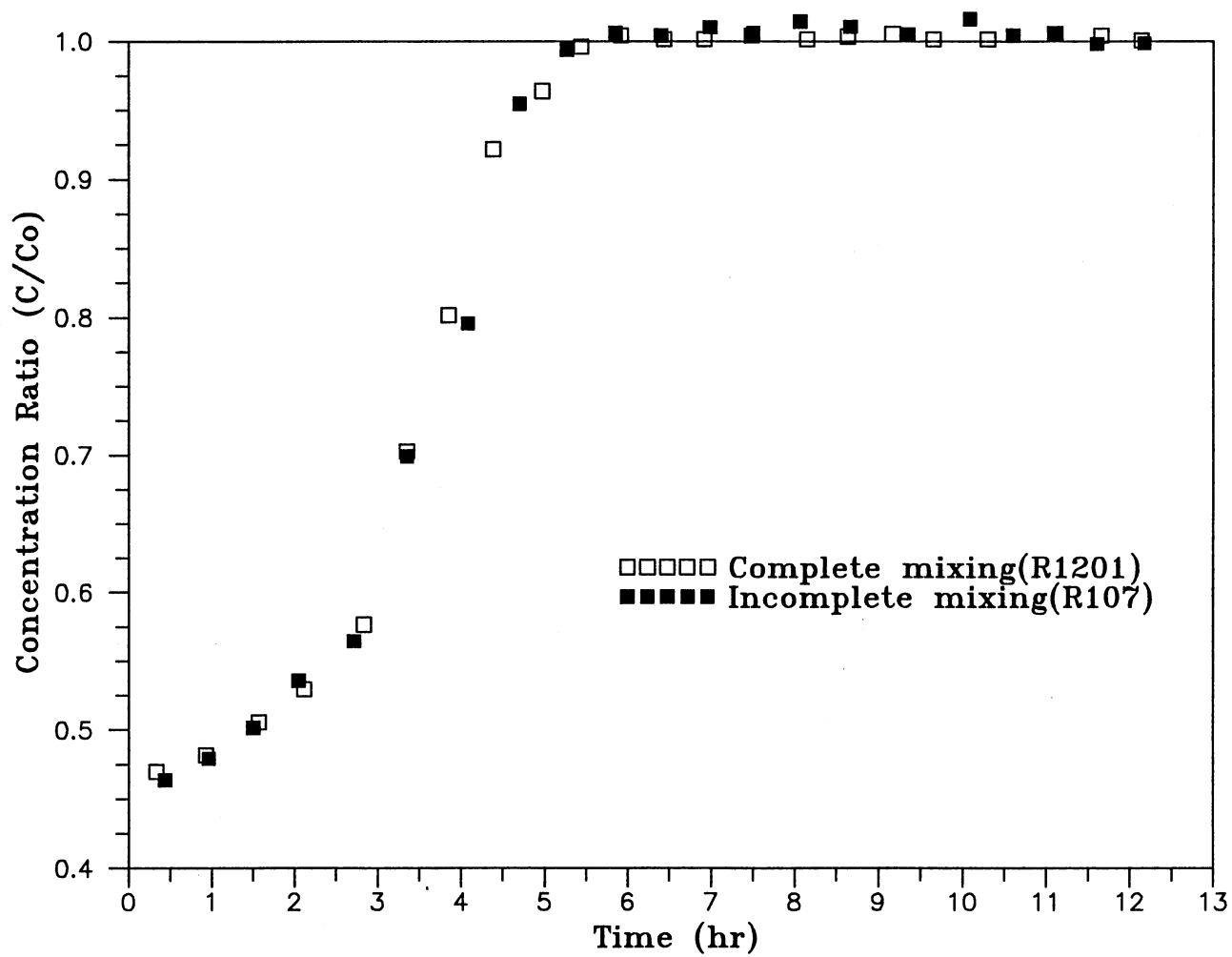


Figure 16. The Effect of Incomplete Mixing of Resins on Chloride Breakthrough Curve with FCR=0.6

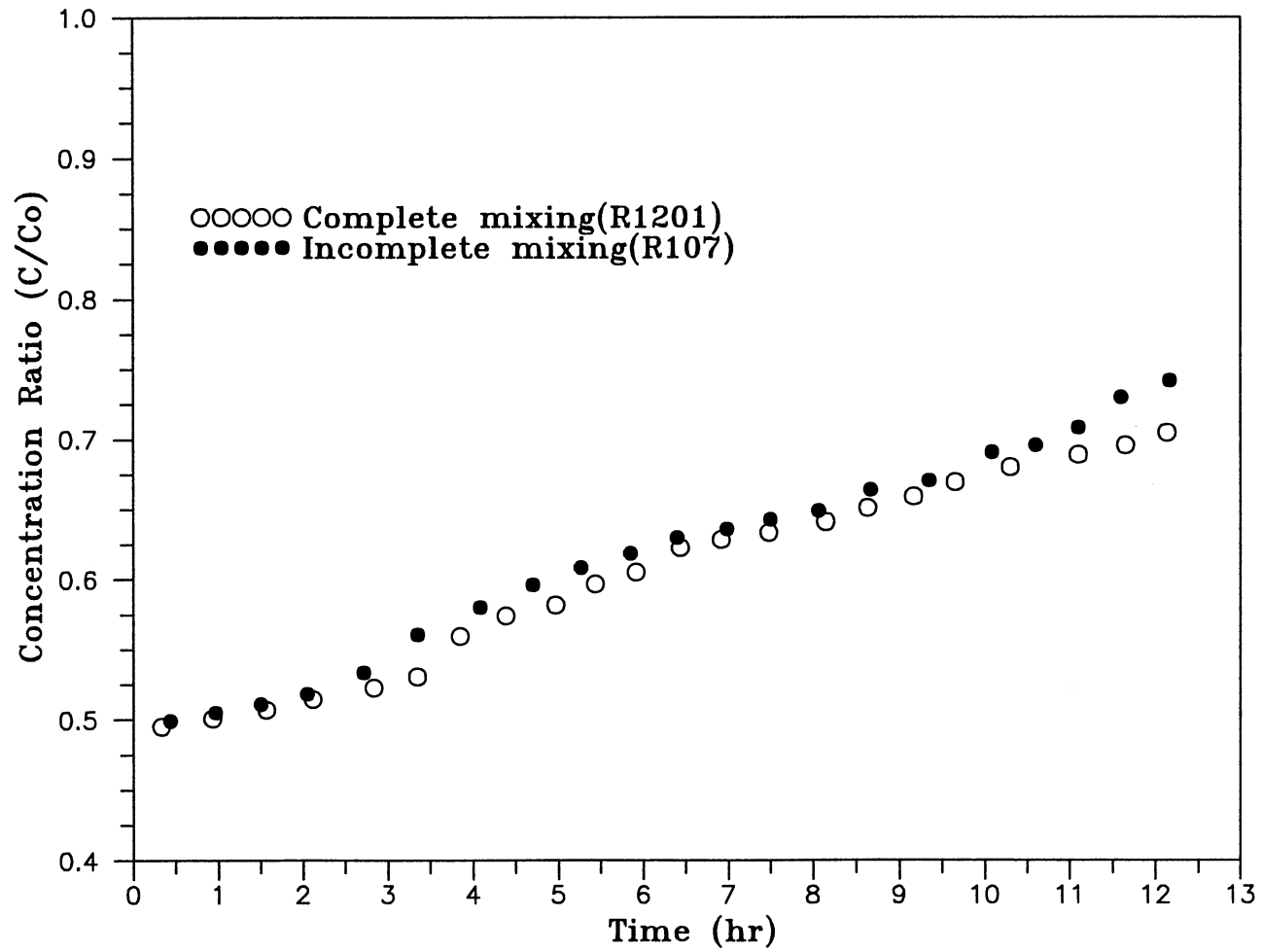


Figure 17. The Effect of Incomplete Mixing of Resins on Sodium Breakthrough Curve with FCR=0.6

change in the anion leakage seems to be slightly greater than that of the cation leakage; The initial leakage in Run R2101 was 0.39 chloride and 0.56 sodium and in Run R213, 0.47 chloride and 0.50 sodium. Therefore, it is worthwhile to mention that the level of anion leakage is slightly more sensitive to the change in resin fraction than that of cation leakage.

In Figures 16 and 17, it is also found that incomplete mixing of the resins has less effect on breakthrough curves of chloride and sodium with more cation resin. Comparison of breakthrough curves in these figures with those in Figures 13 and 14 shows inconsistency in the pattern of the effect of incomplete mixing on breakthrough curves of both ions at the early stage of the exchange processes. Figures 13 and 14 indicate an increased cation exchange rate and a decreased anion exchange rate with incomplete mixing of the resins. For the same case, Figures 16 and 17 shows a slightly increased anion exchange rate and a slightly decreased cation exchange rate, even though the differences in breakthrough curves in each figure are negligible. This inconsistency could result from the small differences in the actual experimental conditions of Runs R213 and R216. But, it can be concluded firmly that pH effect on the cation and anion exchange rates decreases as the cation resin ratio increases. Model predictions on Runs R213 and R216 with exactly the same conditions will be shown and discussed in the next chapter.

Figure 18 shows the comparison of pH profiles obtained from Runs R213 and R216. Compared with Figure 15, the highest value of pH at the beginning of the process decreases with more cation resin. Also, it indicates more acidic effluent with incomplete mixing in the first 2 - 3 run hours. This pH profile would mean a slower cation exchange rate and a faster anion exchange rate at the bottom portion of the bed, which are shown in Figures 16 and 17. If the runs were continued after the present experimental period, pH will be expected to increase by the same rate as the cation exchange rate decreases.

Analysis of Water Samples from PSO

With cooperation of Public Services of Oklahoma (PSO), one of the industrial supporters of the present research, it was possible to collect influent and effluent data around a condensate polisher at the Tulsa Riverside Power Plant. Table IX shows their operating conditions of the condensate polisher.

Recently, they replaced 15 years old resins with new Dow Monosphere resins. Figures 19 and 20 present typical profiles of influent and effluent concentrations of the polisher in the plant before and after the replacement of old resins, respectively. As shown in Figure 19, water sample analysis shows three prominent ions; sodium, chloride, and ammonia. This figure also shows that there were no sudden changes in the influent concentrations of

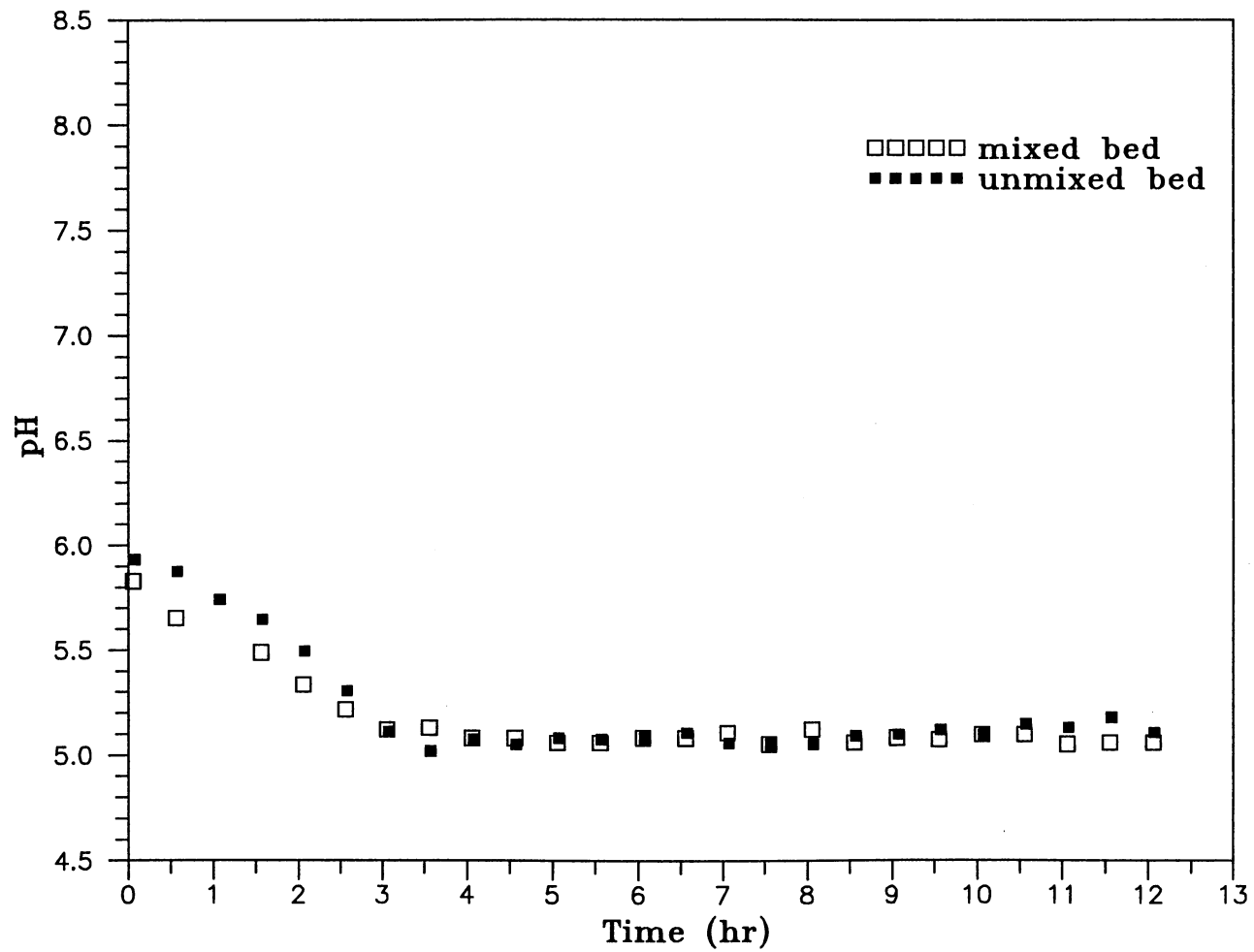


Figure 18. Comparison of pH in Incompletely and Completely Mixed Bed with FCR=0.6

TABLE IX
OPERATING CONDITIONS OF A CONDENSATE POLISHER
AT TULSA RIVERSIDE PLANT

Number of Unit	2
Number of Bed per Unit	4
Bed Depth	
Actual, ft	8.24
Resin Packed, ft	4.12
Bed Diameter, ft	6.0
Flow Rate per Bed, GPM	500 - 1300
pH of Feed Solution	9.1 - 9.3
Old Resin	
Cation	Dowex HGR-W2-H
Anion	Dowex SBR-P-C-OH
New Resin	
Cation	Dowex Monosphere 650C-H
Anion	Dowex Monosphere 550A-OH
Cation-Resin Fraction	0.667
Temperature, °F	105 - 120
Regeneration Period, day	21

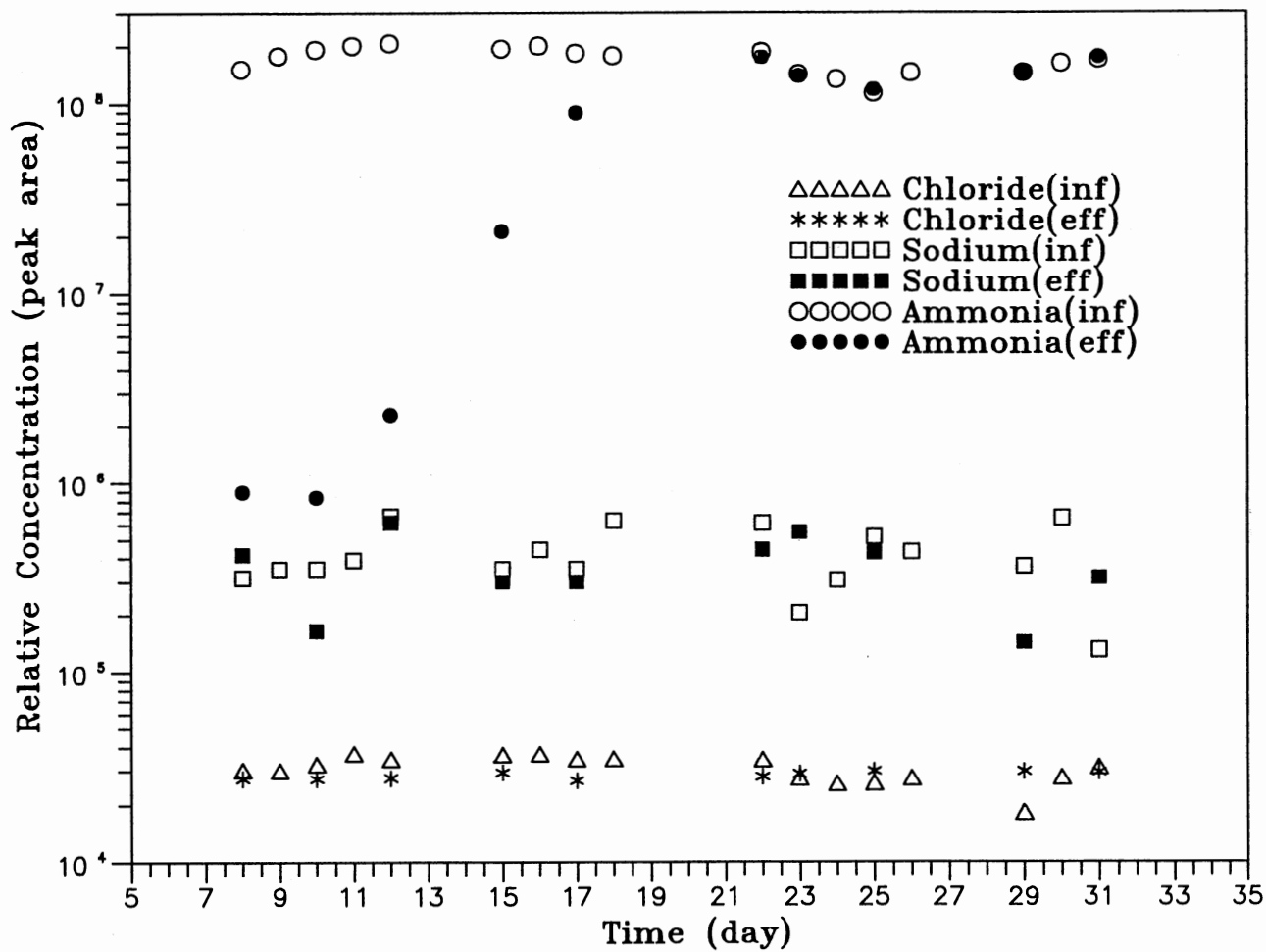


Figure 19. Influent and Effluent Profiles of a Condensate Polisher with Old Resins at the Tulsa Riverside Power Plant

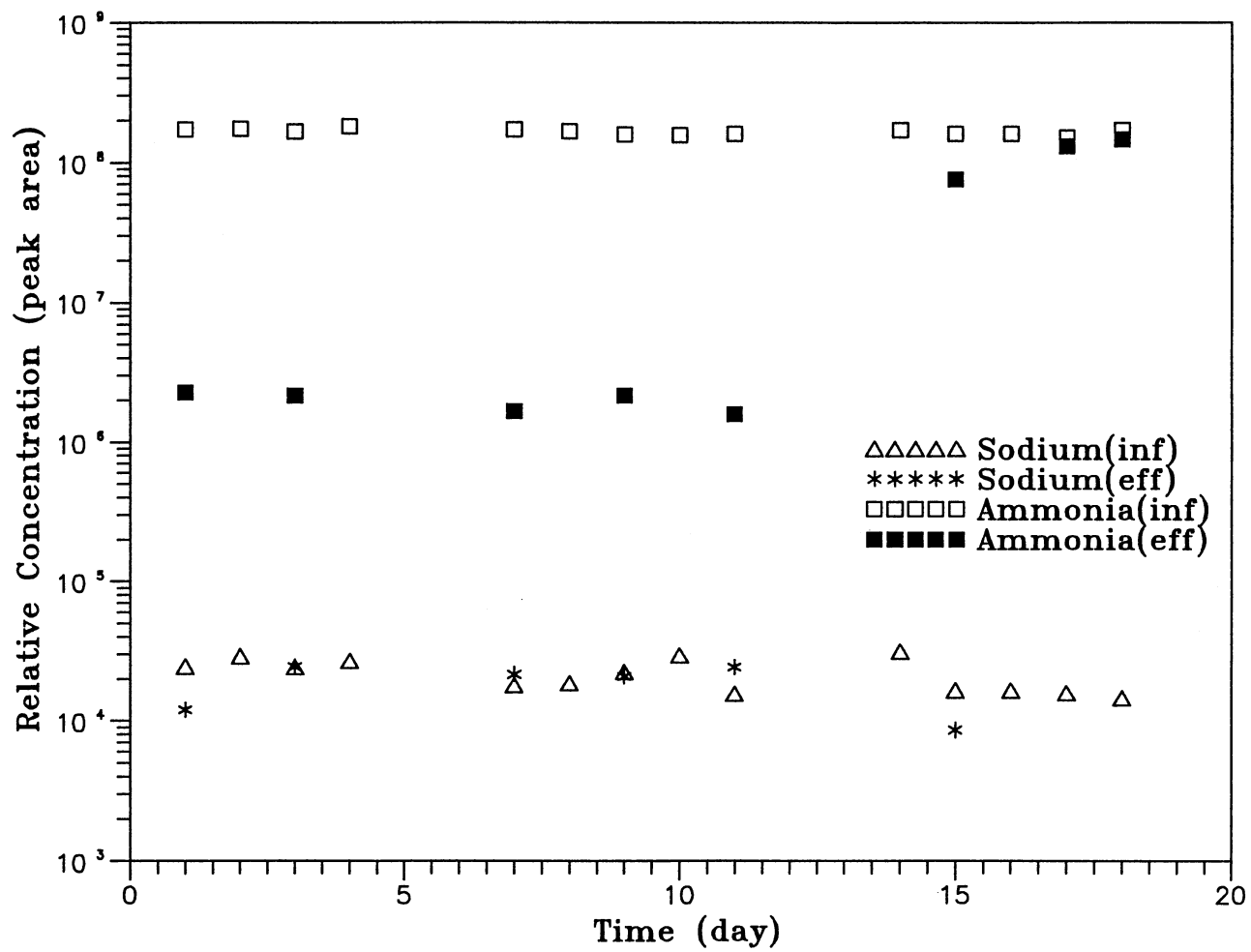


Figure 20. Influent and Effluent Profiles of a Condensate Polisher with New Resins at the Tulsa Riverside Power Plant

chloride and sodium, which might result from major cooling tube leaks. Therefore, it may not be possible to evaluate the mathematical model for the case of step changes in feed concentration using these data. The IC could not produce stable peak areas for chloride and sodium to observe any differences between influent and effluent concentrations. This is because the concentrations of these ions are below or near the lower detection limit of the IC. Based on the ranges of their peak areas, the concentrations of chloride and sodium are calculated to be less than 0.1 ppb and about 1 ppb, respectively.

Figure 19 presents an interesting point that the effluent concentration of ammonia is breaking through at an operation time of about 10 days and will be the same as the influent concentration after about 20 days in use. According to a plant operator, the resins had been regenerated every 3 weeks. For the present work, this regeneration period increased to 5 weeks. The concentration of ammonia in the feed solution is less than 2.0 ppm. Ammonia is used in many existing power plants as a pH control agent to reduce corrosion and erosion problems due to contaminants present within the steam cycle. It increases pH to the range of 9.2 - 9.6 in the absence of copper alloys to reduce the amount of hydrogen ions available for interaction with metal surface (Sawochka, 1988). In recent years, alternatives to ammonia have been considered due to unfavorable selectivity of the typical

cation resins for sodium over ammonia and high ammonia volatility. Morpholine (C_4H_8ONH) is frequently considered as a proper alternative (Sadler and Darvill, 1986).

Figure 20 indicates the performance of the new resins compared with that of the old resins. It shows no chloride leakage and lower concentration of sodium (less than 0.1 ppb). The concentrations of ammonia in the effluent are close to those with the old resins. The ability of the old resins to remove chloride and sodium ions seems to decrease with age. The resin degradation will be discussed using the data in the next chapter. The Steam Generators Owners Group (SGOS) in collaboration with the Electrical Power Research Institute (EPRI) recommends for the feed water concentration to steam generators to be less than 0.2 ppb chloride and sodium (Rios and Maddagiri, 1985). By using the new resins, the plant appears to meet this guideline.

CHAPTER V

DISCUSSION

The most significant contribution of this work is the experimental data for the cases of variable feed concentration and incomplete mixing of resins. The data obtained for the conditions will provide a valuable data base for understanding the performance of mixed-bed ion exchange at ultralow concentration. The data can also be used to simulate a mathematical model, which describes the performance of mixed-bed ion exchange at ultralow concentration, under various conditions observed in full-scale industrial units such as major cooling water leakage and incompletely mixed beds.

The incompletely mixed-bed experiments were conducted under much higher flow rates than the variable feed concentration experiments or the previous experiments performed by Yoon (1990) and King (1991). Thus, flow rates can be studied to determine kinetic effects on bed performance and to provide valuable information for the model performance.

In this chapter, the experimental results of the present work are compared with the predicted values by Haub and Foutch's (1986a) hydrogen-cycle model, which has an ability to predict the performance of mixed-bed ion exchange at

ultralow ionic concentration. The comparisons are presented as plots of C/C_0 , the ratio of effluent concentration to feed concentration, versus run time in hours. The computer programming method for the model was modified to address variable feed concentration and incomplete mixing of resins. The deviations between the experimental and the predicted data will be discussed in terms of property data which affect strongly the model prediction. For incomplete mixing of resins, the effects of nonionic mass-transfer coefficients and resin capacity on the model prediction will be addressed. The results of analysis of water samples from the Tulsa Riverside Power Plant will also be discussed for the effect of resin degradation on the performance of industrial mixed-bed ion exchange.

Accuracy and Reproducibility

The main purpose of this work is the experimental data, so their accuracy and reproducibility should be taken into consideration.

Some preliminary runs with high flow rates for incomplete mixing of resins indicated the possibility of contamination from air. In these runs, numerous air bubbles were introduced into the experimental column with the feed solution. Carbonate or bicarbonate from air will replace chloride ions exchanged with hydroxide ions on anion resin, and thus, affects the shape of breakthrough curve. The experimental system was physically unstable with such high

flow rate as 12.0 ml/s. The air bubbles may result from any mechanical deficiency in the system due to the instability. The flow rate was reduced to have a stable experimental system by using a column of smaller diameter. The experiments for incomplete mixing were conducted with the reduced flow rate of about 7.0 ml/s and produced satisfactory results. To check if the anion resin was contaminated by carbonate or bicarbonate, the fresh and the used resin were analyzed by a Laser Raman Spectroscopy. The comparison of the results of the analysis indicates no difference between the fresh and the used resin, which means that the used resin does not contain any contaminant from air. The results of analysis of the fresh and the used resin are shown in Appendix B.

Errors are basically associated with the quantitative measurements; effluent concentrations by the IC and system parameters by laboratory measurement devices. Measurement of the system parameters such as resin volume, bed depth, and flow rate appeared to cause the biggest error. All errors are discussed and calculated in Appendix B. The accumulated error of the data are found to be ± 6.5 %.

Duplicated experiments were conducted to verify the general reproducibility of the experiments. The experimental conditions of the duplicated runs were shown in Tables VII and VIII. The reproducibility of the variable feed concentration experiments and the incompletely mixed-bed experiments is presented in Appendix B. The

reproducibility appears to be satisfactory with the maximum difference of less than 2.0 %.

Mathematical Model

The model of Haub and Foutch (1986a, b) was developed with the assumptions; uniform bulk liquid and surface compositions for a given exchange particle, equilibrium at the particle-film interface and instantaneous neutralization reactions compared to the rate exchange, constant activity coefficients, pseudo steady state mass transfer across the film layer, isothermal system, and neglected dispersion in the bed (Haub and Foutch, 1986a). The validity of these assumptions, with the modeling process, are described in details elsewhere (Haub, 1984). In this section, the mathematical model will be reviewed briefly. The ionic flux equations were obtained by using Nernst-Planck equation for the flux of each ion and given as;

$$J_i = - D_i \left[\frac{\partial C_i}{\partial r} + \frac{C_i F}{RT} \frac{\partial \phi}{\partial r} \right] \quad (1)$$

These ionic flux equations were used to obtain the effective liquid-phase diffusivity (D_e). The interface concentrations were used to determine appropriate flux expressions and described in terms of bulk-phase concentrations. The rate of exchange of resin-phase compositions was obtained by using the static film model as follows;

$$\frac{\partial y_i}{\partial t} = k_i \left\{ \frac{D_e}{D_i} \right\}^{2/3} a_s \frac{C_i^o}{Q_i} \left[1 - \frac{C_i^*}{C_i^o} \right] \quad (2)$$

Column material balances, with the rate expressions and effective diffusivities, were used to predict the outlet concentrations;

$$\frac{\mu_s}{\epsilon} \frac{\partial X_i'}{\partial Z} + \frac{\partial X_i'}{\partial t} + \frac{f_c (1-\epsilon) Q_i}{C_i^f \epsilon} \frac{\partial y_i}{\partial t} = 0 \quad (3)$$

Dimensionless distance and time coordinates used to simplify the column material balances were defined as;

Dimensionless distance;

$$\xi_c = \frac{k_c (1 - \epsilon)}{\mu_s} \frac{Z}{d_{pc}} \quad (4)$$

Dimensionless time;

$$\tau_c = \frac{k_c C_c^f}{d_{pc} Q_c} \left[t - \frac{Z \epsilon}{\mu_s} \right] \quad (5)$$

The cation resin was selected as a basis for the dimensionless variables. Thus, common increments of distance and time will be used in the integration of the material balance for the two resins. The final rate of exchange and column material balance equations for both

cation and anion in terms of the dimensionless distance and time are as follows;

Cation;

$$\frac{\partial X'_a}{\partial \xi_c} + (1 - f_c) \frac{Q_a}{Q_c} \frac{\partial y_a}{\partial \tau_c} = 0 \quad (6)$$

$$\frac{\partial y_c}{\partial \tau_c} = 6 R_c \left[\frac{C_c^o}{C_c^f} - \frac{C_c^*}{C_c^f} \right] \quad (7)$$

Anion;

$$\frac{\partial X'_c}{\partial \xi_c} + f_c \frac{\partial y_c}{\partial \tau_c} = 0 \quad (8)$$

$$\frac{\partial y_a}{\partial \tau_c} = 6 \left[\frac{k_a}{k_c} \frac{d_{pc}}{d_{pa}} \frac{Q_c}{Q_a} \right] R_a \left[\frac{C_a^o}{C_c^f} - \frac{C_a^*}{C_c^f} \right] \quad (9)$$

where R_i is the ratio of electrolyte to nonelectrolyte mass transfer coefficients of species i and given as $(De/Di)^{2/3}$. As shown in the above expressions, feed concentration and cation resin fraction affect the outlet concentration directly. In the present work, feed concentration and cation resin fraction are variable and given as functions of time and bed depth, respectively. The computer program modified to address these conditions reads new feed concentration in every step of the dimensionless time loop and new cation resin fraction in every step of the

dimensionless distance loop, when it solves the rate expressions and column material balance equations simultaneously.

Computer Models

The following is a brief description of the computer program to solve the mixed-bed ion exchange model operating at ultralow feed concentrations. It will be followed by parametric studies for the effects of program controlling variables on the predicted breakthrough curves of sodium and chloride. The modification of the programming method for the model to accept the variable feed concentration and incomplete mixing of resins will be discussed. The program has the capability to predict effluent breakthrough curves for the ions of interest, or concentration profiles for all ionic species at a given bed depth. It was first written in FORTRAN by Haub (1984), who developed the mathematical model (Haub and Foutch, 1986a, b), and has been modified to improve its accuracy. The computer model can run on the IBM or VAX computer system and, with minor changes, on a personal computer.

Main and Subroutines

The program has a main routine and five subroutines to solve simultaneously anion and cation column balances and rate expressions. The main routine reads and prints all the input data used in the program, controls the time loop of

simulation, prints breakthrough curves or effluent concentration profiles, and coordinates the function of the subroutines. The input data are mainly classified into: the resin properties and constants, the ion-exchange bed and system variables, ionic constants, and the program control data. Table X shows a complete listing of the input data used for the computer model operation. Selectivity, ionic diffusivity, and nonionic mass transfer coefficients of each ion in solution are functions of temperature and calculated in the main routine based on the operating conditions, if necessary.

The nonionic mass transfer coefficients for ion-exchange columns are obtained using the correlations of Carberry (1960) for Reynolds numbers above 20 and Kataoka et al. (1972) for Reynolds numbers below 20. The mass transfer coefficients account for the bed geometry and fluid flow effects on the ion-exchange rates. The ionic diffusion coefficients depend on the ionic concentration in solution and the operating temperature, but constant coefficients from the literature (Robinson and Stokes, 1959) were first used (Haub and Foutch, 1986b). Using limiting ionic conductances, the coefficients are expressed as functions of temperature (Divekar et al., 1988). In addition to the ionic diffusion coefficients, selectivity coefficients, water dissociation constant, and solution viscosity are also given as functions of temperature.

TABLE X
MODEL INPUT PARAMETERS

Resin Property	Cation resin diameter (cm) Anion resin diameter (cm) Bed void fraction Selectivity coefficient for chloride-hydroxide exchange* Selectivity coefficient for sodium-hydrogen exchange*
Resin Constant	Cation resin capacity (meq/ml) Anion resin capacity (meq/ml) Initial loading of cation in the cation resin Initial loading of anion in the anion resin Cation resin volume fraction
Column Parameter	Feed concentration (meq/ml) Volumetric flow rate (ml/sec) Column diameter (cm) Packed resin Height (cm)
Solution Property	Solution viscosity (cp) Solution density (g/ml) Temperature (°C) pH
Ionic Constant*	Diffusivity of hydrogen(cm^2/sec) Diffusivity of hydroxide(cm^2/sec) Diffusivity of chloride(cm^2/sec) Diffusivity of sodium(cm^2/sec)
Program Control Data	Dimensionless time increment Dimensionless distance increment Time limit for column operation (min) Effluent sodium concentration limit Number of increments used for the Runge-Kutta Routine Number of half increments used in Simpson Method

* These parameters are functions of temperature and must be calculated in the program for operating temperatures other than 25 °C

Subroutines BULK and FILM are the two most important subprograms and evaluate the rate expressions of anions and cations at each calculation point based on the ion concentrations in the bulk phase. These subroutines correspond to the bulk-phase neutralization and the film reaction model, respectively. In the bulk-phase neutralization model, the neutralization reaction between hydrogen and hydroxide ions takes place in the bulk liquid phase, and the effective film thickness surrounding the resin is assumed to be constant due to equal cation and anion concentration driving forces. In the film reaction model, the reaction occurs in the liquid film surrounding the resins. This model take into account the relative position of the reaction front to the total film thickness and, as a result, has much more complicated calculation procedures for the ionic concentrations at the interface than the bulk- neutralization model. The other three subroutines are called by subroutine Film and used to calculate the interface concentrations.

Numerical Techniques

The flux expressions for the bulk-phase neutralization model are independent of the number of coions in the film. The inclusion of the reaction only affects the bulk-phase boundary conditions and not the diffusion equations. Thus, the solution scheme of the flux equations is relatively simple. However, the solution scheme of the flux

expressions for the film-reaction model is more complicated. The diffusion of one coion is coupled to the remaining coions in the film and thus, the flux equations of all ionic species must be considered. The Quartic Runge-Kutta method and Simpson's method are used to solve numerically the flux equations for the film-reaction model. An interpolation routine combined with Simpson's method is used to relate values for the hydrogen and chloride ion concentrations.

The column material-balance equations for the cation and anion resins are transformed by defining dimensionless time and distance. The method of characteristics is used to solve the set of equations. A grid structure is defined along curves of constant dimensionless time and distance. Evaluation along these lines reduces the system of partial differential equations to a system of ordinary differential equations. The improved Euler method is used to determine the concentration profiles down the column at a constant dimensionless time by integrating the material balances with respect to dimensionless distance. This results in a horizontal sweep across the calculational matrix. The equations are then integrated with respect to dimensionless time using the backward finite difference method and another horizontal sweep is made. With this approach, the calculations are continued until the ion concentrations in the column effluent reach a predetermined fraction of the concentrations in the feed solution.

Alternative programs capable of handling specific conditions have been developed. These conditions include; 1) the addition of ammonia or an alternative amine, such as morpholine, used as a pH controller to inhibit corrosion throughout the steam cycle, 2) the addition of other chemical additives, and 3) the additions of organic acid anions (Zecchini, 1990). The computer program to solve Haub and Foutch's hydrogen model has been developed to solve Zecchini's multi-component model. For the solution of the material balance equations, the Adams-Bashforth-Moulton implicit method is employed in dimensionless distance and the explicit Adams-Bashforth method in dimensionless time. These numerical techniques are superior for accuracy and stability to those adopted in the program to solve the hydrogen model (Zecchini, 1990).

Parametric Studies

Hu (1986) conducted a series of parametric studies to determine the numerical limits of five variables at a fixed temperature in the compute program. The five variables are: the initial equivalent fractions of chloride and sodium ions in anion and cation resins, respectively; the cation resin volume fraction; the feed solution concentration; and the volumetric flow rate. Moon (1988) tested the numerical limits of the same variables for varying temperatures. The goals of their studies were to make the data input procedure more convenient for the user and to inform the user about

the numerical restrictions imposed upon the system variables to eliminate unnecessary computer runs and save on computer money.

For the same purposes, the effects of the program controlling parameters, dimensionless distance (XI) and time (TAU) increment, were studied in this work. The column material-balances for the cation and anion resins are integrated simultaneously along characteristic lines of constant TAU and XI in the program. The results of the integrations were found to depend on these increments (Haub, 1984). For the evaluation of the effect of XI on the performance of the computer model, the program was run with a constant TAU of 0.01 and seven different XI. Figures 21 and 22 present the effect of XI on chloride and sodium breakthrough curves, respectively. Other input data for the program are shown in these figures. The error in predicted concentration profiles of both ions gradually decreases as XI decreases from 0.1 to 0.001. This can be explained by quickly reduced solution concentration with progression through the exchange column. XI smaller than 0.005 shows negligible error and is considered as the effective numerical limit for the program. However, this limit can be changed by changes in any one of the column parameters. XI of 0.005 corresponds to approximately 0.083 cm for the given conditions. This means the loop to distance increment repeats $4.8/0.083 = 58$ times for each loop to time increment. For the present work, XI of 0.005 is used.

Figures 21 and 22 show an interesting thing about the shape of the sodium curve. The slope of the sodium concentration profile changes after the first 6-7 hours. The effluent concentration of chloride reaches the equilibrium around the same time (Figure 21). Therefore, the change of the slope is likely to be due to mixed-bed behavior such as shifting to a cation single bed as active sites on the anion resin are exhausted. This phenomena was also detected in the experimental data for incomplete mixing of resins (Figures 14 and 17).

For the investigation of the effect of TAU, a constant XI of 0.005 and nine different TAU were used for the execution of the program. The results are shown in Figures 23 and 24. Similar with those for XI, the error in the concentration profiles becomes smaller as TAU decreases to 0.0025. TAU smaller than 0.0025 results in unexpected curve shapes. These unstable curves for both chloride and sodium may result from the accumulated error stemmed from differentiating and integrating the flux equations and column material balances. The effective numerical limits of TAU are thus considered to be 0.01-0.0025 for the given conditions. Any changes in feed concentration or column parameters will alter the numerical limits of TAU. Closer inspection of the figures shows that the effluent profiles of both ions are less sensitive to variations in TAU than in XI. This fact confirms that the solution concentrations at a given distance from the column inlet are relatively stable

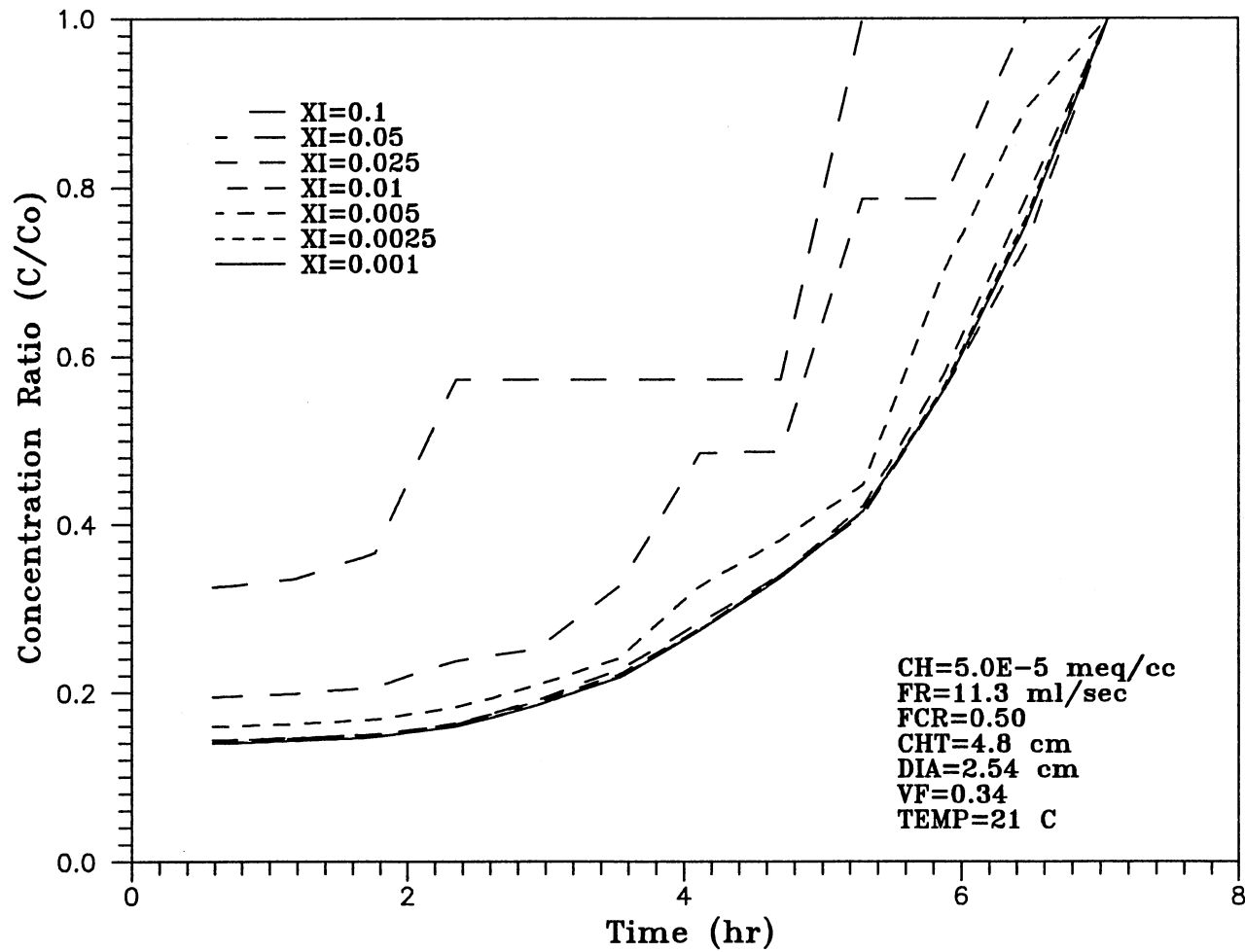


Figure 21. The Effect of Dimensionless Distance Increment on Chloride Breakthrough Curve (TAU=0.01)

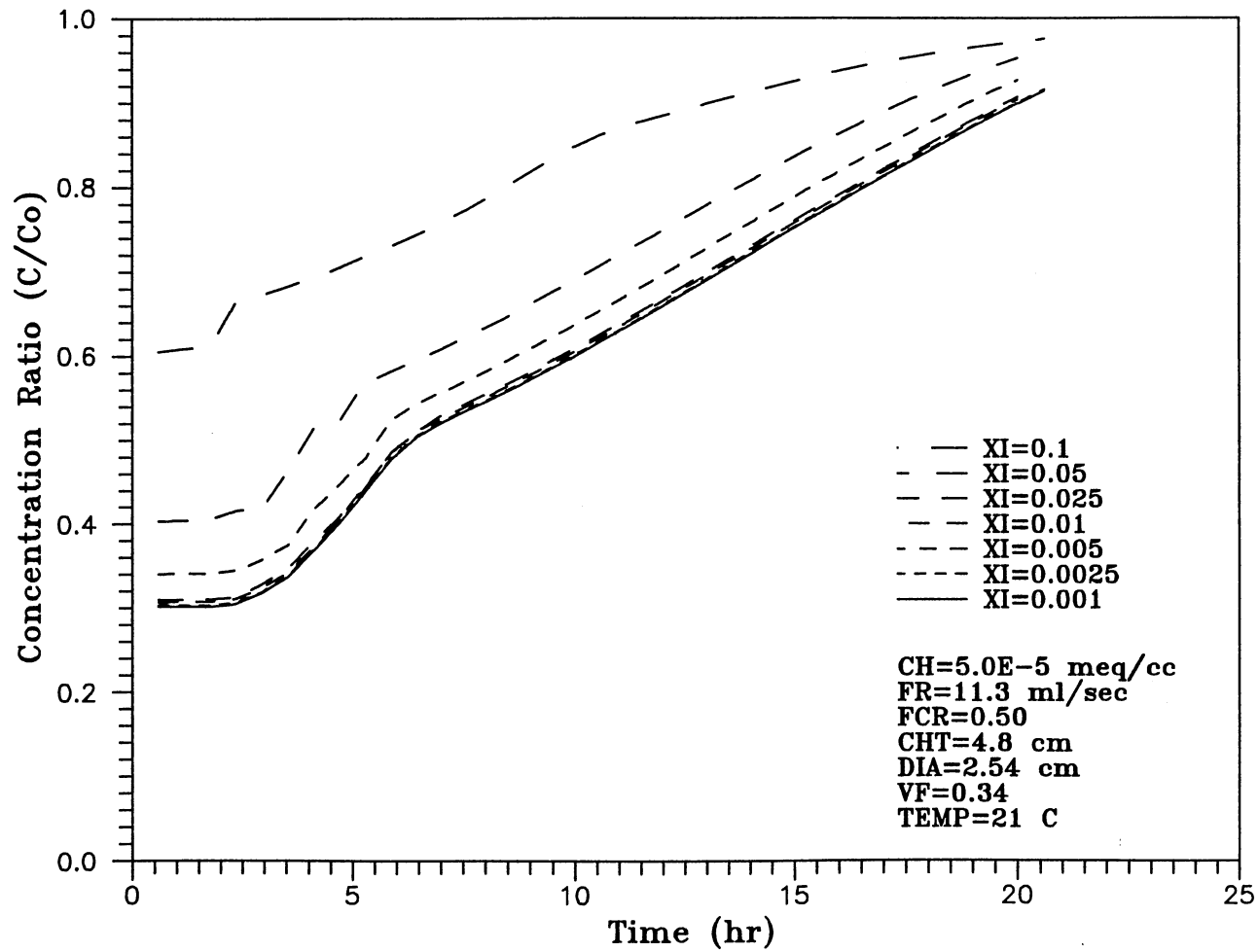


Figure 22. The Effect of Dimensionless Distance Increment on Sodium Breakthrough Curve (TAU=0.01)

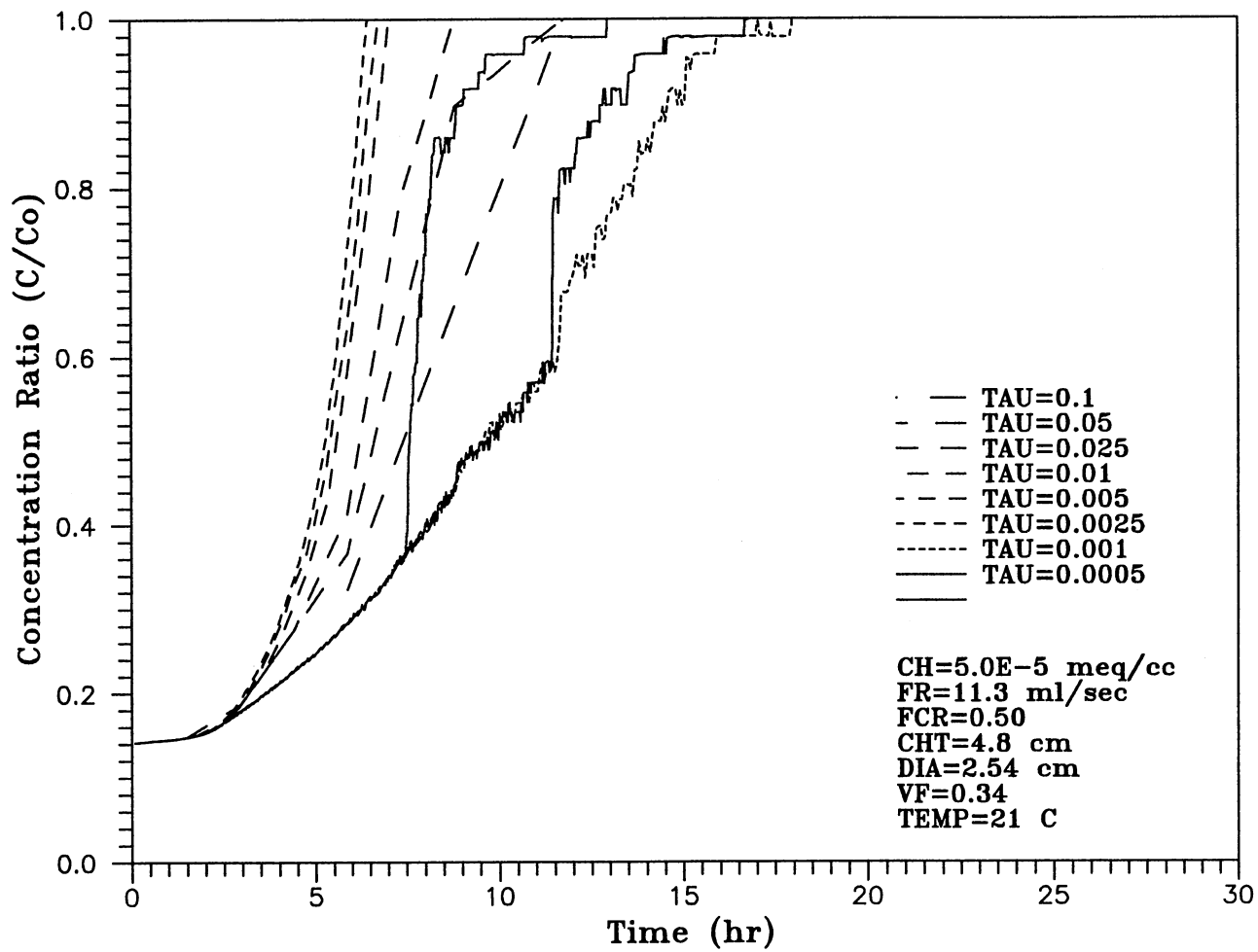


Figure 23. The Effect of Dimensionless Time Increment on Chloride Breakthrough Curve (XI=0.005)

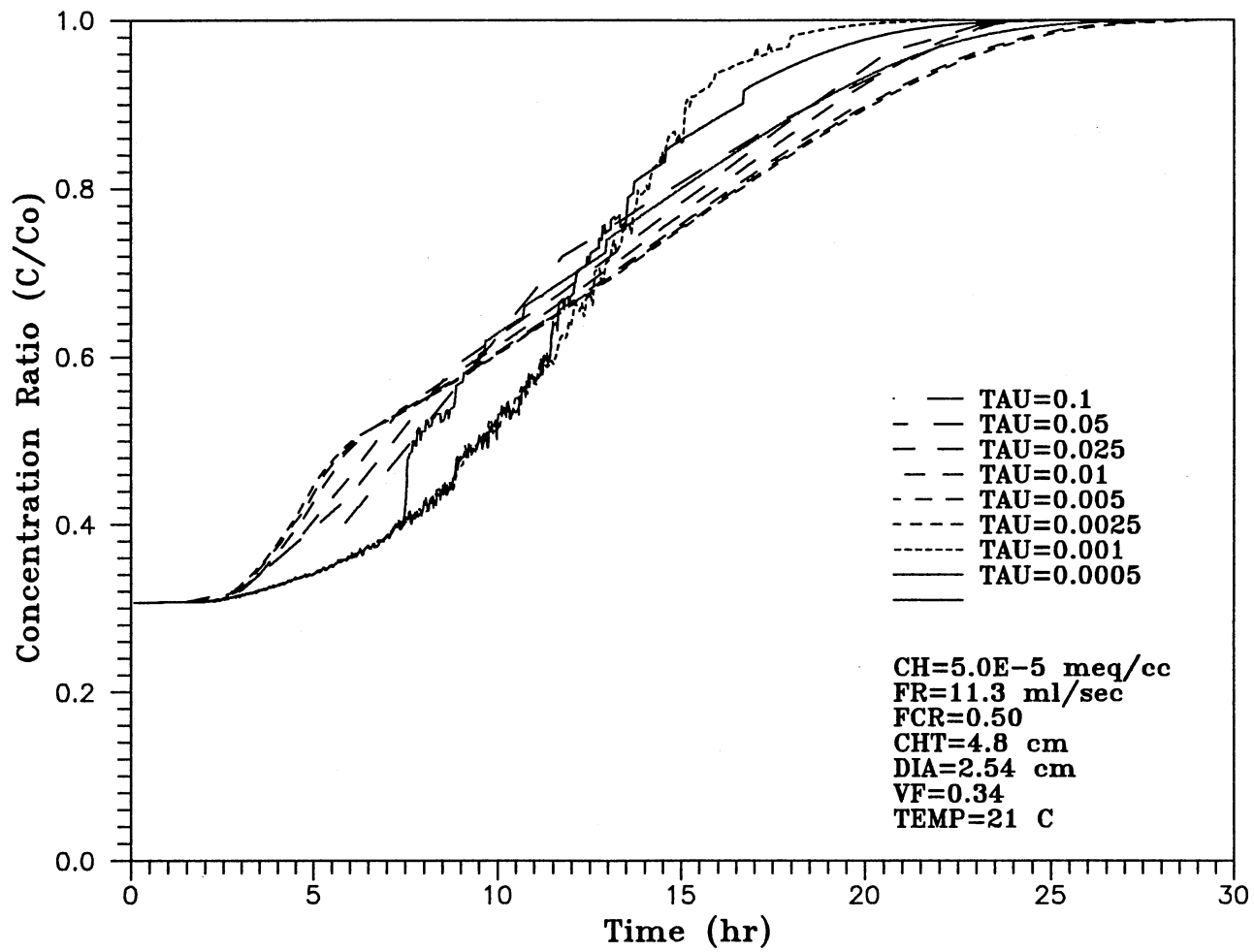


Figure 24. The Effect of Dimensionless Time Increment on Sodium Breakthrough Curve (XI=0.005)

with time as the active ion exchange zone moves slowly down the column.

Modification of Programming Method

The computer program developed by Haub (1984) could address only constant feed concentrations and homogeneously mixed beds. The programming method was modified to allow the models to accept variable feed concentrations and variable cation-resin fraction along the bed. The input data file for the program contains the feed concentration history with other property data. In the program, TAU is given as;

$$\text{TAU} = \frac{(\text{KLC})(\text{CF})}{(\text{QC})(\text{PDC})(60)} (\text{DELT}) \quad (10)$$

KLC is the nonionic mass-transfer coefficient of cation, CF is feed concentration, QC is cation resin capacity, PDC is cation resin-particle diameter, and DELT is real time increment in minutes. For a given operating condition, KLC, QC, and PDC are always constant. In fact, KLC must be changed according to feed concentration because it is a function of feed concentration (Harries and Ray, 1984). However, no attempt has been made to include the concentration effect on KLC in the programming method because TAU is also a function of KLC. In the main routine of the program, KLC affects the real time increment and the

loop to the dimensionless distance. As in the above expression, DELT is constant for constant feed concentrations because TAU is given as constant input data. However, as feed concentration increases, DELT decreases with constant TAU or TAU increases with constant DELT. For the present work, constant TAU is taken because, if DELT is taken as input data and then, TAU is calculated in the program, the calculated TAU often deviates from the effective numerical limits and results in inaccurate effluent profiles or error during the execution of the program. Thus, TAU is given as input data in the input data file for the program and DELT is calculated in the program based on feed concentration. The effluent concentration is given in constant real time increment in output files when feed concentration is constant. When step changes are introduced in feed concentration, the effluent concentration is given in a decreased real time increment. As an example, the real time increment with TAU of 0.0025 is 14.16 min for the feed concentration of 10^{-4} eq/l and decreases to 1.416 min as the feed concentration increases to 10^{-3} eq/l. For the case of an incompletely mixed-bed, cation-resin fraction can be given as a function of bed depth in the program or as numerical values with bed depth in the input file for the program.

The present computer model can thus predict the performance of ion-exchange units under a wide range of on-line operating conditions. As a result, the computer model

makes it possible to determine rational resin regeneration schedules and response times after a major cooling water tube leak in plant operations. The School of Chemical Engineering at Oklahoma State University continues its effort to make the handling of the computer program easier to the user. The user friendly program uses HI-SCREEN to create interactive screens which supply required input data for the program. Input data can be changed in the input data file, retaining other values, and the program can be executed. The effluent concentration profile obtained from the execution of the program is written to the output file and can be viewed.

Variable Feed Concentration

In order to evaluate the effect of the variable feed concentration on the performance of mixed-bed ion exchange, the experiments were designed to obtain data for the cases of step changes in feed concentration. The results of the experiments were compared to those of the constant feed concentration experiments. The comparisons are shown and discussed in the previous chapter. In this section, the performance of the hydrogen-cycle model of Haub and Foutch (1986a, b) will be evaluated for the cases of variable feed concentration by comparing the predicted values of the model to the experimental data.

Model Prediction For The System

For the execution of the computer model, the resin and ionic constants from the resin manufacturer and the literature (Divekar et al., 1987) are used directly. The mass transfer coefficients of sodium and chloride are obtained from the correlation equation of Kataoka et al. (1972). Initial loading of cation and anion on each resin is assumed to be zero. Figures 25 through 30 illustrate the comparisons between the experimental data and the model predictions for the cases of one and two peaks in feed concentration. In the figures, the experimental data are presented as symbols, and the model predictions are shown as solid and dashed lines for the constant and variable feed concentration, respectively. All figures are plotted as C/C_0 versus run time in hours. The feed concentration, C_0 , is held constant for the calculation of concentration fractions. When peaks in feed concentration are introduced, the initial feed concentration is taken as C_0 . The early portions of the breakthrough curves of both ions are amplified in the figures to investigate the model performance around the breakthroughs of both ions. This is more important than investigating the entire resin life because the resins are regenerated before the effluent concentration reaches the breakthrough point in industry.

As shown in Figures 25 through 30, the model predicts slightly lower effluent concentrations of both ions than

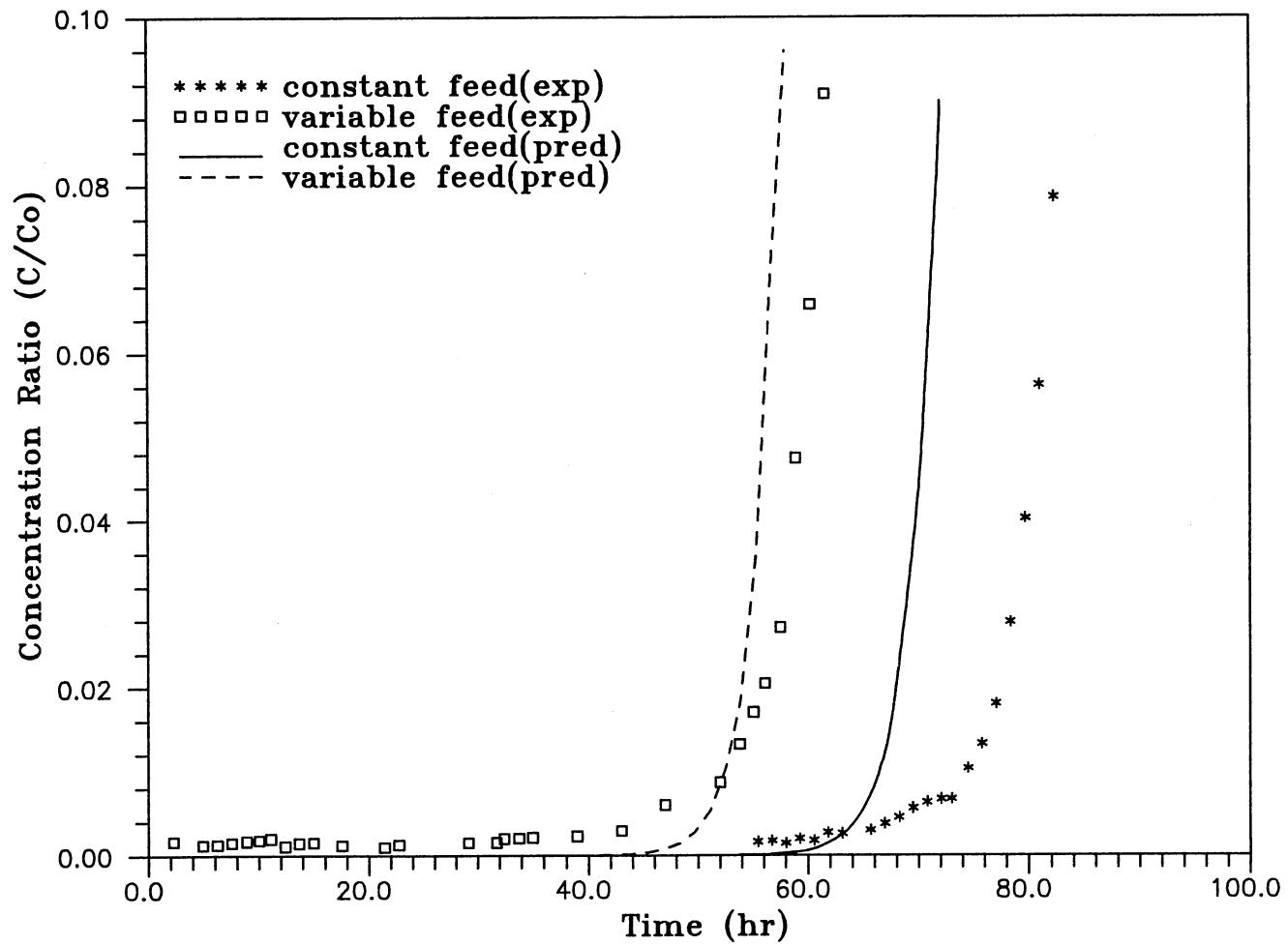


Figure 25. Experimental Data and Model Predictions for the Effect of One Peak in Feed Solution on Chloride Curve

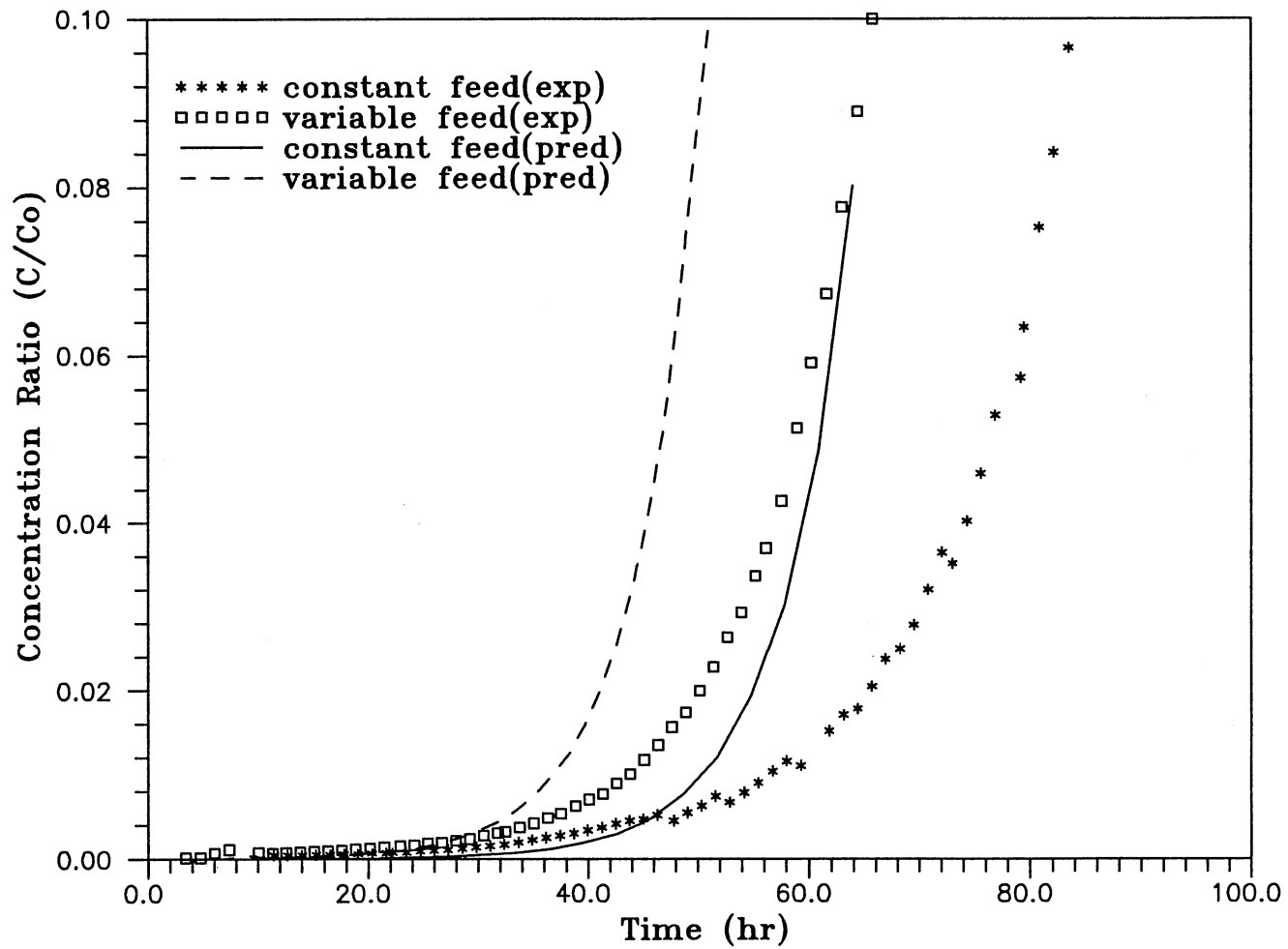


Figure 26. Experimental Data and Model Predictions for the Effect of One Peak in Feed Solution on Sodium Curve

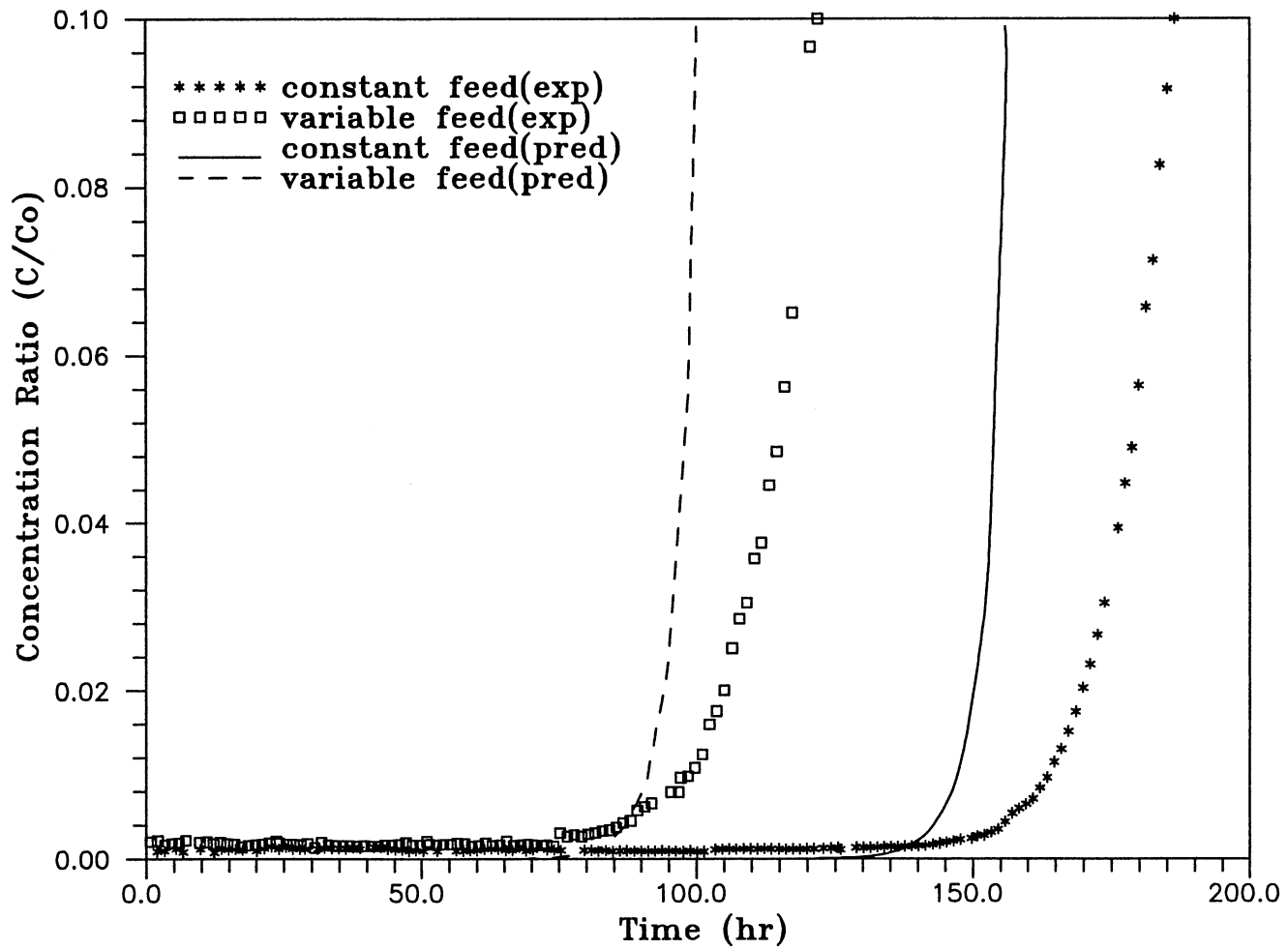


Figure 27. Experimental Data and Model Predictions for the Effect of Two Peaks in Feed Solution on Chloride Curve

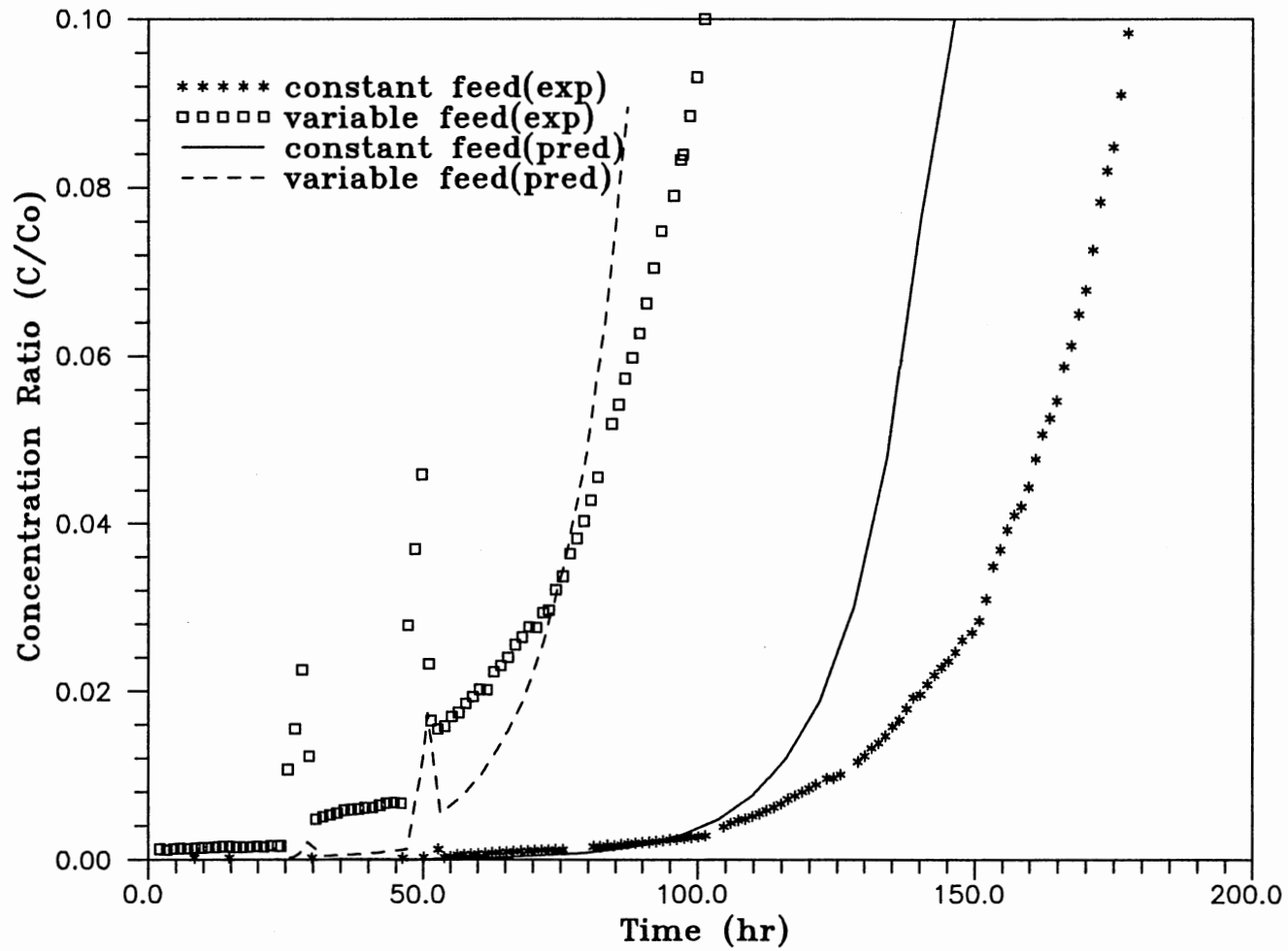


Figure 28. Experimental Data and Model Predictions for the Effect of Two Peaks in Feed Solution on Sodium Curve

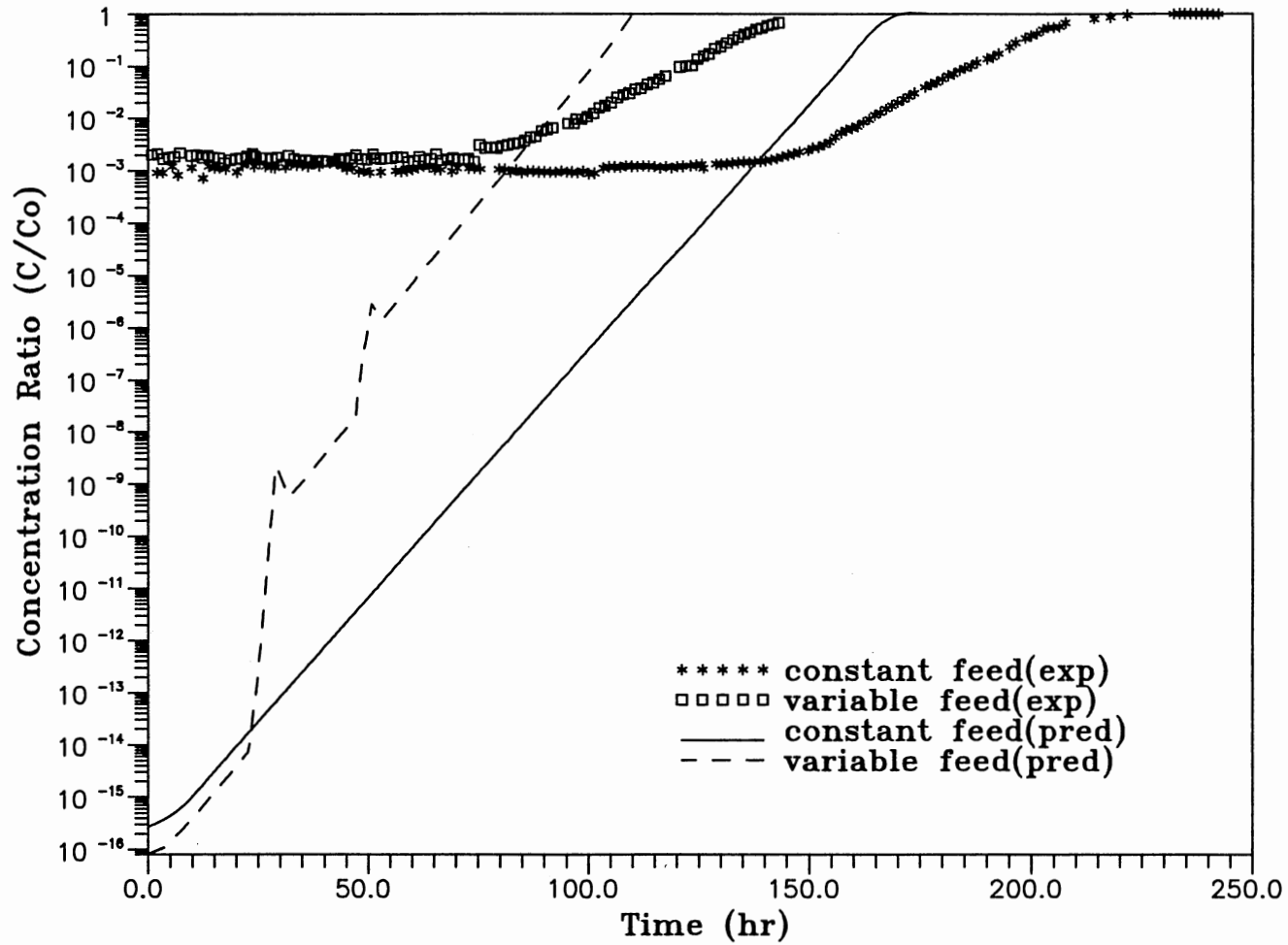


Figure 29. Semilog Plot of Experimental Data and Model Predictions for the Effect of Two Peaks in Feed Solution on Chloride Curve

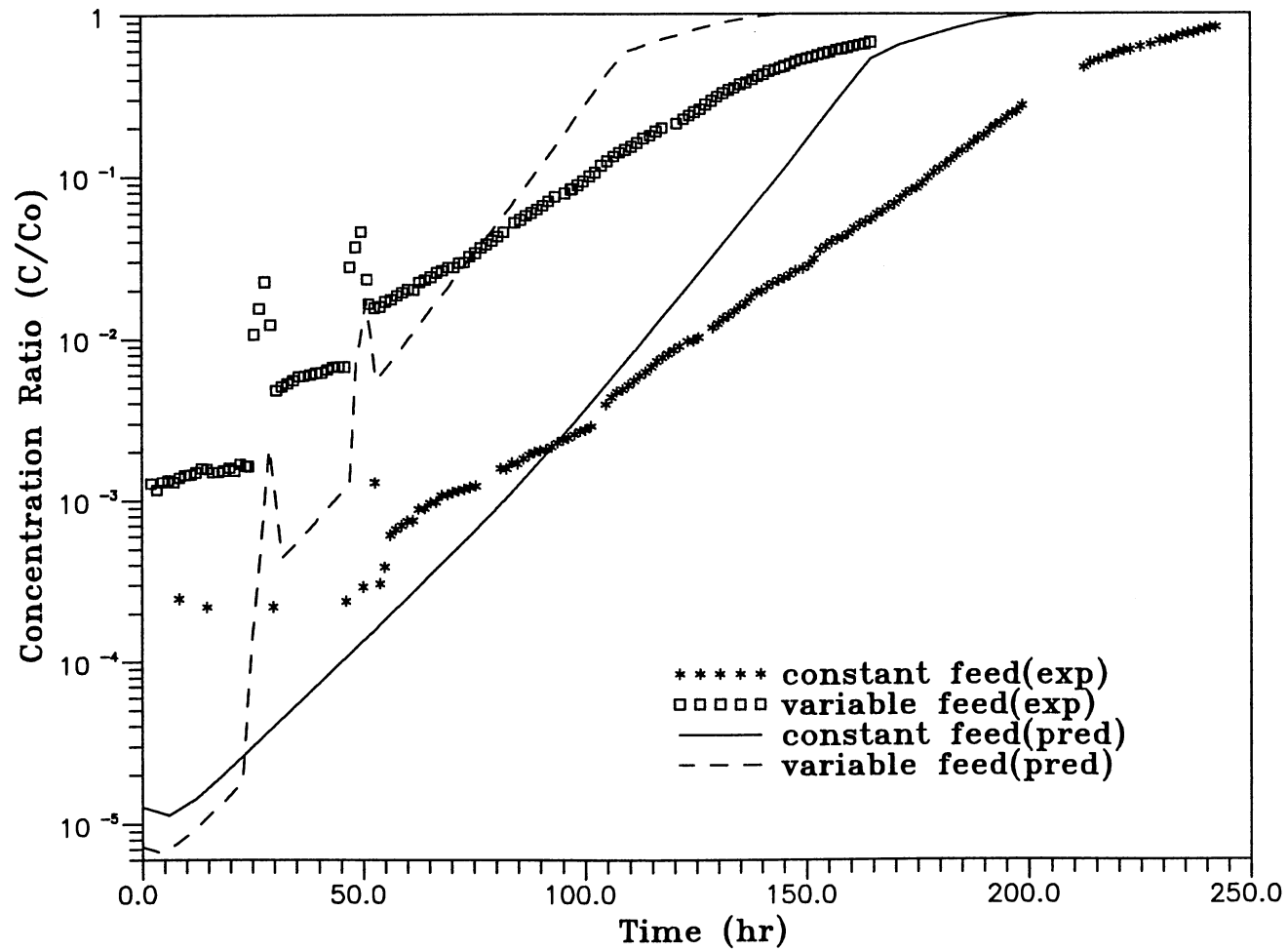


Figure 30. Semilog Plot of Experimental Data and Model Predictions for the Effect of Two Peaks in Feed Solution on Sodium Curve

those from the experiments, for both constant and variable feed concentration. Also, the slopes of the curves predicted by the model are steeper than those from the experiments. After breakthrough, the model starts to predict higher effluent concentrations. Since then, the deviation of the model predictions from the experimental data becomes larger. Generally, the figures show breakthrough times predicted by the model match moderately the breakthrough times from the experiments for both chloride and sodium.

Although the model predictions do not closely match the experimental data through the whole resin life, it can be said through close investigation of the figures that the model predicts the correct trends for the effect of peaks in feed concentration on mixed-bed ion exchange performance. Especially, Figures 28 and 30 indicate the possibility of the model to predict exactly the effect of peaks in feed concentration. Figure 30 is plotted in the semilog scale. The small peaks in the effluent concentration from the experiment might result from the kinetic leakage due to insufficient contact time between solution and the cation resin. The model appears to be able to predict the leakage and higher effluent concentrations after the leakage than those from the constant feed concentration experiment. In Figure 29, which is plotted as log concentration fraction versus run time, the model prediction for chloride also shows peaks in the effluent concentration when and where

peaks in feed concentration are introduced. However, the peaks in the experimental data are not clearly detected. This is due to the measurement limits of the IC at such low concentrations.

System Parameters

Based on the comparisons presented in the figures, a possible way to match the experimental data and the model predictions is to vary property data for the model, such as selectivity coefficients, ionic diffusivities, and nonionic mass transfer coefficients. These parameters are given as functions of temperature in the program and influence strongly the model prediction and impact the shapes of the breakthrough curves of chloride and sodium. Initial loading of each ion on corresponding resin also affects the model prediction, but was not considered in this work. As the selectivity coefficients increase, the breakthrough curve becomes steeper and reaches the equilibrium faster (Helfferich, 1962a, b). Therefore, the coefficients used in the model simulation need to be reduced to fit the experimental data. The ionic diffusion coefficient and the mass transfer coefficient are interrelated. For a given system, the mass transfer coefficient decreases as the diffusivity decreases. With the decreased mass transfer coefficient, the effluent concentration profiles of cation and anion are breaking through earlier. Therefore, the model may predict correctly the breakthroughs of both ions

with the decreased mass transfer coefficients. However, the difference between the predicted values and the experimental data after breakthrough will increase.

There are significant limitations of the property data available in the ultralow concentration range, which must be lower than 20 part per billion (ppb) NaCl equivalent. Most of the property data used for the simulation of the computer model were obtained at relatively high concentrations of 0.001 M or higher. The solution concentration is one of the factors on which the parameters are dependent (Myers and Boyd, 1956; Graham and Dranoff, 1982; Harries and Ray, 1984). Therefore, it is doubtful to expect the correct model prediction by applying these data to the concentration range of three to five orders of magnitude less.

The selectivity coefficients are functions of the resin properties such as the resin capacity, the degree of resin saturation, the resin crosslinking, and the nature of counter ions and the functional group, in addition to temperature and solution concentration (Wheaton and Hatch, 1968, Divekar et al., 1987). The coefficients from the resin manufacturer would, therefore, give a reasonable approximation and were used in the present work.

The ionic diffusion coefficient in water has been measured by many investigators (Robinson and Stokes, 1960; Harries and Ray, 1984, Petruzzell et al., 1987). However, the values in literature show differences of more than four times for hydrogen and two times for chloride from each

other. The coefficient is supported by a small amount of experimental data and thus, the extended measurements should be done for various conditions. Recently, Yoon (1990) attempted to match his experimental data to the theoretical values from Haub and Foutch's model (1986a, b) by applying coefficients approximately one order of magnitude lower than those from the literature (Robinson and Stokes, 1959). The literature data were obtained by experiments and supported by other investigations (Tyrell and Harries, 1984). Therefore, there should be serious consideration for the validity of his correlation equations.

The nonionic mass transfer coefficient for packed beds accounts for the bed geometry and flow field effects on the mass transfer rate. The coefficient is related to the ionic diffusion coefficient and a hydrodynamic factor in liquid phase. Harries and Ray (1984) showed the mass transfer coefficient decreases with solution concentration because the hydrodynamic factor, film thickness, increases as the solution concentration decreases. In this work, the numerical model employs the mass transfer coefficient correlation of Kataoka et al. (1972) for Reynolds number less than 20. However, the equation was obtained from relatively high solution concentration of 0.01 M (Kataoka et al., 1973), and the coefficient should thus be reduced for the present system.

Carberry (1960) proposed a theoretical equation for mass transfer in a packed bed of spherical particles. However,

in the low Reynolds number region, it deviates from the experimental data (Kataoka et al., 1972). Kataoka et al. (1972) suggested an approximate solution for the liquid-phase mass transfer coefficient in a packed bed at low Reynolds number less than 10. Reynolds numbers of the system for the present work are about 1.2 and 0.9 for sodium and chloride, respectively. At such low Reynolds numbers, the mass transfer coefficient was reported to be much lower than obtained from the equations of Carberry and Kataoka et al. (Rowe, 1975; Koloini et al., 1977).

Table XI presents the result of a sample calculation of the mass transfer coefficients of cation and anion using low Reynolds number using the various correlation equations shown in Table III, with the parameter values used to calculate the coefficients. Based on the effective Reynolds number regions to which the equations can be applied, all equations except Carberry's can be used for this work. However, the table shows the mass transfer coefficients obtained from the equation of Kataoka et al. are greater than those from other equations. The coefficients from Rahman and Streat's equation are close to those from Zarraa's equation and approximately 40 % lower for both cation and anion than those from Kataoka's equation. Rowe's equation gives the coefficients of about 70 % lower than Kataoka's. The coefficients from Rowe and Yoon's are close, especially for cation. A detailed discussion for the effect of the mass transfer coefficient on the model prediction

TABLE XI
 A SAMPLE CALCULATION* FOR THE MASS TRANSFER
 COEFFICIENTS** AT LOW REYNOLDS NUMBER

Correlation Equation	Cation	Anion	Applicable Re number
Carberry (1960)	5.381	8.191	10<Re<100
Kataoka et al. (1972)	6.670	10.64	Re<10
Rowe (1975)	1.685	2.661	0.01<Re<100
Rahman and Streat (1981)	3.945	6.014	2<Re<25
Yoon (1990)	2.877	2.662	Re<1
Zarraa (1992)	3.965	6.587	0.23<Re<2.27

* Calculation conditions

- . Reynolds number of cation = 1.173
- . Reynolds number of anion = 0.88
- . Bed void fraction = 0.34
- . Column diameter, cm = 2.54
- . Column height, cm = 13.0
- . Cation resin diameter, cm = 0.08
- . Anion resin diameter, cm = 0.06

** All values are given by 10^3 cm/sec.

will be shown in the next section for the case of incomplete mixing of the resins.

The explanation given above confirms that the property data for the model simulation should be somehow reduced for the present study. The current comparisons between the experimental data and the predicted values show the slight difference in two curves around breakthrough, while big difference after breakthrough. The reduced selectivity coefficients tend to fit the model prediction to the experimental data, especially after breakthrough. But the selectivity data are very limited. The reduced mass transfer coefficients will result in better match of two curves around breakthrough and worse after that. The model prediction is much more sensitive to the change in the mass transfer coefficient than in the selectivity coefficient. With the moderately reduced selectivity and mass transfer coefficients, the model can predict the breakthrough times of sodium and chloride more closely. But, the deviation of the model prediction from the data will be larger after breakthrough. As a conclusion, applying only the reduced property data to the model seems not to improve satisfactorily the model predictions at very low Reynolds number.

Incompletely Mixed-bed Ion Exchange

In a practical point of view, there is little interest in the region of Reynolds number less than 1. A 50

gal/min/ft² (3.4 cm/sec) service flow rate is recommended to be satisfactory for the operation of a condensate polisher without loss of a resin efficiency in industry (Caddel and Moison, 1984). As given in Table IX, the actual data from the Tulsa Riverside Power Plant show the flow rates of 500 - 1300 gal/min, which are equivalent to the superficial velocities of 1.2 - 3.12 cm/sec. To have an experimental condition closer to industrial practice, the flow rates of the experimental system for this dissertation needed to be about 20 times higher than those used for the variable feed concentration experiments.

Experiments to investigate the effect of incomplete mixing of the resins on mixed-bed ion exchange performance were conducted under high flow rates of approximately 2.5 cm/sec. The results of the experiments are presented and discussed in the previous chapter. In this section, the experimental data will be compared to predicted values by Haub and Foutch's (1986a, b) model. In addition, the effects of the mass transfer coefficients and resin capacity on the model prediction will be discussed in attempting to match the data to the model prediction.

Model Prediction For The System

Comparisons of the results of the experiments to the model prediction are plotted as effluent concentration fraction versus run time in hours. The experimental data are shown as symbols in the figures, and the model

predictions are as solid and dashed lines for the cases of complete and incomplete mixing of the resins, respectively. For the model simulation, the resin constants and selectivity coefficients from the resin manufacturer are used. The ionic diffusion coefficients are given as functions of temperature (Divekar et al., 1987). The mass transfer coefficients are obtained from the correlation equations of Kataoka et al. (1972) and Carberry (1960). The zero initial loading of cation and anion on each resin are assumed.

Figures 31 and 32 show comparisons between the results of the experiments conducted with the cation resin fraction of 0.5 and the model prediction for chloride and sodium, respectively. As mentioned in the previous chapter, the results of the experiments show that incomplete mixing of the resins appears not to affect the performance of the mixed-bed ion exchange as much as expected. But, it causes slight increase of the sodium exchange rate and slight decrease of the chloride exchange rate at the early stage of run. These changes of the exchange rates would be due to an increased mass transfer coefficient of sodium and a decreased mass transfer coefficient of chloride in an alkaline solution than a neutral or acidic solution (Harries, 1988). The experiment was performed with only anion resin in about the upper 20 % of the column. The feed solution is fed downward and meets only anion resin in the upper portion of the column. This results in a more

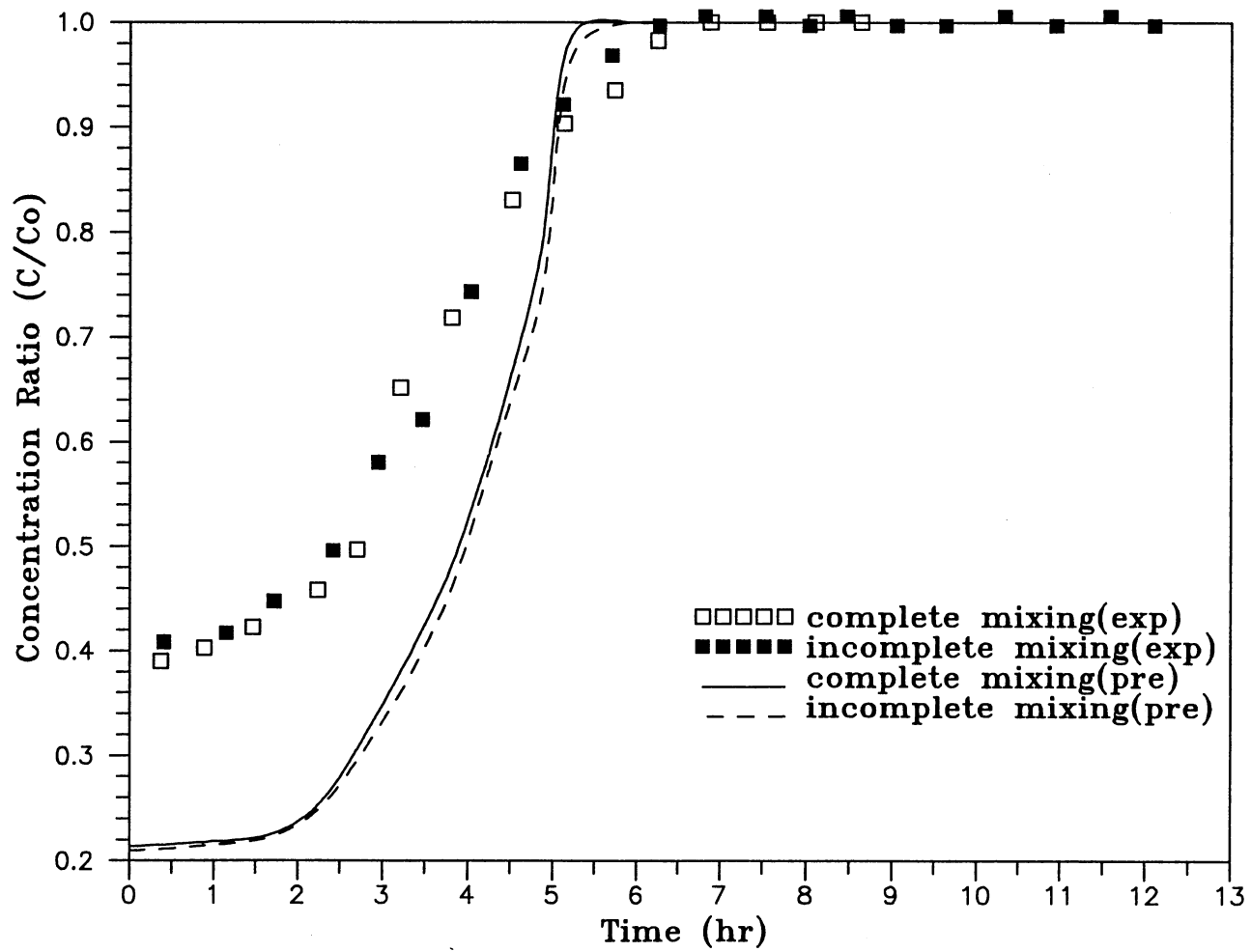


Figure 31. Experimental Data and Model Predictions for the Effect of Incomplete Mixing of Resins on Chloride Breakthrough Curve with FCR=0.5

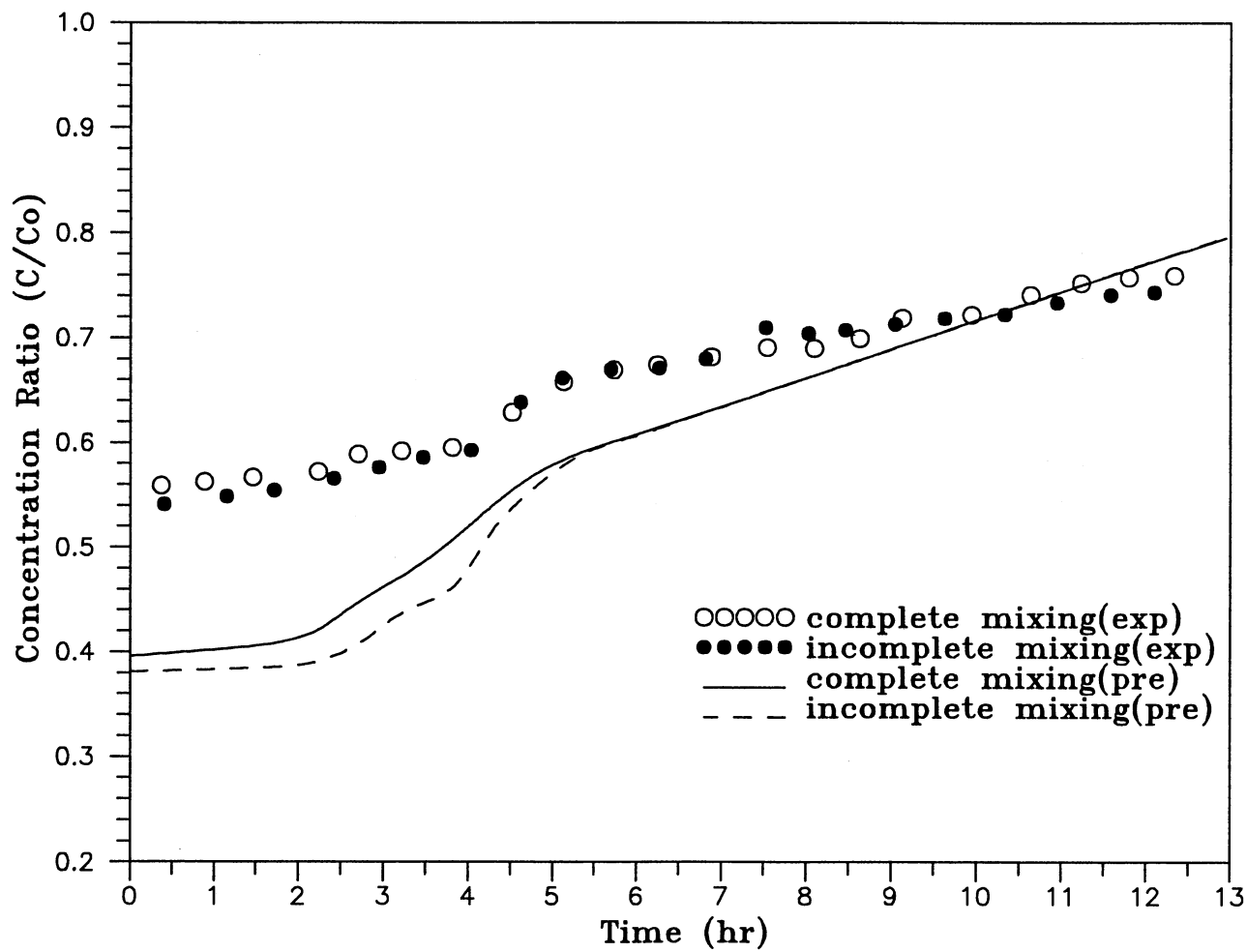


Figure 32. Experimental Data and Model Predictions for the Effect of Incomplete Mixing of Resins on Sodium Breakthrough Curve with FCR=0.5

alkaline solution and thus, an increase in the sodium mass transfer coefficient and a decrease of the chloride mass transfer coefficient. The model predicts the same trend as the experimental data for the effect of incomplete mixing of the resins. However, the model prediction shows the bigger effect of incomplete mixing on the exchange rate of sodium than chloride. As the chloride breakthrough curves reach equilibrium, the model prediction and the experimental data show the effect of incomplete mixing on the effluent concentration profiles for sodium disappears. This is because the mixed-bed acts like a single cation bed after active sites of the anion resin are exhausted. The figures also illustrate that slope changes in the sodium curves found in the experimental data for both complete and incomplete mixing are also shown in the model prediction. These slope changes might result from the complete exhaustion of the anion resin.

The model also predicts the initial leakage of chloride and sodium resulted from insufficient contact time between solution and the resins. In order for exchange rates to occur completely, the solution and resins must have a minimum contact time in an exchange bed. For a strong acid and basic resin, flow rate for the minimum contact time is usually 30 - 40 bed volumes per hour (BV/h) (Hill and Lorch, 1988), which is equivalent to approximately 1.5 - 2.0 min of contact time of the solution with the resin. For the present work, the bed volume is 10.7 cm^3 with bed diameter

of 1.849 cm and bed depth of 4.0 cm, and flow rate is 2312.8 BV/h. This flow rate causes the contact time less than the minimum and the leakage of both ions from the beginning of the exchange processes. As reference, the minimum bed depth to remove the leakage is theoretically about 230 cm for the present experimental conditions. The model prediction and the experimental data show the lower level of initial leakage of chloride than sodium. The difference in the level of leakage of both ions might be due to the difference in the selectivity coefficients of both resins. Because the selectivity coefficient of the anion resin is much higher than the cation resin, chloride curves show lower initial leakage and are steeper than sodium curves.

Figures 33 and 34 show the comparison of the results of the experiments performed with relatively large cation resin fraction of 0.6 to the model prediction for chloride and sodium, respectively. As expected, the model prediction and the experimental data show the lower initial leakage of sodium and the higher initial leakage of chloride than those of the previous case with the cation resin fraction of 0.5. However, the model prediction and the experimental data show inconsistency in the pattern of the effect of incomplete mixing on the effluent concentration profiles of both ions. This inconsistency may result from the differences in the experimental conditions of two runs. The volume of the cation resin was 6.4 ml for the completely mixed-bed experiment and 6.0 ml for the incompletely mixed-bed.

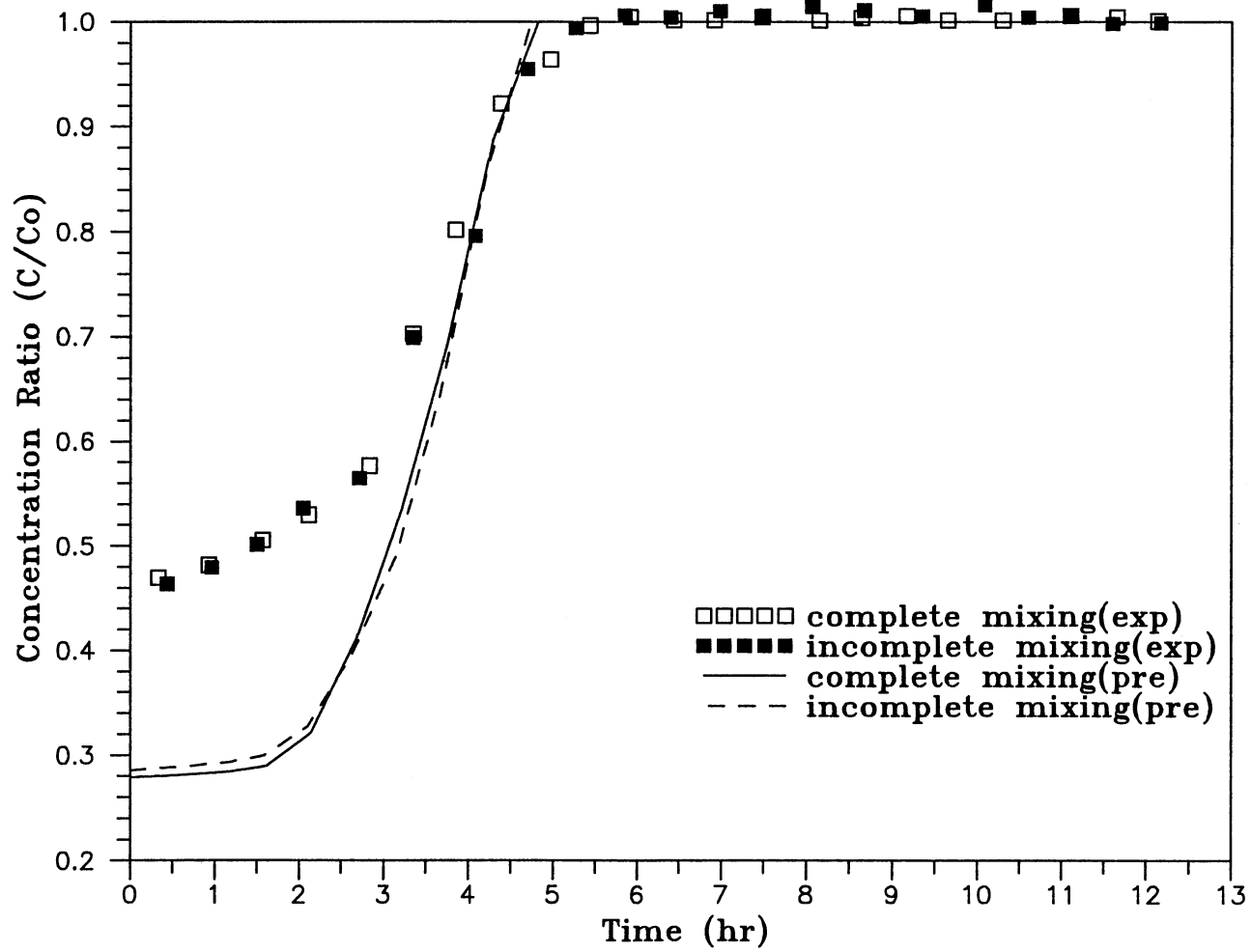


Figure 33. Experimental Data and Model Predictions for the Effect of Incomplete Mixing of Resins on Chloride Breakthrough Curve with FCR=0.6

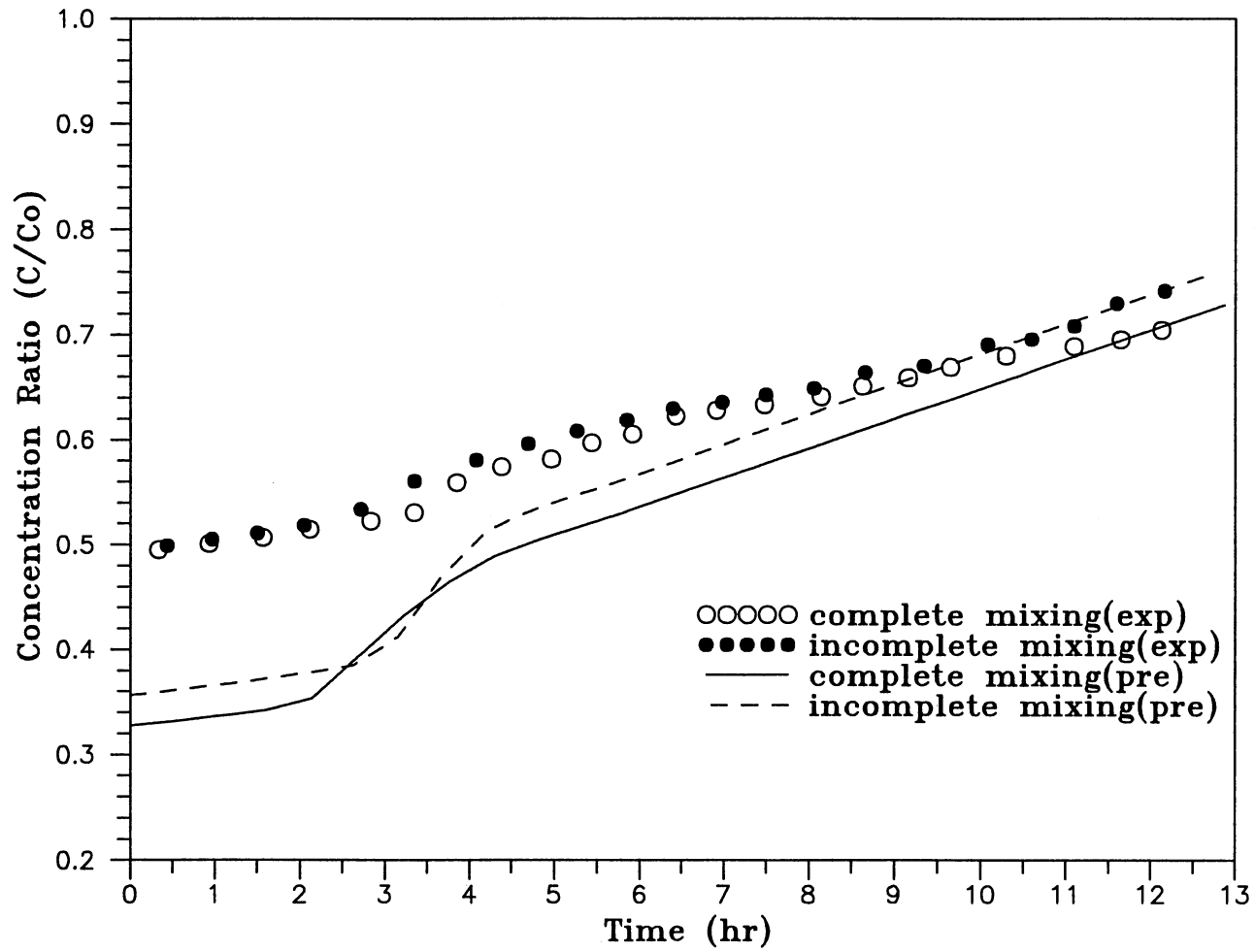


Figure 34. Experimental Data and Model Predictions for the Effect of Incomplete Mixing of Resins on Sodium Breakthrough Curve with FCR=0.6

Figure 35 presents the model predictions with close conditions for the same runs. The model predicts an increased cation exchange rate and a decreased anion exchange rate at the early run times. But, comparison of the model prediction presented in Figure 35 to those in Figures 31 and 32 shows that incomplete mixing of the resins has less effect on the sodium breakthrough curve with more cation resin. This is also shown in the results of the experiments. Therefore, it can be said that the model has an ability to predict the correct trend for the effect of incomplete mixing of the resins on the mixed-bed ion exchange performance.

As discussed to this point, the model appears to predict the correct trend of the effluent concentration profiles of chloride and sodium for both cases of complete and incomplete mixing of the resins. However, at a first glance over Figures 31 through 34, it could be known that the model predicts much lower effluent concentrations of both ions than the experimental data. The deviation is largest at the beginning of the exchange process and diminishes as the process continues. As explained in the previous section for the case of the variable feed concentration, disagreement of the model prediction with the experimental data is due likely to the use of inaccurate property data in the model. Thus, the effect of the property data on the model prediction will be discussed in the following section.

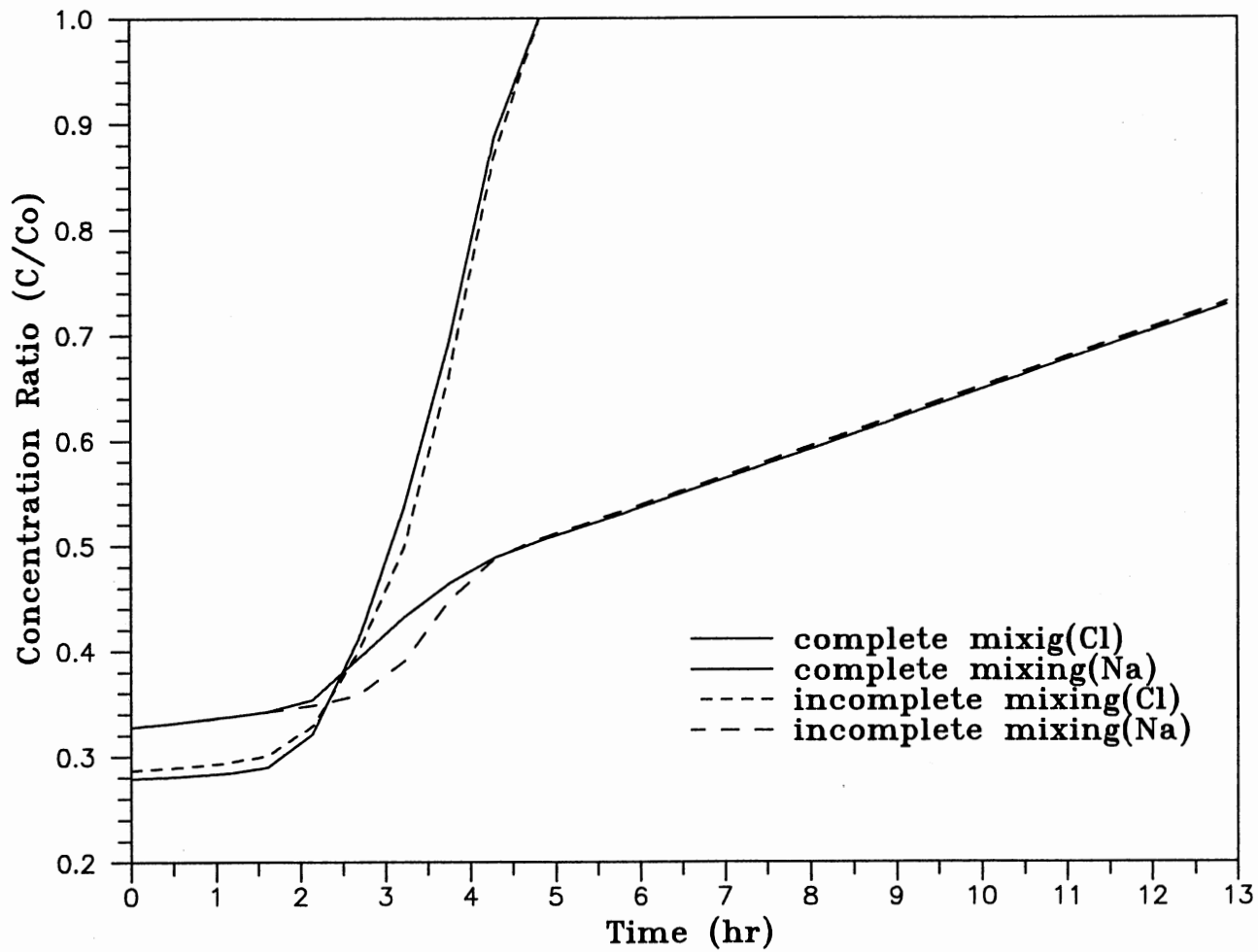


Figure 35. Model Predictions for Effect of Incomplete Mixing on Mixed-bed Ion Exchange (FCR=0.6)

Effects of System Parameters

As discussed early, the property data available for the model were very limited and/or measured in relatively high concentration and may not be appropriate for ultralow concentrations because they depend on the solution concentration. Among the property data, the mass transfer coefficient is an important factor which affects strongly the model prediction and has a reasonable reason to be changed at ultralow concentration (Harries and Ray, 1984). In this section, the effect of the mass transfer coefficient on the model prediction will be investigated.

There are several correlation equations of the mass transfer coefficient in literature. They are summarized and shown in Table III. Table XII gives the results of the coefficient calculation at moderate Reynolds number of about 20 using various correlation equations. Carberry's equation is used in the model simulation for the present work. The coefficients from Carberry's equation are close to those from Rahman and Streat's equation and slightly higher than those from Kataoka's equation. Zarraa's equation gives the largest coefficients for cation and anion, which may be inaccurate because Reynolds number of the system is out of the effective range of the equation. Rowe's equation gives the smallest values for both ions, and the values are about 80 % lower than those from Carberry or Rahman and Streat. Yoon's equation gives the second smallest values.

TABLE XII

A SAMPLE CALCULATION* FOR THE MASS TRANSFER
COEFFICIENTS** AT MODERATE REYNOLDS NUMBER

Correlation Equation	Cation	Anion	Applicable Re number
Carberry (1960)	1.807	2.737	10<Re<100
Kataoka et al. (1972)	1.306	2.075	Re<10
Rowe (1975)	0.302	0.590	0.01<Re<100
Rahman and Streat (1981)	1.663	2.519	2<Re<25
Yoon (1990)	1.189	1.095	Re<1
Zarraa (1992)	1.992	3.327	0.23<Re<2.27

* Calculation conditions

- Reynolds number of cation = 21.3
- Reynolds number of anion = 16.0
- Bed void fraction = 0.34
- Column diameter, cm = 1.85
- Column height, cm = 4.20
- Cation resin diameter, cm = 0.08
- Anion resin diameter, cm = 0.06

** All values are given by 10^2 cm/sec.

Certainly, the coefficient from Carberry's equation should be reduced to match the model prediction to the experimental data. However, the answer to what equation will give the correct mass transfer coefficients at ultralow concentration is still doubtful.

In order to match the model prediction to the experimental data, a series of arbitrarily reduced mass transfer coefficients of sodium and chloride were tried in the model simulation. Then, the results of the simulation were compared to the results of the completely mixed-bed experiment with the cation-resin fraction of 0.5. Figure 36 shows the result of one of the trials. The mass transfer coefficients from Carberry's (1960) correlation equation were $0.1796\text{E-}1$ cm/s for sodium and $0.2722\text{E-}1$ cm/s for chloride at the experimental conditions. These coefficients were multiplied by a factor of 0.7 for sodium and 0.6 for chloride to produce $0.1257\text{E-}1$ cm/s and 0.1633 cm/s, respectively. Mass transfer coefficients for morpholine from Oldbury P.S. resin as a function of feed concentration have been measured. The values are $1.5\text{E-}4$ m/s for a feed concentration of 40 ppm, $1.25\text{E-}4$ m/s for 5 ppm, and $1.25\text{E-}4$ m/s for 2.4 ppm (Bates, 1992). These data show that the mass transfer coefficient decreases with feed concentration and that the effect of feed concentration is more significant at lower feed concentration. Based on the above data, the reduced mass transfer coefficients in this study seem to be reasonable.

Figure 36 indicates the model prediction is reasonably close to the experimental data, especially for sodium. For chloride, the model appears to predict the correct level of initial leakage, but still lower effluent concentrations as the exchange process continues. For sodium, the model prediction shows slightly lower level of initial leakage, but fairly correct effluent concentrations. More reduced mass transfer coefficient of chloride will improve the model prediction in the middle of the process, but result in the higher level of initial leakage than that shown in the experimental data.

Figure 36 also illustrates the effect of the mass transfer coefficients on the model prediction. With the reduced mass transfer coefficients of both ions, the transfer rates decrease and after all, the exchange rates decrease. Thus, the more ionic contaminants that exist in the effluent, the more the levels of initial leakage increases. The mass transfer coefficient also affects the slope of the breakthrough curve. For sodium and chloride, the slopes of the curves decrease as the coefficients decrease.

In addition to the mass transfer coefficient, another parameter which affects strongly the model prediction is the resin capacity. The resin capacity describes the quantitative performance of a resin and is provided by the resin manufacturer. The capacity supported by the manufacturer are 1.1 meq/ml for anion resin and 2.18 meq/ml

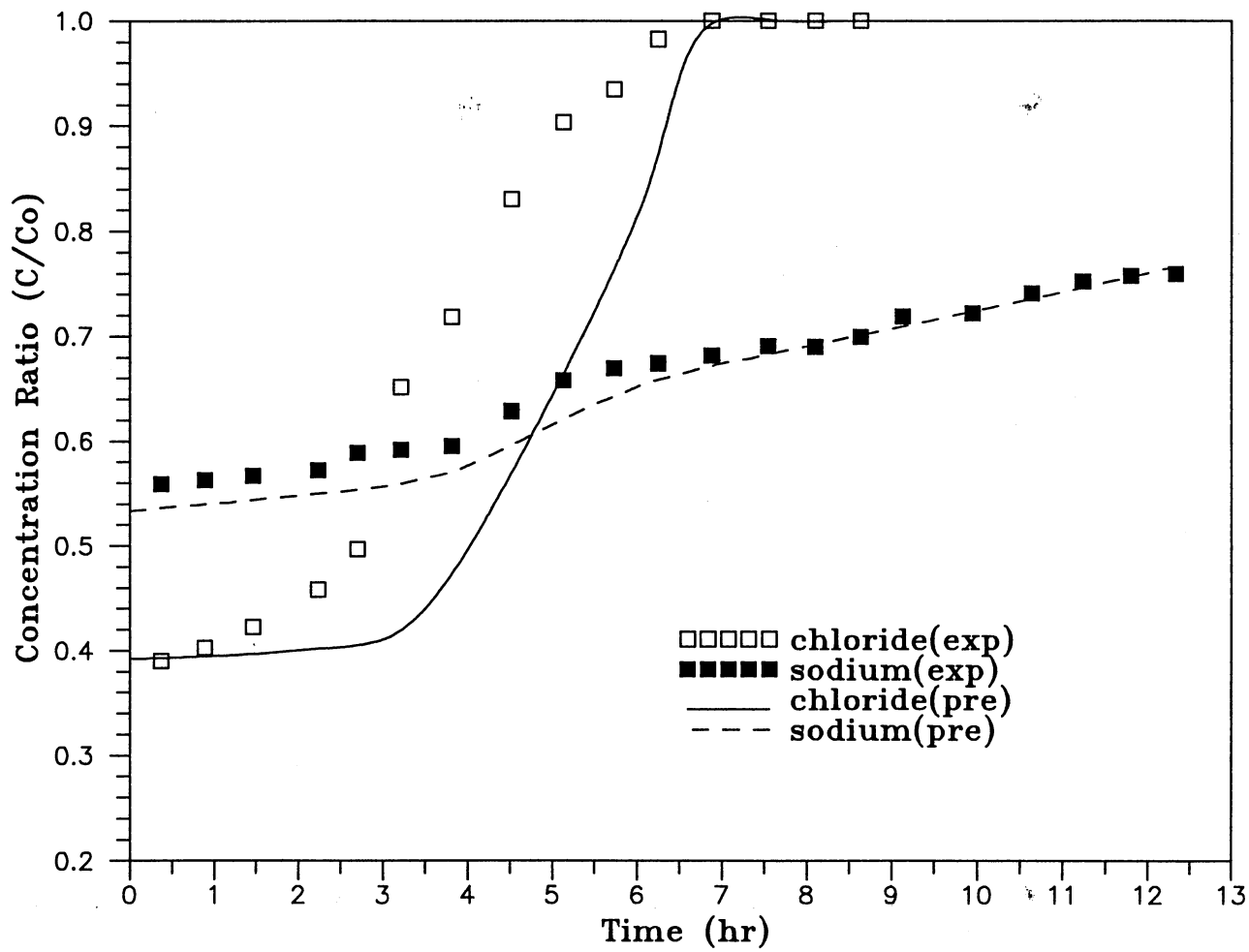


Figure 36. Experimental Data and Model Predictions with the Modified Mass Transfer Coefficients

for cation resin. But, these values are for Cl^- form anion resin and Na^+ form cation resin. When these resins are converted to OH^- and H^+ form, they will lose some of their capacity. In fact, cation-resin capacity decreases to less than 2.0 meq/ml for H^+ form (Dow Chemical, 1990). The anion-resin capacity informed by the manufacturer is, in practice, usually reduced by 15 % and 40 % for the design of a monobed and a mixed-bed ion exchange system, respectively (McClinton, 1992). Therefore, there is a possibility for the resin to be overrated in term of the capacity. The overrated resin capacity results in overrated performance of the mixed-bed. For the present work, the model could predict the correct breakthrough curves of sodium and chloride with the reduced cation and anion-resin capacity.

Figures 37 and 38 show the effect of the anion-resin capacity with reduced cation-resin capacity of 2.0 meq/ml on the breakthrough curves of chloride and sodium, respectively. The cation-resin capacity is decreased by about 10 % from that indicated by the manufacturer. Solid lines in the figures are the model prediction with the reduced mass transfer coefficients. As shown in the figures, the curves of both ions are breaking through earlier and closer to the experimental data as the anion-resin capacity decreases. The figures also show that the anion-resin capacity does not affect the levels of initial leakages of both ions. This is because the initial leakage results from kinetically insufficient contact time between

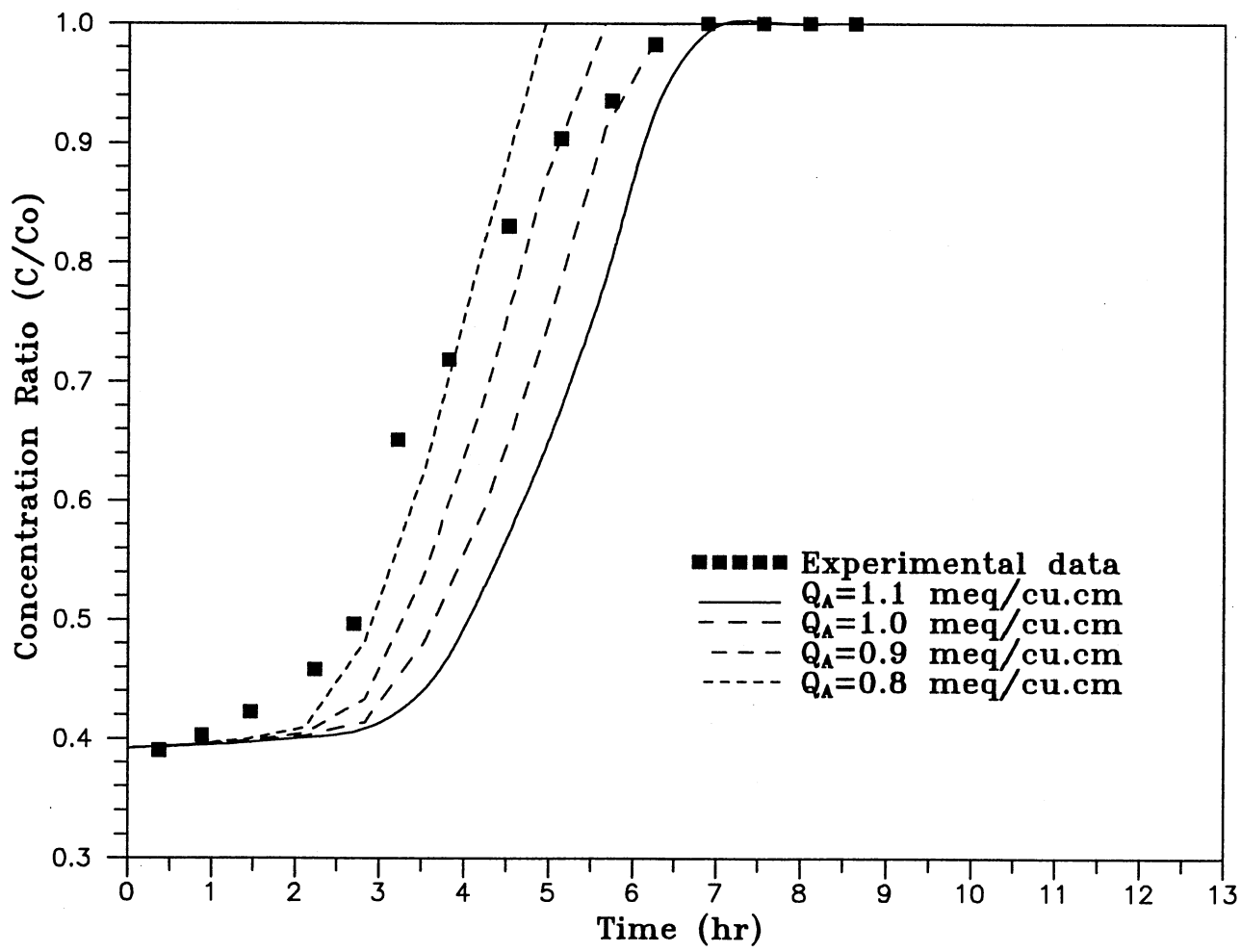


Figure 37. Effect of Anion Resin Capacity on Chloride Breakthrough Curve ($Q_c=2.0$ meq/cu.cm)

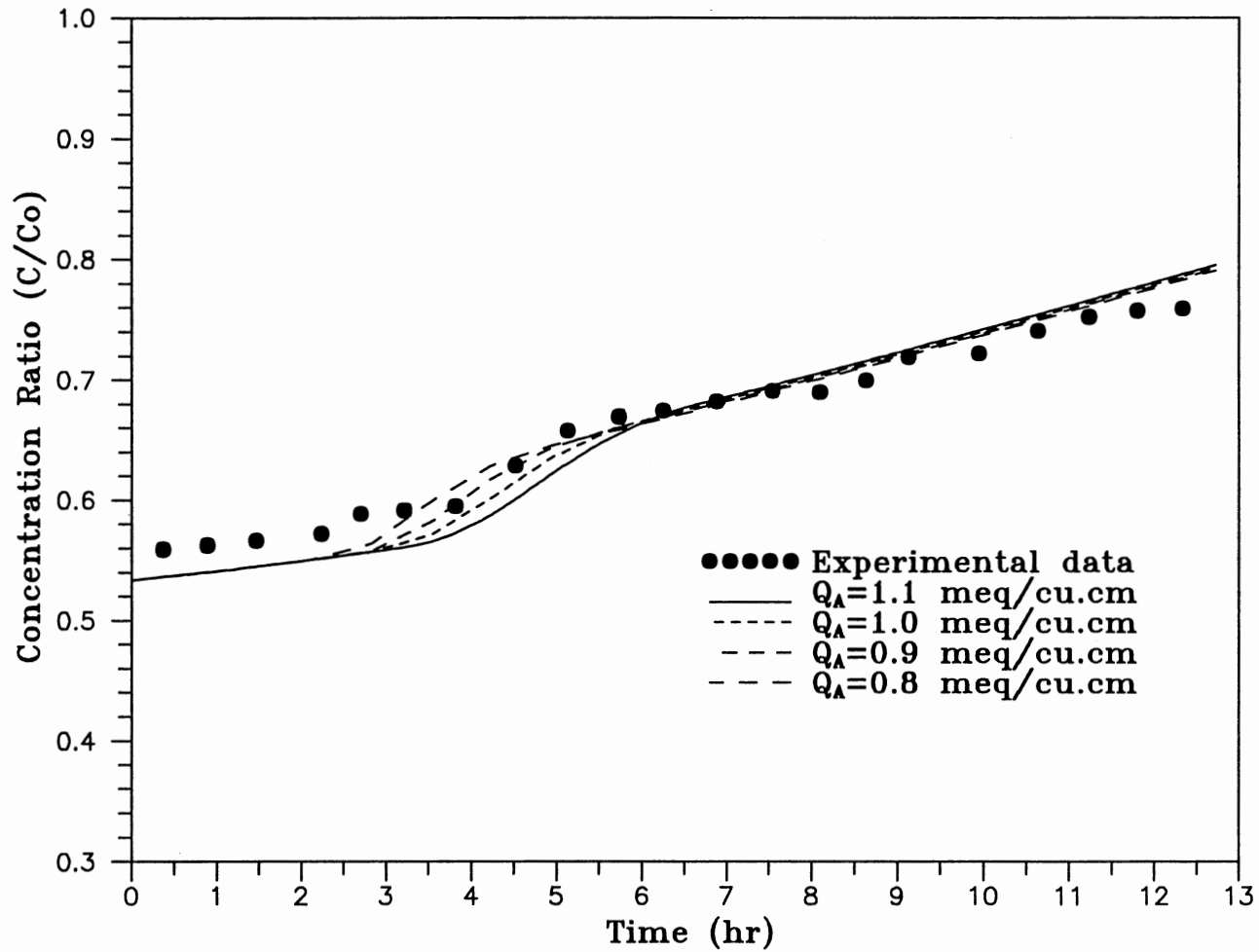


Figure 38. Effect of Anion Resin Capacity on Sodium Breakthrough Curve ($Q_C = 2.0$ meq/cu.cm)

the feed solution and the resins, and is only affected by factors of how fast ions in the solution can be removed, such as the mass transfer coefficient. Figure 38 indicates the anion-resin capacity has less effect on the sodium curve. An interesting point is, however, that it begins to affect the shape of the sodium curve when the chloride curve begins to break and ends when the chloride curve reaches the equilibrium. This confirms that in a mixed-bed process, the anion-exchange rate affects the cation exchange rate or vice versa, and that the mixed-bed acts like a single bed after the anion resin is exhausted.

Figures 36 through 38 show that the model prediction matches the experimental data well with the reduced mass transfer coefficients and anion-resin capacity of 0.8 meq/ml and the cation-resin capacity of 2.0 meq/ml. The anion-resin capacity of 0.8 meq/ml is about 70 % of the capacity indicated by the manufacturer. The model prediction with these modified values for the cases of complete and incomplete mixing of the resins with the cation-resin fraction of 0.5 and 0.6 are illustrated in Figures 39 and 40, respectively. These figures confirm that the model of Haub and Foutch (1986a, b) has an ability to predict correctly the performance of mixed-bed ion exchange under various conditions, provided the correct values or correlation equations for the property data are available.

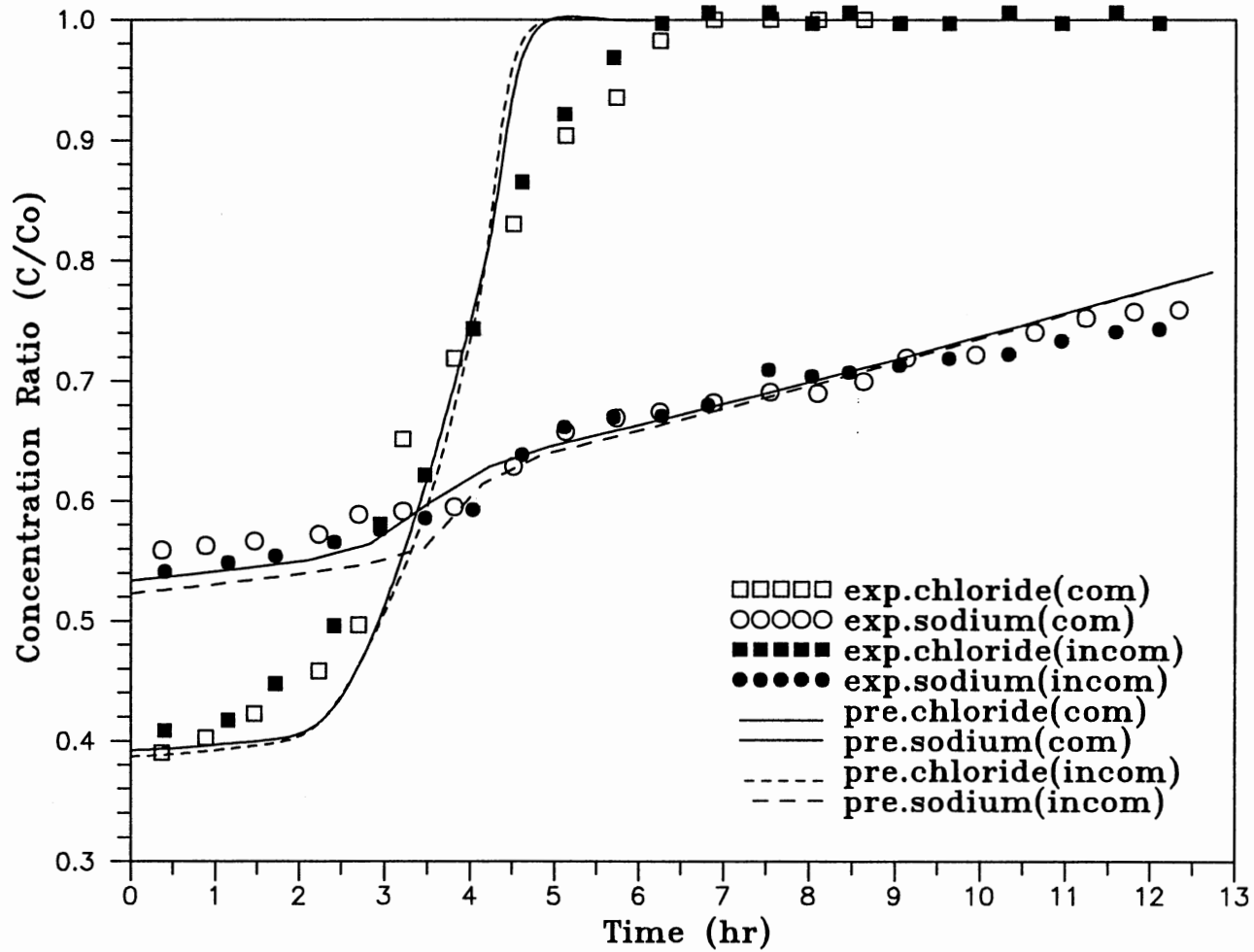


Figure 39. Experimental Data and Model Predictions for Complete and Incomplete Mixing of Resins with Modified MTC and Resin Capacity (FCR=0.5)

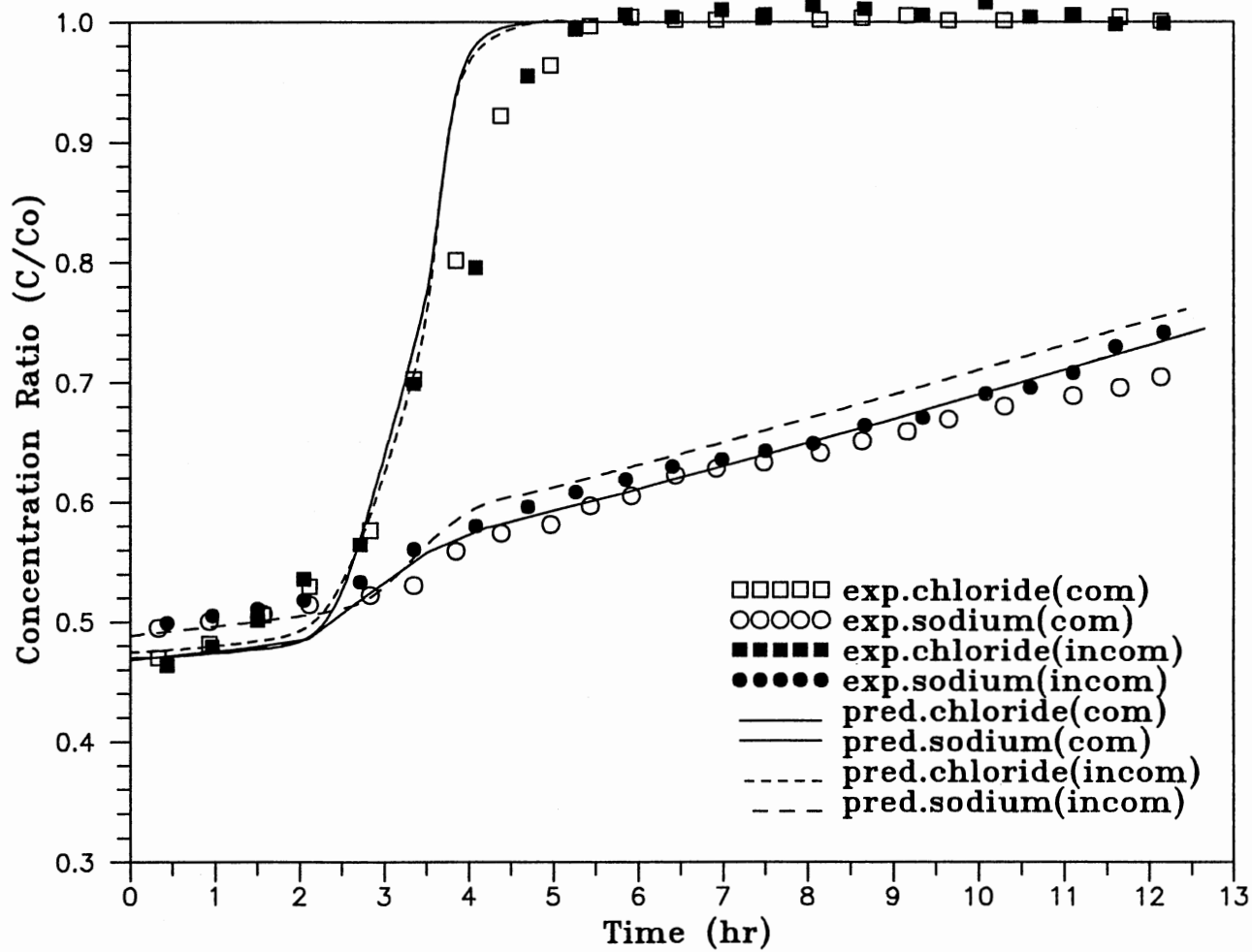


Figure 40. Experimental Data and Model Predictions for Complete and Incomplete Mixing of Resins with Modified MTC and Resin Capacity (FCR=0.6)

On-Line Operating Data From PSO

As shown in Figures 19 and 20 in the previous chapter, influent and effluent data around a full scale condensate polisher were obtained by analyzing water samples from the Tulsa Riverside Power Plant. The figures indicate no substantial differences between the influent and effluent concentrations of sodium and chloride. The figures also show no sudden increases in influent concentration resulted from a condenser tube leak.

Because of uncertainties in measuring the exact concentration of each ion in the solution, the data were not used for the evaluation of the model under the operating conditions of a full scale polisher in this work. Instead, it appears to be possible to investigate the effect of resin degradation on the performance of the polisher by comparing the data obtained from the old resins and the new resins. In fact, Dowex Monosphere resins, the new products of Dow Chemical, have superior properties to the old resins, which are provided by the same company. The physical properties of the old and the new resins are given in Tables IV and XIII, respectively. Comparison between the properties of the old and new resins indicates slightly smaller size of the new cation particle than the old, but almost the same anion particle size. The particle sizes of the new resins are extremely uniform with 95 % of the particles within 100 microns of the average sizes for both cation and anion

TABLE XIII
 PHYSICAL PROPERTIES OF NEW DOWEX RESINS*

parameter	cation	anion
name	Monosphere 650C	Monosphere 550A
capacity (meq/ml)	1.90	1.1
selectivity	Na-H 1.13	Cl-OH 22.0
water retention capacity (%)	46 - 51	44 - 50
density (lb/ft ³)	50.0	40.0
diameter(cm)	0.065	0.059
appearance	hard, black, spherical beads	hard, white, spherical beads
particles within range of ± 0.01 cm from diameter (%)	95 minimum	95 minimum

* From the vendor

particle. The small particle sizes and the uniformity of the new resins may lead to certain kinetic and hydraulic advantages in system performance. However, the anion-resin capacity is the same for both resins, and the cation-resin capacity is lower for the new resins. Therefore, no significant difference between the performances of these resins can be expected, based on their physical properties.

Figure 20, which presents the data from the new resins, shows the sodium concentration of approximately one order of magnitude less than from the old resin (Figure 19) and no chloride leakage. According to a plant operator, the old resins had been in service for 15 years until they were replaced in 1991. Therefore, the exchange performance of the old resin must have been reduced with age.

The mechanism of resin degradation and the effect of a certain mechanism are not fully understood because of the lack of suitable methods for measuring quantitatively, and even qualitatively, changes in the resin structures. The possible mechanisms are many: physical change of the resin structure, decross-linking and resulting increased swelling, loss of total exchange capacity, loss in acidity or basicity of functional group, irreversible adsorption of functional group, and fouling from precipitation (Kunin, 1958; Inczedy, 1966). Each of these may be independent, or dependent on, or related to, other factors.

Usually, the term degradation of resin includes both physical and chemical changes in the resin structure. The

physical changes which may be related to chemical modifications include resin softening, swelling, and particle-size reduction. Poor resin performance is closely related to chemical changes, which may involve either irreversible loss of the exchange sites or fouling (Kunin, 1958). In the present work, the preliminary approach to evaluate the effect of resin degradation is attempted by considering the effect of the exchange-sites loss and fouling. These factors affect the total resin capacity and mass transfer rate, as shown in the previous section of this chapter.

The anionic exchange sites which can be interchanged with anions in solution can be lost by replacing with a species of higher selectivity such as sulfonate and carbonate. Thermal degradation or oxidation near the surface of the resin particle also causes anionic exchange sites loss by converting the strongly basic sites to the weakly basic sites (Kunin, 1958; Inczedy, 1966). In general, however, resin performance is not correlated directly with the measurement of the reduced resin capacity because only a small portion of the active exchange sites is used in the exchange process.

The fouling increases the physical resistance to ionic mass transfer in the resin. This fouling may result from the adsorption of fouling agents such as organics, iron oxides, and particulates (Kunin, 1958). The adsorbed agents will accumulate within the resins with time. However, the

extent of degradation will be different depending on water quality, column history, and regeneration schemes because the fouling agents are different from station to station. Thus, fouling effects on the performance of ion-exchange resin can not be predicted accurately.

One possible approach to characterize the effect of resin degradation on a system performance is to measure the mass transfer coefficients of an old resin and a new resin and compare them. Harries and Ray (1984) suggested a simple method for the measurement of the actual mass transfer coefficient. With influent and effluent data from a plant, the actual mass transfer coefficient can be determined by using Harries method.

As a conclusion, the reduced exchange performance of the old resins at the Tulsa Plant can be considered as the result of either the loss of the anionic-exchange sites or the increase of the ionic mass transfer resistance within the resins, or from a combination of these factors. Close investigation of Figures 19 and 20 indicates the effect of resin degradation is much greater on chloride than sodium. Chloride leakage is shown with the old resins, while no leakage is observed with the new resins. This confirms that anion exchange performance progressively deteriorates with service in a condensate purification plant although the rate varies from system to system (Harries, 1987). The on-line data shown in the figures may not be accurate enough for the calculation of the actual mass transfer coefficients to

evaluate the effects of resin degradation. Thus, more laboratory work is recommended to measure the coefficient using the old resin from the plant.

CHAPTER VI

CONCLUSIONS AND RECOMMENDATIONS

For this work, the experiments were designed to collect data for the cases of variable feed concentration and incomplete mixing of resins observed in large scale industrial plants. To evaluate the effect of the variable feed concentration, step changes in feed concentration were arbitrarily introduced into the experimental column. For the incompletely mixed bed, only anion resin was loaded in about the upper 20 % of the column and more cation resin in the lower portion. Downflow was used for the experiments. The results of the experiments for both cases were compared to the predicted values from the hydrogen cycle model of Haub and Foutch (1986a, b), which has the ability to predict the performance of industrial mixed-bed ion exchange. Water samples from the Tulsa Riverside Power Plant were analyzed to obtain on-line operating data from a full scale condensate polisher. From this work, the following conclusions are drawn;

1. The experimental system is updated to include on-line pH measurement. Thus, this system can be used to collect on-line/off-line data such as temperature, resistivity, pH, and concentration of influent and/or effluent of the experimental column.

2. Introducing step changes in feed concentration affects the breakthrough times of chloride and sodium, but not the slopes of curves. After the peaks are introduced, there is a low level of leakage of both ions due to insufficient contact time between the solution and the resin. When the feed returns to the normal concentration, the leakage of chloride disappears. But, the sodium effluent starts to have higher concentrations after the peaks are introduced. Therefore, the amount of sodium removed until breakthrough is more sensitive to the step changes in feed concentration than the amount of chloride. This would be due to the much lower selectivity coefficient of sodium than chloride.

3. Incomplete mixing of the resins increases the sodium exchange rate slightly and decreases the chloride exchange rate slightly at the early stage of the exchange processes. This is due to the difference of the mass transfer coefficients of sodium and chloride in an alkaline and an acidic solution. The effect of incomplete mixing of the resins diminishes as active sites on the anion resin are exhausted.

4. The effect of incomplete mixing of the resin on the sodium breakthrough curve decreases as cation-resin fraction increases. For the chloride breakthrough curve, the effect is less sensitive to an increase of cation-resin fraction.

5. The programming method is modified to allow the model to accept the variable feed concentration and variable

cation-resin fraction along the bed. The input data file for the program contains the inlet concentration, as a function of time, and other property data. Cation-resin fraction is given as a function of bed depth in the program. The present computer model can thus predict the performance of ion exchange units under a wide range of on-line operating conditions.

7. System parametric studies show the error in predicted concentration profiles of chloride and sodium gradually decreases as dimensionless distance (XI) and time (TAU) increments decrease. But, very low TAU could cause an unstable output due to the accumulated error resulted from differentiating and integrating the flux equations and column material balances.

7. The analysis of water samples for the Tulsa Riverside Power Plant shows three prominent ions; sodium, chloride, and ammonia. The influent and effluent concentrations of beds with 15 years old resin are approximately 0.1 ppb and 1 ppb of chloride and sodium, respectively. New Dow Monosphere resins give no chloride leakage and sodium concentration less than 0.1 ppb.

8. The model predicts correctly the effects of step changes in feed concentration and incomplete mixing of the resins on the performance of mixed-bed ion exchange. However, deviation between the model prediction and the experimental data is significant.

9. Difference between the model prediction and the data depends on flow conditions. At very low Reynolds number near 1.0, the model predicts lower effluent concentrations of chloride and sodium until breakthrough and higher after breakthrough than the experiments. At moderate Reynolds number around 20, the model predicts generally much lower concentrations of both ions even after breakthrough.

10. The nonionic mass transfer coefficients affect the initial leakages and the shapes of the effluent concentration profiles of sodium and chloride. As the coefficient decreases, the initial leakage increases, and the curve slope becomes wider. The coefficient itself decreases as the inlet concentration and flow rate decrease.

11. The anion-resin capacity affects the breakthrough time of each ion, but not the initial leakage or the curve shape. With the reduced anion capacity, the effluent concentration profiles of both ions are breaking earlier. But, this effect is less on sodium than chloride.

12. To match the model prediction to the experimental data, the nonionic mass transfer coefficient from Carberry's (1960) correlation equation is reduced by 30 % for sodium and 40 % for chloride, and the anion-resin capacity is decreased by 30 % from the value supplied by the resin manufacturer. The model prediction with the reduced coefficients and resin capacity fits satisfactorily the data obtained for the case of incomplete mixing of the resins.

To understand the mixed-bed ion exchange process better and improve the performance of the model, the following recommendations based on the results of the present work are made;

1. To maintain consistency and remove a possible source of contamination in the experimental procedure, the experimental system should be updated to endure a high pressure drop resulted from a high flow rate close to an industrial condition. A continuous feed system is also strongly recommended to obtain data from deep beds and to avoid the contamination of the feed solution by air.

2. For the accurate simulation of the model, the computer programming method should be modified to address the mass transfer coefficient as a function of feed concentration and inlet pH. Also, accurate values of the resin capacity, resin particle size, particle size distribution, and bed void fraction should be obtained. The exchange rate would decrease as the resin particle size and bed void fraction increase and the resin capacity decreases.

3. The whole modeling process needs to be reviewed for very low flow rates. The effect of axial dispersion should be considered at very low Reynolds number regions (Helfferich, 1962). This may reduce the nonionic mass transfer coefficient significantly in particular beds (Wakao et al., 1977).

BIBLIOGRAPHY

- Bajpai, R. K., Gupta, A. K., and Rao, M. G., "Single Particle Studies of Binary and Ternary Cation Exchange Kinetics," AICHE Journal, Vol.20, No.5, pp.989-995 (1974).
- Ball, M., Jenkins, A., and Burrows, R. J., "Ammonium Form Cation Resin Operation of Condensate Purification Plant," in "Ion Exchange Technology," Edited by D. Naden and M. Streat, Ellis Horwood Limited, Chichester, England, 1984.
- Bates, Personal Communication, 1992.
- Bird, R. B., Stewart, W., E., and Lightfoot, E. N., "Transport Phenomena," John Wiley & Sons, Inc., New York, 1960.
- Bonner, O. D. and Pruett, R. R., "The Effect of Temperature on Ion Exchange Equilibria. II. The Ammonia-Hydrogen and Thallous-Hydrogen Exchanges," Journal of Physical Chemistry, Vol.63, No.9, pp.1417-1420 (1959a).
- Bonner, O. D. and Pruett, R. R., "The Effect of Temperature on Ion Exchange Equilibria. III. Exchangers Involving Some Divalent Ions," Journal of Physical Chemistry, Vol.63, No.9, pp1420-1423 (1959b).
- Boyd, G. E., Adamson, A. W., and Myers, L. S. Jr., "The Exchange Adsorption of Ions from Aqueous Solutions by Organic Zeolites. II. Kintetics," Journal of the American Chemical Society, Vol.69, No.11, pp.2836-2848 (1947).
- Caddel, J. R. and Moison, R. L., "Mixed-Bed Deionization at High Flow Rates," Chemical Engineering Progress Symposium Series, Vol.50, No.14, pp.1-5 (1954).
- Carberry, J. J., "A Boundary-Layer Model of Fluid-Particle Mass Transfer in Fixed Beds," AICHE Journal, Vol.6, No.3, pp.460-463 (1960).
- Cobble, J. W. and Turner, P. J., "Additives for pH Control in PWR Secondary Water," EPRI NP-4209, Project 1571-3, August 1985.
- Cooney, D., "The Importance of Axial Dispersion in Liquid-Phase Fixed-Bed Adsorption Operations," Chemical Engineering Comm., Vol.110, pp217-231 (1991).

- Copeland, J. P. and Marchello, J. M., "Film-Diffusion-Controlled Ion Exchange with a Selective Resin," Chemical Engineering Science, Vol.24, No.9, pp.1471-1474 (1969).
- Crits, G. J., "Questions and Answers on Condensate Polishing Design and Performance," Proceedings of the American Power Conference, Vol.43, pp.1131-1137 (1981).
- Crits, G. J., "Condensate Polishing with the Ammonex Procedure," in "Ion Exchange Technology," Edited by D. Naden, and M. Streat, Ellis Horwood Limited, Chichester, England, 1984.
- Daniels, F. and Alberty, R. A., "Physical Chemistry," John Wiley & Sons, Inc., New York, 1979.
- Diamond, R. M. and Whitney, D. C., "Chapter 8. Resin Selectivity in Dilute to Concentrated Aqueous Solutions," in "Ion Exchange," Volume 1, Edited by J. A. Marinsky, Marcel Dekker, Inc., New York, 1966.
- Divekar, S. V., Foutch, G. L., and Haub, C. U., "Mixed-Bed Ion Exchange at Concentrations Approaching the Dissociation of Water. Temperature Effects," Industrial & Engineering Chemistry Research, Vol.26, No.9, pp.1906-1909 (1987).
- Dowex, "Dowex: Ion Exchange," The Dow Chemical Company, Midland, Michigan, 1958.
- Frisch, N. W. and Kunin, R., "Kinetics of Mixed-Bed Deionization: I," AIChE Journal, Vol.6, No.4, pp.640-647 (1960).
- Glaski, F. A. and Dranoff, J. S., "Ion Exchange Kinetics: A Comparison of Models," AIChE Journal, Vol.9, No.3, pp.426-431 (1963).
- Golding, L. S., "Chapter 6. Heterogeneity and the Physical Chemical Properties of Ion Exchange Resins," in "Ion Exchange," Volume 1, Edited by J. A. Marinsky, Marcel Dekker, Inc., New York, 1966.
- Gomez-Vaillard, R., and Kershenbaum, L. S., "The Performance of Continuous Cyclic Ion-Exchange Reactors-II. Reaction with Intraparticle Diffusion Controlled Kinetics," Chemical Engineering Science, Vol.36, No.2, pp.319-326 (1981).
- Graham, E. E. and Dranoff, J. S., "Application of the Stefan-Maxwell Equations to Diffusion in Ion Exchangers. 2. Experimental Results," Industrial and Engineering Chemistry Fundamentals, Vol.21, No.4, pp.365-369 (1982).

- Gregor, H. P., "A General Thermodynamic Theory of Ion Exchange Processes," Journal of American Chemical Society, Vol.70, No.3, pp.1293 (1948).
- Gregor, H. P., "Gibbs-Donnan Equilibria in Ion Exchange Resin Systems," Journal of American Chemical Society, Vol.73, No.2, pp.642-? (1951).
- Grimshaw, R. W. and Harland, C. E., "Ion Exchange Kinetics: Introduction to Theory and Practice," The Chemical Society, London, England, 1975.
- Harries, R. R., "Water Purification by Ion Exchange Mixed Bed," Ph.D. Dissertation, Loughborough University of Technology, 1986.
- Harries, R. R., "Ion Exchange Kinetics in Condensate Purification," Chemistry and Industry, No.4, pp104-109 (1987).
- Harries, R. R., "The Role of pH in Ion Exchange Kinetics Kinetics," in "Ion Exchange for Industry," Edited by Streat, M., Ellis Horwood Limited, Chichester, England, 1988.
- Harries, R. R. and Ray, N. J., "Anion Exchange in High Flow Rate Mixed Beds," Effluent and Water Treatment Journal, Vol.24, No.4, pp.131-139 (1984).
- Harris, F. E. and Rice, S. A., "Model for Ion Exchange Resins" Journal of Chemical Physics, Vol.24, No.6, pp.1258 (1956).
- Haub, C. E., "Model Development for Liquid Resistance-Controlled Reactive Ion Exchange at Low Solution Concentrations with Application to Mixed Bed Ion Exchange," M.S. Thesis, Oklahoma State University, Stillwater, Oklahoma, 1984
- Haub, C. E. and Foutch, G. L., "Mixed-Bed Ion Exchange at Concentrations approaching the Dissociation of Water. 1. Model Development," Industrial and Engineering Chemistry Fundamentals, Vol.25, No.3, pp.373-381 (1986a).
- Haub, C. E. and Foutch, G. L., "Mixed-Bed Ion Exchange at Concentrations Approaching the Dissociation of Water. 2. Column Model Applications," Industrial and Engineering Chemistry Fundamentals, Vol.25, No.3, pp.381-385 (1986b).
- Helfferich, F., "Ion Exchange," McGraw-Hill Book Company, New York, 1962.

- Helferich, F., "Ion-Exchange Kinetics. V. Ion Exchange Accompanied by Reactions," The Journal of Physical Chemistry, Vol.69, No.4, pp.1178-1187 (1965).
- Helferich, F., "Chapter 2. Ion Exchange Kinetics," in "Ion Exchange," Vol.1, Edited by J. A. Marinsky, Marcel Dekker, Inc., New York, 1966.
- Hill, R. and Lorch, W., "Chapter 7. Ion Exchange," in "Handbook of Water Purification," 2nd Edition, Edited by Lorch, W., John Wiley and Sons, 1988.
- Hsu, T. and Pigford, R. L., "Mass Transfer in a Thermally Regenerable Ion Exchange Resin by Continuous Cycling," Industrial & Engineering Chemistry Research, Vol.30, No.5, pp.1067-1075 (1991).
- Hu, F. C., "Mixed-Bed Ion Exchange Simulations at Low Solution Concentrations," M.S. Report, Oklahoma State University, Stillwater, Oklahoma, 1986.
- Inczedy, J., "Analytical Applications of Ion Exchangers," Pergamon Press Ltd., London, 1966.
- Jackson, M. B. and Bolto, B. A., "Effect of Ion Exchange Resin Structure on Nitrate Selectivity," Reactive Polymers, Vol.12, No.3, pp.277-290 (1990).
- Kataoka, T., Sato, N., and Ueyama, K., "Effective Liquid Phase Diffusivity in Ion Exchange," Journal of Chemical Engineering of Japan, Vol.1, No.1, pp.38-42 (1968).
- Kataoka, T., Yoshida, H., and Yeyama, K., "Mass Transfer in Laminar Region Between Liquid and Packing Material Surface in the Packed Bed," Journal of Chemical Engineering of Japan, Vol.5, No.2, pp.132-136 (1972).
- Kataoka, T., Yoshida, H., and Yamada, Y., "Liquid Phase Mass Transfer in Ion Exchange Based on the Hydraulic Radius Model," Journal of Chemical Engineering of Japan, Vol.6, No.2, pp.172-177 (1973).
- King, D. W., "The Influence of Temperature and Amines on Mixed-Bed Ion Exchange Column Performance for Ultra-Low Concentrations of Sodium and Chloride," Ph.D. Dissertation, Oklahoma State University, Stillwater, Oklahoma, 1991.
- Koloini, T., Sopcic, M., and Zumer, M., "Mass Transfer in Liquid-Fluidized Beds at Low Reynolds Numbers," Chemical Engineering Science, Vol.32, pp.637-641 (1977).

- Kraus, K. A. and Raridon, R. J., "Temperature Dependence of Some Cation Exchange Equilibria in the Range 0 to 200," Journal of Physical Chemistry, Vol.63, No.11, pp.1901-1907 (1959).
- Kunin, R., and McGrvey, F. X., "Monobed Deionization with Ion Exchange Resins," Industrial and Engineering Chemistry, Engineering and Process Development, Vol.43, No.3, pp.734-740 (1951).
- Kunin, R., "Ion Exchange Resins," 2nd ed. John Wiley & Sons, Inc., New York, 1958.
- Kunin, R., "Elements of Ion Exchange," Reinhold, New York, 1960.
- Kuo, J. C. and David, M. M., "Single Particle Studies of Cation-Exchange Rates in Packed Beds: Barium Ion-Sodium Ion System," AIChE Journal, Vol.9, No.3, pp.365-370 (1963).
- McClinton, I., Personal Communication, Glegg Water Conditioning, Inc., 1992.
- Moon, B. H., "Mixed-Bed Ion Exchange Simulations at Low Solution Concentrations for Various Temperatures," M.S. Report, Oklahoma State University, Stillwater, Oklahoma, 1987.
- Myers, G. E. and Boyd, G. E., "A Thermodynamic Calculation of Cation Exchange Selectivity," Journal of Physical Chemistry, Vol.60. No.5, pp.521-529 (1956).
- Naden, D. and Streat, M., "Ion Exchange Technology," Ellis Horwood Limited, Chichester, England, 1984.
- Nelson, P. A. and Galloway, T. R., "Particle-To-Fluid Heat and Mass Transfer in Dense Systems of Fine Particles," Chemical Engineering Science, Vol.30, No.1, pp.1-6 (1975).
- O'Sullivan, D. J., "Condensate Polishing at Aghada Generating Station - a Review of Five Years Operating Experience," Chemistry and Industry, No.4, pp.113-118 (1987).
- Petruzzelli, D., Liberti, L., Passino, R., Helfferich, F. G., and Hwang, Y. L., "Chloride/Sulfate Exchange Kinetics: Solution for Combined Film and Particle Diffusion Control," Reactive Polymers, Vol.5, No.3, pp.219-226 (1987).
- Rahman, K. and Streat, M., "Mass Transfer in Liquid Fluidized Beds of Ion Exchange Particles," Chemical Engineering Science, Vol.36, No.2, pp.293-300 (1981).

- Rao, M. G. and David, M. M., "Single-Particle Studies of Ion Exchange in Packed Beds: Cupric Ion-Sodium Ion System," AICHE Journal, Vol.10, No.2, pp.213-219 (1964).
- Rao, M. G. and Gupta, A. K., "Ion Exchange Processes Accompanied by Ionic Reactions," The Chemical Engineering Journal, Vol.24, No.2, pp.181-190 (1982).
- Reichenberg, D., "Chapter 7. Ion Exchange Selectivity," in "Ion Exchange," Volume 1, Edited by J. A. Marinsky, Marcel Dekker, Inc., New York, 1966.
- Rios, J. and Maddagiri, M., "Use of Two Bed Polishers in Side Stream to Reduce Introduction of Insoluble and Soluble Solids into PWR Steam Generators," Proceedings of the American Power Conference, Vol. 47, pp.1066 (1985).
- Robinson, R. A. and Stokes, R. H., "Electrolyte Solutions," Butterworths Scientific Publications, London, 1960.
- Rowe, P. N., "Particle-To-Liquid Mass Transfer in Fluidized Beds," Chemical Engineering Science, Vol.30, No.1, pp.7-9 (1975).
- Sadler, M. A. and Darvill, M. P., "Condensate Polishers for Brackish Water-Cooled PWR's," EPRI NP-4550, PROJECT 1571-5, July 1986.
- Sadler, M. A., O'Sullivan, D. J., Bates, J. C., and Costello, M. E., "Ammonium-Form Operation of Condensate Polishing Plant at Aghada Generating Station," Proceedings of the American Power Conference, Vol.45, No.3, pp.1058-1063 (1983).
- Sawochka, S. G., "Morpholine Gains Interest in Search for Improved Reliability of PWR Steam Generators," Power, Vol.32, No.4, pp. 67-70 (1988).
- Schlogle, R. and Helfferich, F., "Comment on the Significance of Diffusion Potentials in Ion Exchange Kinetics," The Journal of Chemical Physics, Vol.26, No.1, pp.5-7 (1957).
- Slejko, F. L., Ultrapure Water, Vol.7, No.1, pp.4 (1990).
- Smith, T. G. and Dranoff, J. S., "Film Diffusion-Controlled Kinetics in Binary Ion Exchange," Industrial and Engineering Chemistry Fundamentals, Vol.3, No.3, pp.195-200 (1964).

- Soldatov, V. S. and Bichkova, V. A., "Ion Exchange Selectivity and Activity Coefficients as Functions of Ion Exchange Composition," in "Ion Exchange Technology," Edited by D. Naden and M. Streat, Ellis Horwood Limited, Chichester, England, 1984.
- Tittle, K., "Mixed-Bed Performance in a Condensate Polishing Plant," Proceedings of the American Power Conference, Vol.43, pp.1126-1130 (1981).
- Tittle, K., "Condensate Polishing at AGR Stations," Chemistry and Industry, No.4, pp.110-113 (1987).
- Triay, I. R. and Rundberg, R. S., "Determination of Selectivity Coefficient Distributions by Deconvolution of Ion Exchange Isotherms," Journal of Physical Chemistry, Vol.91, No.20, pp.5269-5274 (1987).
- Turner, J. C. and Snowdon, C. B., "Liquid-Side Mass Transfer Coefficients in Ion Exchange: An Examination of the Nernst-Planck Model," Chemical Engineering Science, Vol.23, No.3, p.221-230 (1968a).
- Turner, J. C. and Snowdon, C. B., "Liquid-Side Mass Transfer Coefficient in Ion Exchange, the H⁺/Cu⁺⁺ - Cl⁻ System," Chemical Engineering Science, Vol.23, No.9, pp.1099-1103 (1968b).
- Tittle, K., "Condensate Polishing at AGR Satations," Chemistry and Industry, No.4, pp.110-113 (1987).
- Wakao, N., Kaguei, S., and Shiozawa, B., "Effect of Axial Fluid Thermal Dispersion Coefficient on Nusselt numbers of Dispersion-Concentric Model of Packed Beds at Low Flow Rates," Chemical Engineering Science, Vol.32, No.4, pp.451-454 (1977).
- Wang, S., Personal Communication, The School of Physics, Oklahoma State University, 1992.
- Wheaton, R. M. and Hatch, M. J., "Chapter 6. Synthesis of Ion Exchange Resins," in "Ion Exchange," Volume 2, Edited by J. A. Marinsky, Marcel Dekker, Inc., New York, 1969.
- Wilke, C. R., "Estimation of Liquid Diffusion Coefficients," Chemical Engineering Progress, Vol.45, No.3, pp.218-224 (1949).
- Wilke, C. R. and Chang, P., "Correlation of Diffusion Coefficients in Dilute Solutions," AIChE Journal, Vol.1, No.2, pp.264-270 (1955).

- Wirth, L. F., Jr., "The Status of Condensate Polishing, 1980," Paper presented at the 41st International Water Conference, Sponsored by the Engineers' Society of Western Pennsylvania, Pittsburgh, 1980.
- Yoon, T. K., "The Effect of the Cation to Anion Resin Ratio of the Mixed-Bed Ion Exchange at Ultra-Low Concentrations," Ph.D. Dissertation, Oklahoma State University, Stillwater, Oklahoma, 1990.
- Zabrodsky, S. S., "Heat Transfer Between Solids Particles and a Gas in a Non-uniformly Aggregated Fluidized Bed," International Journal of Heat and Mass Transfer, Vol.6, pp.23-31 (1963).
- Zabrodsky, S. S., "On Solide-To-Fluid Heat Transfer in Fluidized Systems," International Journal of Heat and Mass Transfer, Vol.10, No.12, pp.1793-1800 (1967).
- Zarraa, M. Z., "Mass Transfer During the Removal of Dissolved Heavy Metals from Wastewater Flows in Fluidized Beds of Ion Exchange Resins," Chemical Engineering and Technology, Vol.15, No.1, pp.21-25 (1992).
- Zecchini, E. J., "Solutions to Selected Problems in Multi-Component Mixed-Bed Ion Exchange Modeling," Ph.D. Dissertation, Oklahoma State University, Stillwater, Oklahoma, 1990.

APPENDIXES

APPENDIX A

EXPERIMENTAL PROCEDURES

Detailed procedures of the mixed-bed ion exchange experiments: chemical compounds preparation for the operation of the ion chromatography, the operation procedures of the ion chromatograph, the procedure of the glass column experiments, and the preparation of feed solution; are given in this section.

Chemical Preparation for IC

There were six plastic bottles used to store and feed eluants and regenerants. They were numbered from 1 to 6. Bottles 1 and 2 were for the anion eluant and Bottles 2 and 3 for the cation eluant. All these four bottles had the same size of 1.5 liters. Bottle 5 was for the anion regenerant and Bottle 6 for cation regenerant; they were of 4 liters.

1. The anion eluant was prepared by pipetting 10 ml of concentrated AS4A ELUANT and dilute up to 1000 ml with 18 Meg-ohm water. The concentrated eluant was made by dissolving 9.54 g sodium carbonate and 7.14 g sodium bicarbonate in a 500 ml flask with 18 Meg-ohm water.
2. The cation eluant was prepared as following;
 - prepared a 10 ml DAP-HCl stock solution by dissolving

- 0.141 g DAP in a 100 ml flask with 18 Meg-ohm water
- pipette 25 ml of the above solution into a 1000 ml flask
 - add 25 ml of 1 M HCl to the flask
 - dilute the above solution up to 1000 ml with 18 Meg-ohm water and mix thoroughly.
3. The anion regenerant was prepared by diluting 100 ml of 0.5 N H₂SO₄ to 1000 ml with 18 Meg-ohm water. The concentrated sulfuric acid was prepared by pipetting 14 ml of 36 N H₂SO₄ into a 1000 ml flask and filling it to mark with 18 Meg-ohm water.
4. The cation regenerant was prepared by diluting 100 ml of 55 % TBAOH to 2000 ml with 18 Meg-ohm water.

IC Operation Procedure

Start Up

1. Turn on two main gas cylinder valves.
2. Turn on the system switch of eluant degas module.
3. After 20 minutes, turn the mode switches to the pressure position. There are two mode switches: the left is for Bottles 1 and 2 and the right for Bottles 3 and 4.
4. After 10 minutes, turn off the main gas cylinder valves and check for gas leaks. If no leaks, turn on the valves again.
5. Check pressures applied to the Bottles. The pressure for the eluant bottles must be regulated to between 5-10 psi.

The membrane suppresser regenerant requires about 25 psi of pressure.

6. Turn on the computer where the AI-450 program is installed.
7. Type "widx" from C prompt and select "run" icon.
8. Click on load and select method or schedule for cation and anion if the operation is for dual-system.
9. Check all figures on the gradient pump module based on those in the selected method or schedule files. The minimum pump pressure for anion and cation is 100 psi. The appropriate operating pressure is about 1000 psi for anion and cation. The maximum pump pressure for both ion is 1500 psi.
10. Wait until conductivity on the conductivity detector settles down around 16.2 for anion and 5.3 for cation. It will take about 2-3 hours.
11. Inject 18 Meg-ohm water 3-5 times to flush out ionic contaminants in the Gradient Pump and the Gradient Mixer. The injection of samples could be done by pushing the green "run" button on the ACI. Samples could be injected through the sampling pumps or the sample ports on the chromatography module.
12. After analyzing all samples, inject 18 Meg-ohm water 3-5 times to prevent build-up of contaminants in the four-valves eluant manifold.

Shut Down

1. Push the yellow "end" button or the red "abort" button.
2. Turn off the main cylinder valves
3. Turn the mode switches to the sparge position.
4. Turn off the system switch.
5. Open the bottles caps to release the pressure applied.
6. Turn off the ACI switch and on it immediately.

Experimental Procedures

Variable Feed Concentration Experiments

1. Rinse the column with 18 Meg-ohm water.
2. Place a frit in the bottom of the column.
3. Measure the desired wet volumes of anion and cation resin in plastic graduated cylinders and record them on a Quattro Pro spreadsheet.
4. Place anion and cation resin into a 250 ml rinsed beaker and mix them well with a plastic rod.
5. Charge the mixed resins into the experimental column. Special caution is required to avoid the separation of the resins.
6. Fill the experimental column with pure water and assemble the whole system and insulate the column.
7. Pump 18 Meg-ohm water through the column for a rinsing period and measure the resin bed depth of the column and record on the Quattro Pro spreadsheet.

8. Check the resistivity monitor to determine temperature and resistivity from channel 2. The resistivity should read greater than 25.1 or the voltage output, monitored on the computer screen, should be 4.90 or higher.
9. If the desired temperature and a high resistivity are reached, then switched the influent line to the desired ionic solution. It has usually taken about 1 hour to get the stable experimental conditions.
10. Monitor the channel 1 of the resistivity meter. When the value of the channel 1 goes down, record the time as the start of the experimental run.
11. Start the ion chromatography and load the LabTech software.
12. Measure the flow rate periodically and record them in milliliter per second.
13. To introduce a step change in feed concentration, switch the influent line to the third container which contains more concentrated solution than the normal feed solution.
14. Monitor the resistivity monitor (channel 1) and record the starting time of the peak.
15. After the desired duration of the peak in feed concentration, switch the influent line back to the normal feed concentration and record the ending time of the peak.
16. Check the chromatograms through "view" or "optimize" option in the Dionex software to terminate the run. When

the effluent concentrations reach equilibrium for cation, stop the operation of the system.

17. To shut down the experimental system, stop the operation of the ion chromatography and the LabTech software, and turn off the feed pump.

Incompletely Mixed-Bed Experiments

- 1-3. Same as those for the variable feed concentration experiments.
4. Place the half of the measured anion resin with cation resin into a 250 ml beaker and mix them well.
5. Charge the mixed resins in the bottom portion of the column and place a thin frit in the upper end of the mixed resin portion. Then, charge the rest of anion resin in the column and place another frit in the upper portion of the column.
- 6-10. Same as those for the variable feed concentration experiments.
11. Start the LabTech software.
12. Measure the flow rate and collect samples at the end of the flow path, periodically.
13. Shut down the system when needed. 14. Analyze the samples using the ion chromatography.

Feed Solution Preparation

1. Prepare a 1000 ml flask and rinse with 18 Meg-ohm water.

2. Measure the calculated amount of salt and dissolve in the flask with 18 Meg-ohm water to make the concentrated solution.
3. Pipette 10 ml of the concentrated solution in a 10 liter carboy and add 18 Meg-ohm water to make the final feed solution.
4. Add the feed solution to the feed containers.

APPENDIX B

ERROR ANALYSIS

The errors caused by the experimental system are analyzed in this section. Analysis of the fresh and the used anion resin using Laser Raman Spectroscopy is also address.

Any experimental measuring device has certain uncertainties associated with it. Most of the uncertainties for the equipment have been determined through calibration or repeated experimental analysis. The whole system error is associated with the errors of ion chromatograph and mixed-bed ion exchange column.

Accuracy of Sample Analysis

The accuracy of the chromatographic analysis was checked regularly through the experiments by injecting the same sample several times successively and then comparing the chromatogram in terms of the peak area. Table XIV shows an example of such analysis. This is when AN_CDM2.MET and CATION6.MET are used. The maximum deviation from average and the standard deviation are 1.22 % and 0.70 %, respectively.

Calibration curves of chloride and sodium concentrations were made from standard solutions to interpolate the peak

TABLE XIV
ACCURACY OF ION CHROMATOGRAPHY ANALYSIS

Ion	Peak Area	Deviation from Average (%)	STD (%)
Chloride	2.347E8	0.34	0.244
	2.336E8	-0.13	
	2.334E8	-0.21	
Sodium	9,980E9	0.63	0.700
	9.821E8	-1.22	
	9.950E8	0.01	

area from the ion chromatograph. The peak area of a sample depends on the the file used for the analysis. The method file controls the time events of ion chromatograph operation. Figures 41 and 42 show the calibration plots with the interpolation equations for chloride and sodium, respectively. They were obtained using ANION6.MET and CATION6.MET files. These figures indicate the close linear relations between peak areas and ion concentrations for both ions. The maximum standard deviations of the coefficients in the correlation equations are $7.51E-5$ and $7.04E-9$ for chloride and sodium, respectively. However, the measurement could vary day to day. Thus, the consistency of the peak area for a certain concentration was always checked before injection of samples. When the other method file was used,

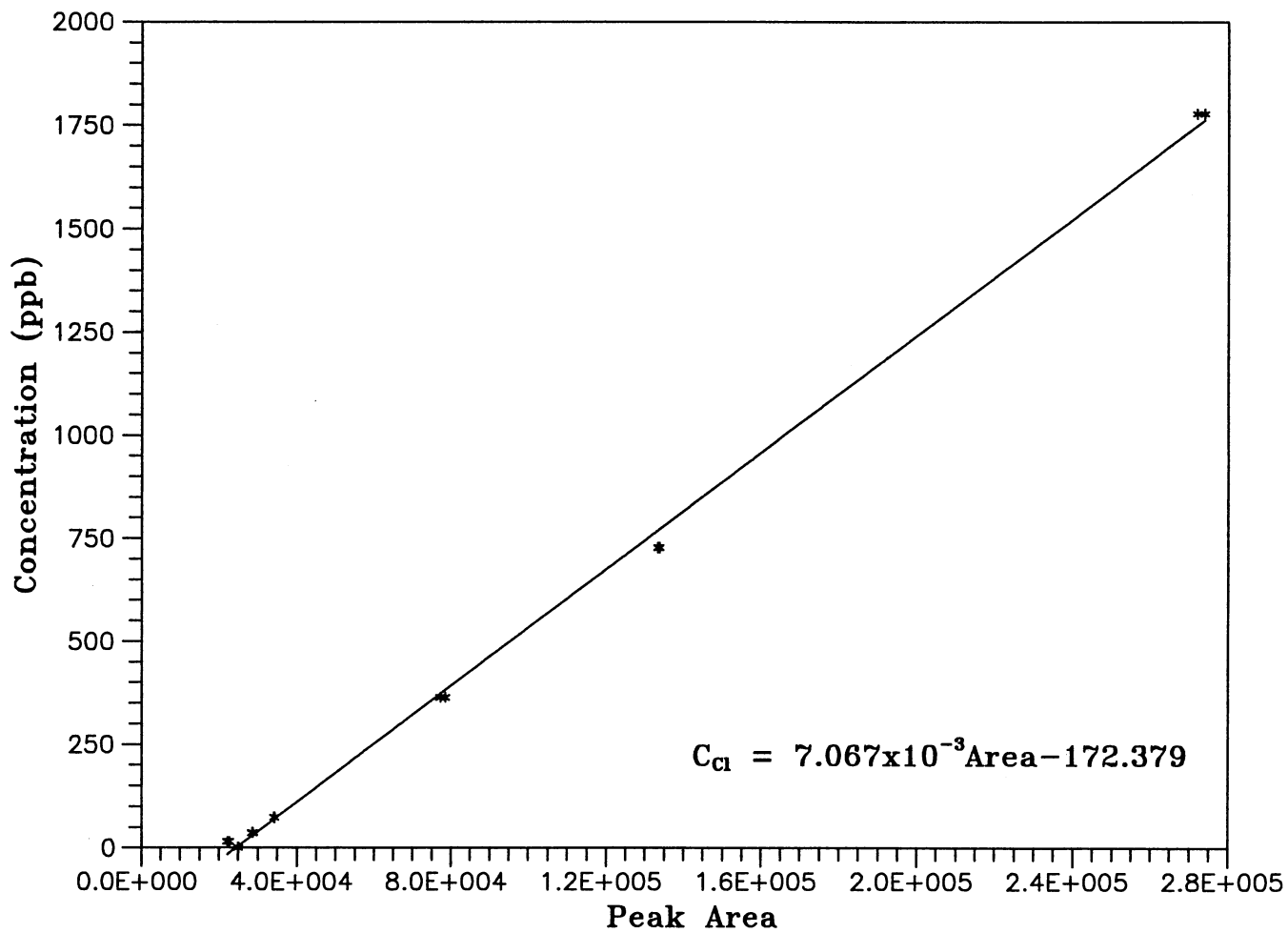


Figure 41. Calibration Curve of Chloride
(Method File : ANION6.met)

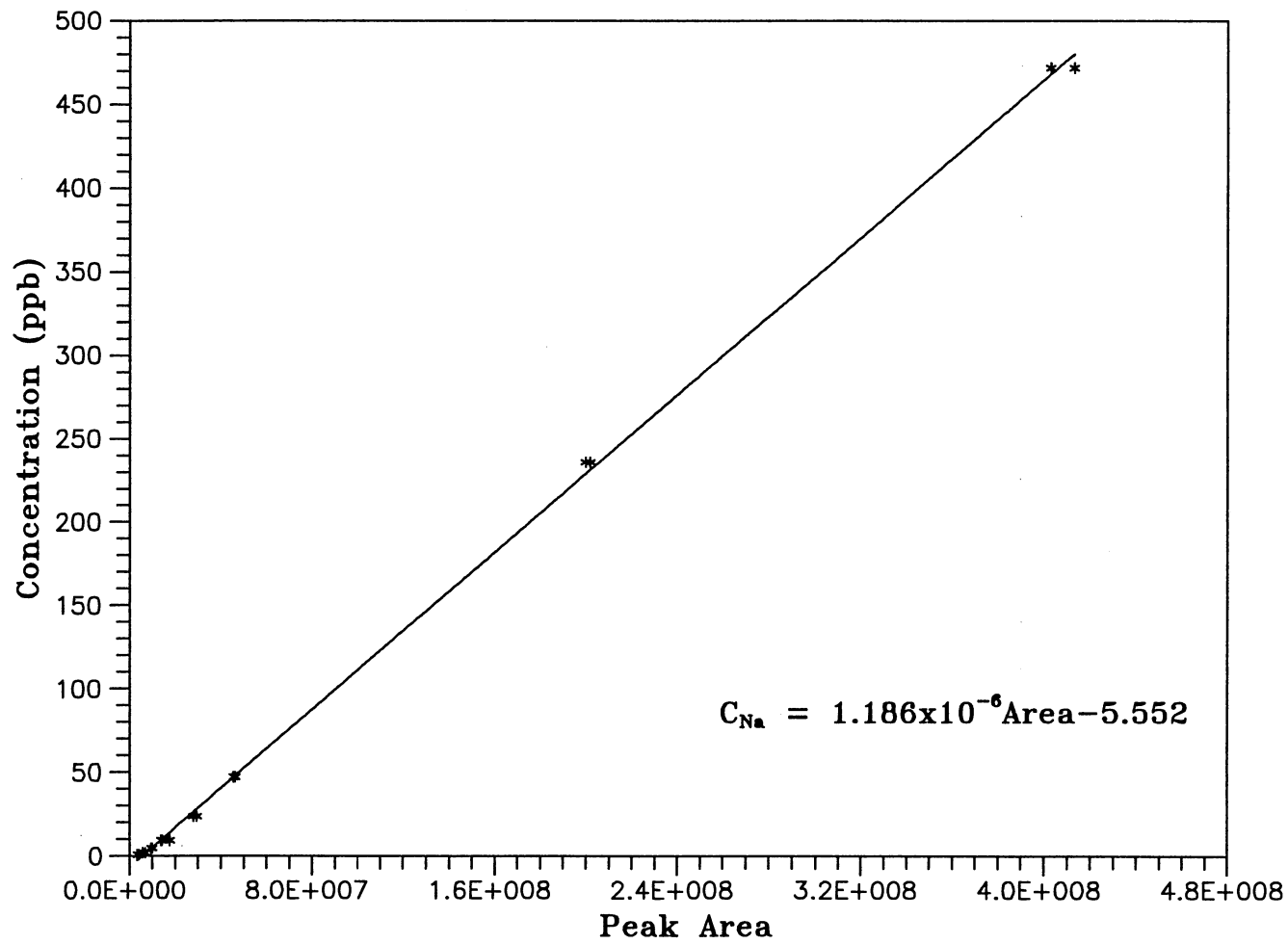


Figure 42. Calibration Curve of Sodium
(Method File : CATIONS6.MET)

or the inconsistency of the peak area was found, the calibration plot was renewed.

Figure 43 presents the calibration curve for on-line effluent pH data. A data file made by Labtech Notebook contains volts data coming from the pH transmitter. Using the linear equation shown in the figure, the actual pH values are calculated. The maximum standard deviation of the coefficients in the equation is 0.034.

Experimental Error for the System

The experimental errors are basically associated with the quantitative measurements. The possible sources of errors are; preparation of feed solution with salt crystals and pure water, measurement of wet resin volume and bed depth, measurement of feed flow rates, and temperature variation.

The accuracy of reading the weights of the sodium chloride crystals by the electronic balance was estimated to be ± 0.0003 g, which is equivalent to 0.51 % error. The measurement accuracy of pure water to a 10 liter carboy is estimated to be ± 50 ml, so the error for water measurement is 0.5 %. The maximum deviation of the solution flow rate for the case of incomplete mixing of the resins was 1.2 %.

The measurement error of wet resin volume and bed depth was estimated to be ± 0.1 cm. This caused the largest error because of inaccurate measurement devices. As an example, the reading of 4.0 ml resin volume and 4.0 cm bed depth, as

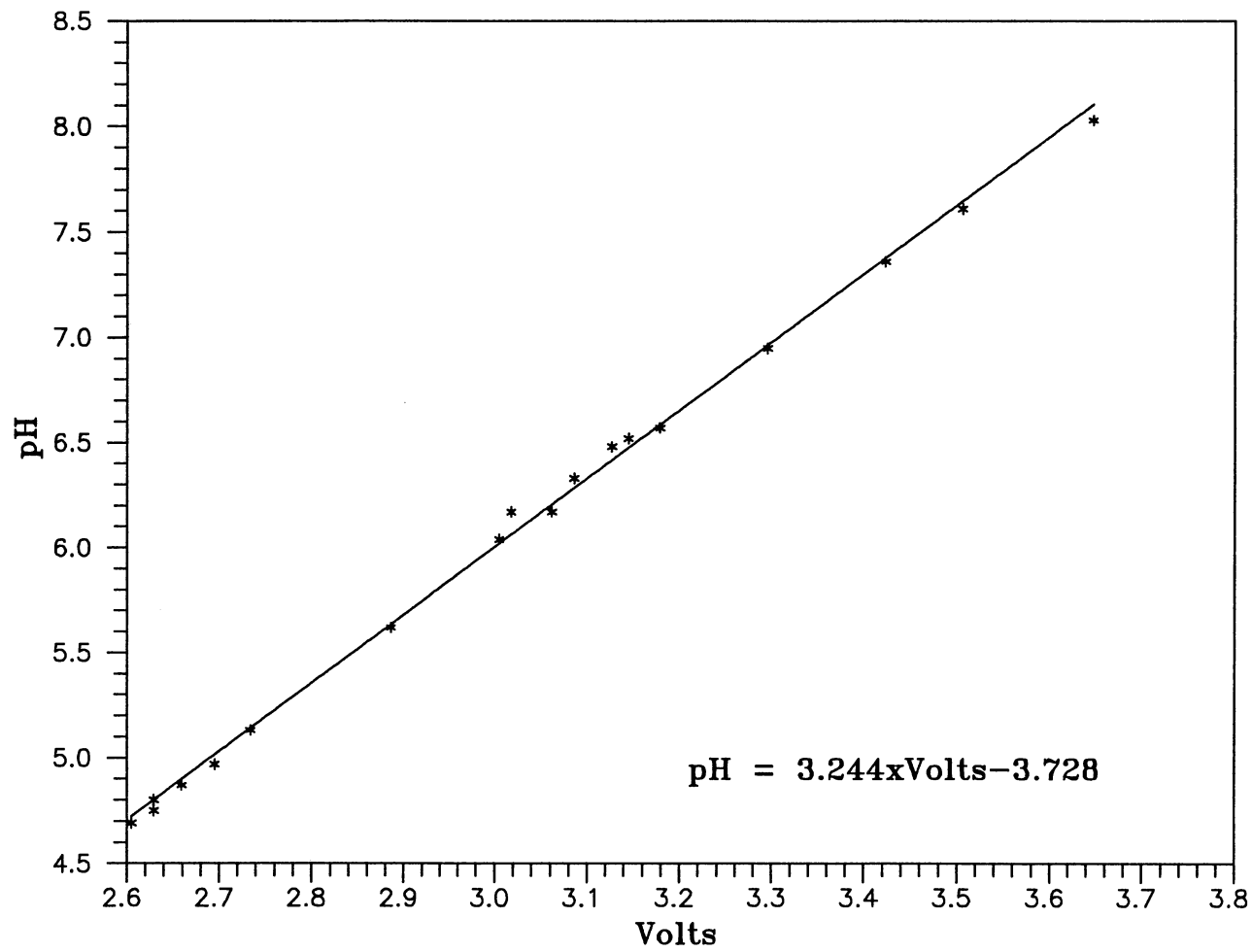


Figure 43. pH Calibration Curve

an example, gives errors of 2.5 %. The temperature probes were calibrated against a standard and was found to be within 1 °C for the temperature range of this study. The temperature variation will affect the resin selectivity coefficients, ionization constant for water, bulk-phase viscosity, and ionic diffusion coefficients in the system. The variation of ± 1 °C shows the maximum deviation of 1.02 %, 0.24 %, 2.4 %, and 1.8 %, respectively.

From the above considerations, the cumulative error of preparation of feed solution, measurement of wet resin volume and bed depth, measurement of feed flow rates, and temperature variation was found to be approximately ± 6.5 %.

Experiments were duplicated in order to check the experimental reproducibility. A sample measurement of the reproducibility of the experiments is illustrated in Figures 44 and 45. The experimental conditions of the duplicated runs are given in Tables VII and VIII. The agreement is entirely satisfactory, with the maximum difference of less than 2.0 %.

Analysis of Anion Resin

Figures 46 and 47 show the results of analysis of the fresh and the anion resin used in an incompletely mixed-bed experiment (R0213) using a Laser Raman Spectroscopy, respectively. The analysis is to check if the resin is contaminated by carbonate or bicarbonate from air. The figures indicate no evidence for significant amount of

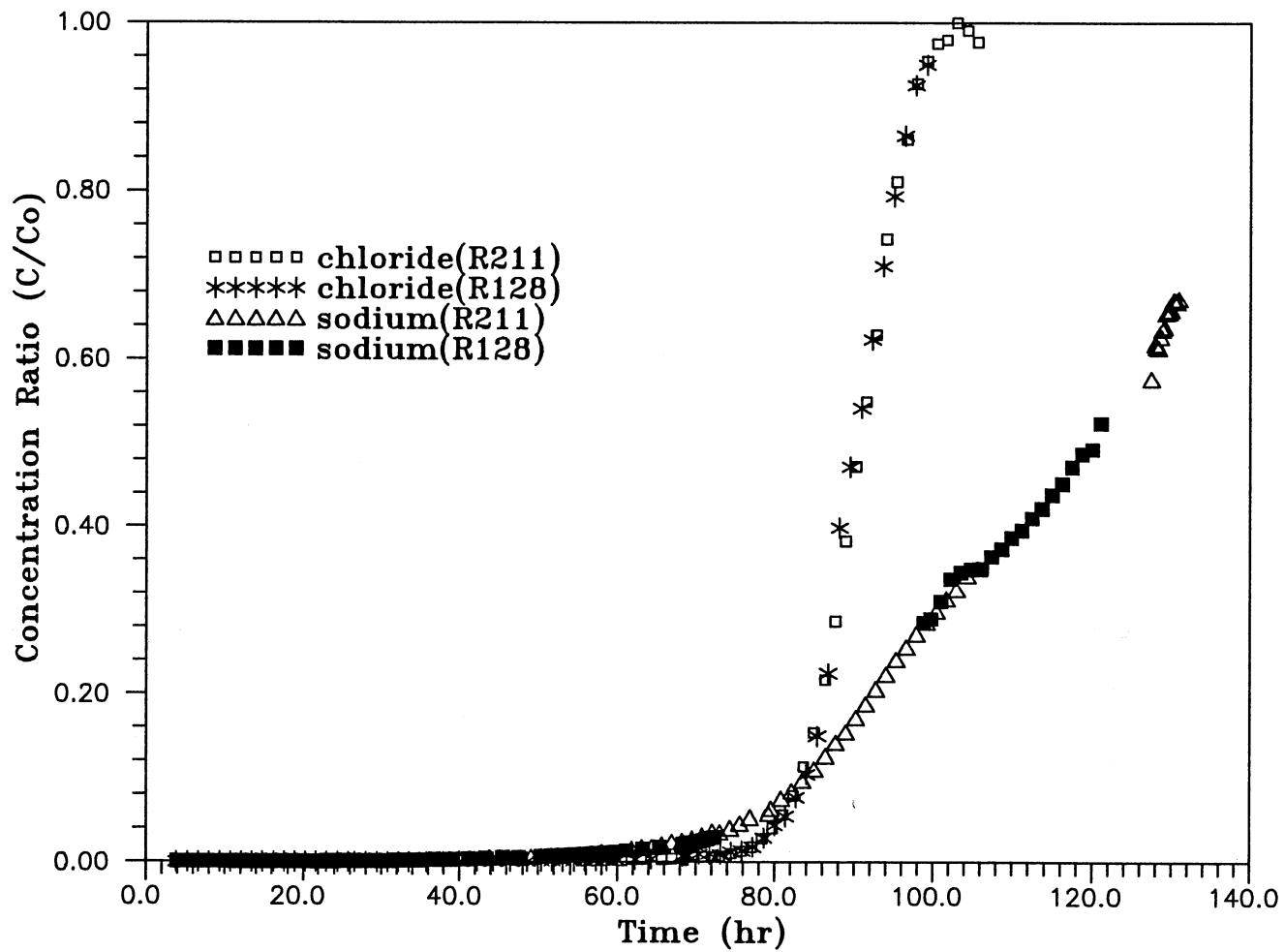


Figure 44. Reproducibility of Variable Feed Concentration Experiments (Runs R128 and R211)

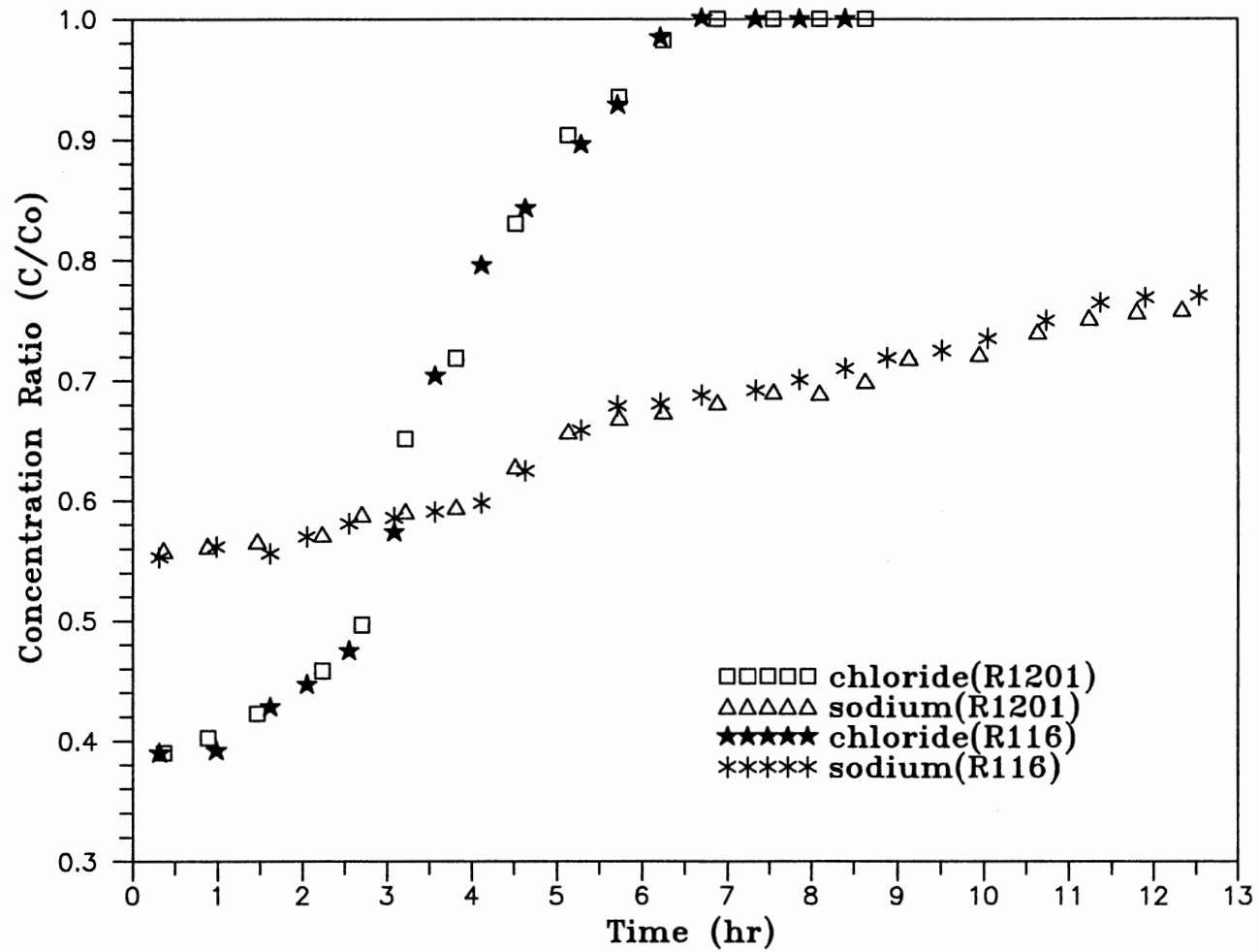


Figure 45. Reproducibility of Incomplete Mixing of Resins
Experiments (Runs R1201 and R116)

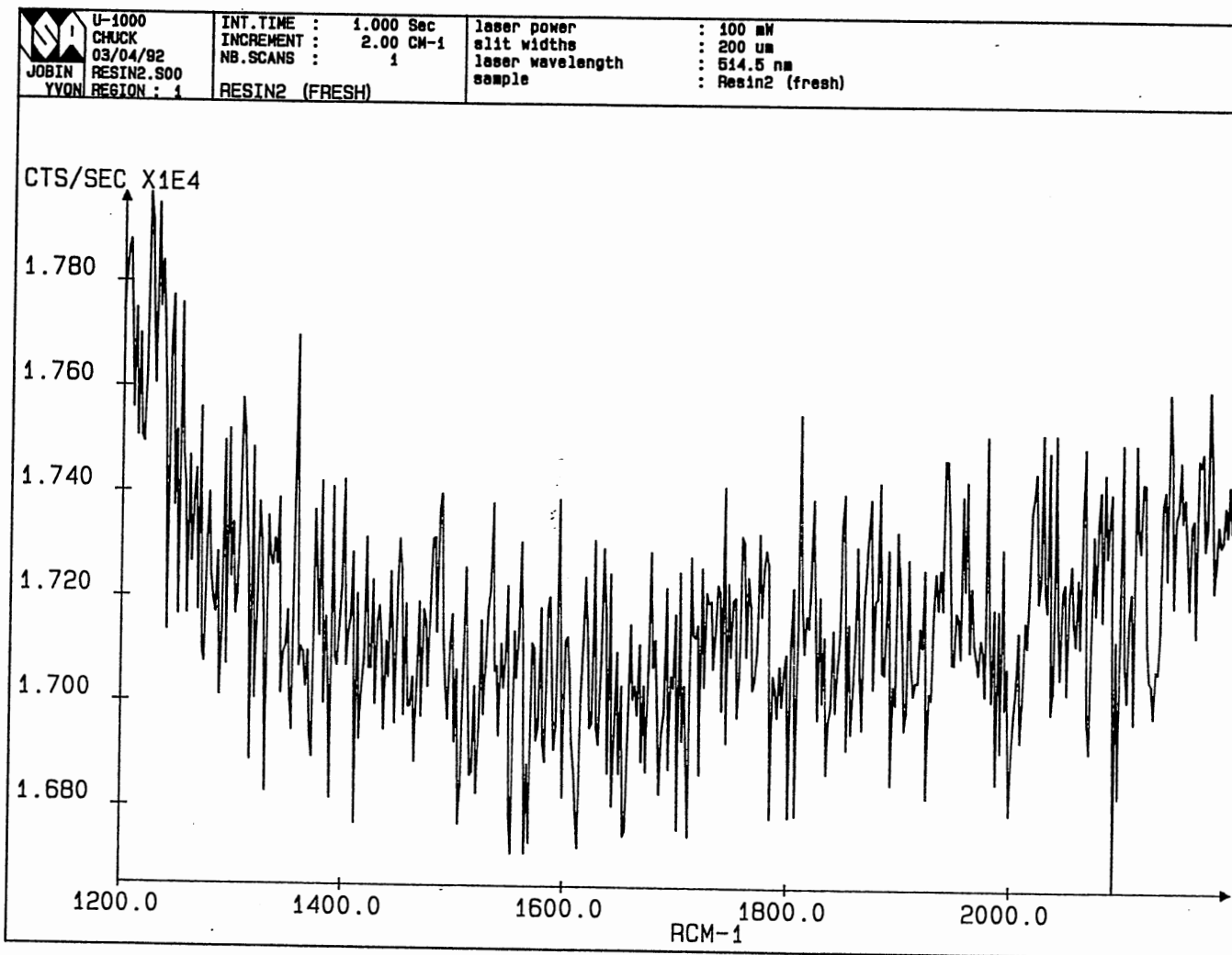


Figure 46. The Result of Analysis of Fresh Anion Resin
Using Laser Raman Spectroscopy

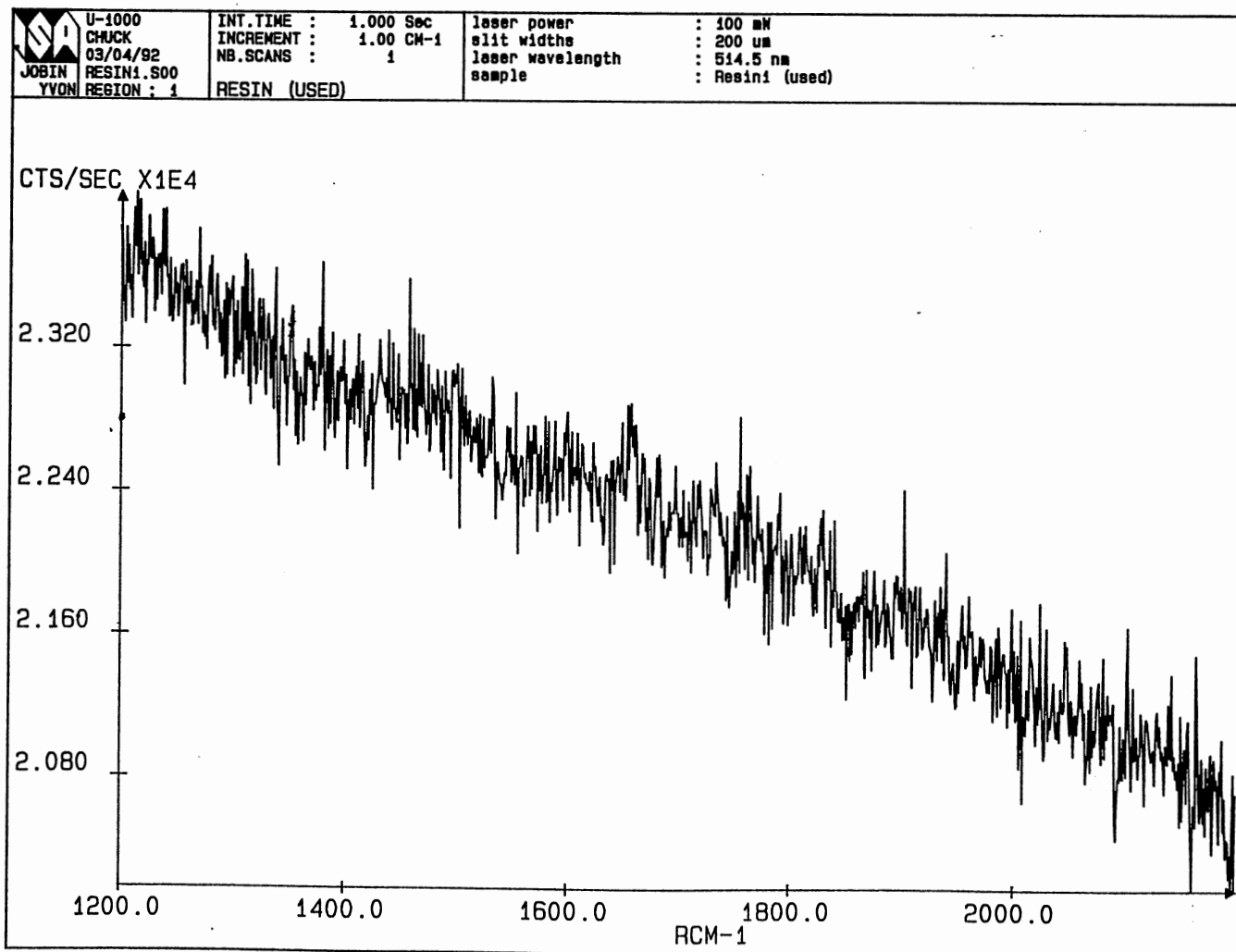


Figure 47. The Result of Analysis of Used Anion Resin Using Laser Raman Spectroscopy

carbonate or bicarbonate. The carbonate peak appears in 2143 RCM^{-1} and the bicarbonate peak does in $1215\text{-}1388 \text{ RCM}^{-1}$ (Wang, 1992). Even though the vertical axis in the figures is amplified, any significant peaks around these points are not found in both figures. This indicates that there is no serious contamination of the anion resins by air and confirms the accuracy of the experiments with high flow rates of about 7.0 ml/s .

APPENDIX C

EXPERIMENTAL DATA

The numerical data obtained in the variable feed concentration and incomplete mixing of resins experiments are presented in the following tables as a function of run time in hours.

TABLE XV
 NUMERICAL DATA OF VARIABLE FEED
 CONCENTRATION EXPERIMENTS

Time (hr)	Chloride (C/Co)	Time (hr)	Sodium (C/Co)
R128 (Constant Feed Concentration)			
3.88	2.13E-07	3.93	0.000323
5.25	2.65E-07	5.30	0.000353
6.62	3.3E-07	6.67	0.000386
7.98	4.12E-07	8.03	0.000421
9.35	5.13E-07	9.40	0.000461
10.72	6.39E-07	10.77	0.000503
12.08	7.96E-07	12.13	0.00055
13.43	9.89E-07	13.50	0.000601
14.80	1.23E-06	14.87	0.000657
16.18	1.54E-06	16.22	0.000717
17.53	1.91E-06	17.58	0.000784
18.90	2.38E-06	18.93	0.000856
20.28	2.97E-06	20.30	0.000935
21.65	3.71E-06	21.67	0.001022
23.02	4.62E-06	23.05	0.001118
24.40	5.77E-06	24.42	0.001222
25.77	7.18E-06	25.78	0.001336
26.62	8.24E-06	26.60	0.001409
28.05	1.04E-05	27.95	0.001538

TABLE XV (Continued)

Time (hr)	Chloride (C/Co)	Time (hr)	Sodium (C/Co)
29.42	1.29E-05	29.32	0.001681
30.80	1.61E-05	30.65	0.001833
32.18	2.02E-05	32.00	0.002001
33.55	2.51E-05	33.35	0.002185
35.77	3.59E-05	34.70	0.002385
37.88	5.04E-05	36.83	0.00274
40.02	7.1E-05	38.97	0.003147
42.18	0.000101	41.13	0.003623
44.33	0.000142	43.27	0.004162
46.47	0.0002	45.40	0.004781
48.62	0.000283	47.53	0.005492
50.35	0.000374	50.33	0.006589
51.75	0.000469	51.68	0.007193
53.12	0.000584	53.03	0.007853
54.50	0.000729	54.38	0.008573
55.90	0.000913	55.73	0.009359
57.27	0.001138	57.08	0.010218
58.63	0.001418	58.45	0.011167
60.00	0.001766	59.80	0.012191
62.22	0.002522	61.17	0.013324
64.33	0.003545	63.27	0.015272
68.33	0.006744	65.42	0.017563
68.55	0.006983	68.37	0.021275
68.78	0.00725	68.58	0.021577
69.00	0.007507	68.80	0.021883
70.37	0.009353	69.03	0.022217
71.73	0.00934	69.25	0.022532
73.10	0.0091	69.47	0.022852
74.47	0.0119	69.70	0.023201
75.83	0.01347	69.92	0.02353
77.20	0.01806	70.15	0.02389
78.57	0.02875	70.37	0.024229
79.93	0.043553	70.58	0.024572
81.30	0.054257	70.80	0.02568
82.67	0.07659	71.02	0.02623
84.03	0.1041	71.25	0.02687
85.40	0.14986	71.47	0.0274
86.77	0.22453	71.68	0.0281
88.13	0.3987	71.90	0.02876
89.50	0.47123	72.13	0.0292
90.87	0.54123	72.35	0.0296

TABLE XV (Continued)

Time (hr)	Chloride (C/Co)	Time (hr)	Sodium (C/Co)
92.23	0.62312	98.80	0.2857
93.60	0.710453	99.73	0.2897
94.97	0.79342	101.00	0.31064
96.33	0.86545	102.27	0.3374
97.70	0.92564	103.53	0.3452
99.07	0.95	104.82	0.34879
		106.08	0.35
		107.37	0.364
		108.63	0.37312
		109.88	0.38673
		111.15	0.3956
		112.42	0.41
		113.68	0.4215
		114.95	0.43789
		116.22	0.45102
		117.48	0.47123
		118.75	0.48672
		120.02	0.49235
		121.10	0.52341

R211 (Constant Feed Concentration)

55.45	0.001638	11.42	0.000454
56.72	0.001754	12.68	0.000455
58.02	0.001462	13.98	0.000478
59.28	0.001998	15.25	0.000532
60.57	0.001774	16.52	0.000555
61.83	0.002733	17.78	0.000605
63.1	0.002606	19.07	0.000643
65.67	0.003021	20.33	0.000719
66.93	0.003804	21.62	0.000765
68.22	0.004533	22.18	0.00081
69.5	0.005658	23.45	0.000846
70.78	0.006346	24.72	0.000992
72.07	0.006674	25.98	0.001075
73	0.006715	27.25	0.001139
74.5	0.010367	28.53	0.00129
75.77	0.013251	29.8	0.001428
77.05	0.018071	31.07	0.001565

TABLE XV (Continued)

Time (hr)	Chloride (C/Co)	Time (hr)	Sodium (C/Co)
78.37	0.027859	32.33	0.001735
79.7	0.040273	33.63	0.001981
80.98	0.056196	34.9	0.002273
82.32	0.078588	36.15	0.002536
83.68	0.11328	37.43	0.002795
85	0.153986	38.7	0.003032
86.38	0.216856	39.98	0.003439
87.65	0.287016	41.25	0.003757
88.92	0.382688	42.53	0.004182
90.2	0.471526	43.8	0.004566
91.47	0.548975	45.07	0.00472
92.73	0.628702	46.33	0.00523
94.02	0.742597	47.8	0.004539
95.28	0.810934	49.07	0.005505
96.55	0.861048	50.35	0.006316
97.83	0.927107	51.62	0.007445
99.12	0.954442	52.88	0.006723
100.38	0.974943	54.2	0.007861
101.65	0.979499	55.47	0.009041
102.92	0.992543	56.75	0.010416
104.25	0.990888	58.05	0.011602
105.52	0.976765	59.32	0.011077
		61.85	0.015191
		63.13	0.01712
		64.42	0.017845
		65.68	0.0205
		66.92	0.023773
		68.25	0.024977
		69.52	0.027841
		70.82	0.032068
		72.08	0.0365
		73.02	0.035182
		74.32	0.040227
		75.57	0.045909
		76.85	0.052841
		79.17	0.057318
		79.47	0.063341
		80.8	0.075205
		82.12	0.084136
		83.48	0.096545
		85.02	0.11025

TABLE XV (Continued)

Time (hr)	Chloride (C/Co)	Time (hr)	Sodium (C/Co)
		86.4	0.126159
		87.68	0.142205
		88.95	0.154682
		90.22	0.171886
		91.48	0.187977
		92.75	0.206159
		94.03	0.223795
		95.3	0.241364
		96.6	0.256136
		97.87	0.272273
		99.15	0.285909
		100.42	0.299545
		101.68	0.313864
		102.95	0.325455
		104.3	0.341136
		105.67	0.349773
		127.45	0.576136
		127.93	0.618182
		128.15	0.615227
		128.38	0.613182
		128.62	0.626818
		128.85	0.635455
		129.08	0.638409
		129.3	0.654773
		129.53	0.655455
		129.75	0.656818
		129.98	0.658864
		130.2	0.670227
		130.43	0.669545
		130.68	0.668182
		130.92	0.672273

Run R218 (One Peak in Feed Concentration)

30.45	0.001105	3.4	0.000183
31.73	0.001499	4.73	0.000174
32.42	0.001916	6.03	0.000713
33.73	0.00192	7.35	0.001142
35.02	0.00126	26.08	0.00061

TABLE XV (Continued)

Time (hr)	Chloride (C/Co)	Time (hr)	Sodium (C/Co)
53.82	0.001273	10.03	0.000781
55.08	0.01613	11.3	0.000786
56.1	0.019378	12.55	0.000789
57.55	0.025672	13.82	0.000848
58.92	0.044852	15.08	0.000916
60.25	0.062164	16.33	0.000997
61.6	0.0859	17.6	0.001101
62.97	0.116993	18.87	0.001213
64.35	0.1659	20.15	0.00133
65.72	0.227107	21.45	0.001451
67.07	0.300683	22.9	0.001576
68.35	0.38041	24.17	0.001705
69.63	0.460137	25.42	0.001857
70.9	0.542141	26.68	0.001994
72.2	0.612756	27.95	0.002209
73.48	0.687927	29.22	0.002402
74.77	0.758542	30.48	0.002782
76.05	0.824601	31.75	0.003073
77.33	0.886105	32.45	0.003257
78.63	0.922551	33.75	0.003773
80.57	0.933941	35.05	0.004245
81.83	0.938497	36.32	0.004875
83.1	0.943052	37.5	0.005402
84.37	0.943052	38.85	0.006266
85.63	0.94533	40.1	0.007061
86.9	0.943052	41.37	0.007695
88.17	0.938497	42.62	0.008945
		43.88	0.010066
		45.15	0.011748
		46.4	0.013518
		47.67	0.015639
		48.95	0.017384
		50.18	0.019975
		51.43	0.022795
		52.7	0.026364
		53.97	0.029341
		55.22	0.033727
		56.13	0.037
		57.57	0.042614
		58.95	0.051341

TABLE XV (Continued)

Time (hr)	Chloride (C/Co)	Time (hr)	Sodium (C/Co)
		60.27	0.059114
		61.62	0.067364
		62.98	0.077636
		64.37	0.089
		65.75	0.102364
		67.08	0.117568
		68.38	0.132023
		69.65	0.147091
		70.93	0.163659
		72.22	0.180045
		73.5	0.197364
		74.78	0.213455
		76.07	0.231364
		77.37	0.247727
		78.65	0.261136
		80.58	0.281591
		81.85	0.296818
		83.12	0.309091
		84.38	0.324545
		85.65	0.338864
		86.92	0.353864
		88.18	0.369318
		89.45	0.383636
		90.72	0.401136
		91.98	0.417045
		93.25	0.431818
		94.52	0.454773
		95.78	0.469091
		97.05	0.486364
		98.32	0.508409
		99.57	0.521136
		100.83	0.545
		102.1	0.564545
		103.8	0.584091
		105.07	0.604545
		106.07	0.622727
		107.33	0.647727
		108.6	0.672727
		109.87	0.695455
		111.13	0.720455

TABLE XV (Continued)

Time (hr)	Chloride (C/Co)	Time (hr)	Sodium (C/Co)
		112.4	0.745455
		113.67	0.765909
		114.93	0.784091
		116.18	0.813636
		117.45	0.838636
		118.72	0.861364
		119.98	0.879545
		121.25	0.895455
		122.52	0.925
		123.83	0.945455
		125.15	0.970455
		126.47	0.992727

Run R326 (Constant Feed Concentration)

2	0.000925	8.4	0.000247
3.28	0.000933	14.73	0.000219
5.4	0.001225	29.82	0.00022
6.67	0.000833	46.2	0.000239
9.8	0.001167	50.05	0.000292
12.37	0.000733	53.88	0.000307
13.65	0.001225	54.93	0.000388
14.93	0.001133	56.23	0.000613
16.18	0.00115	57.5	0.000666
17.5	0.001083	58.78	0.000699
20.07	0.00095	60.05	0.000745
21.42	0.001242	61.32	0.000752
22.68	0.001475	62.63	0.000885
24.02	0.001217	63.95	0.000894
25.3	0.001408	65.22	0.00097
26.57	0.001225	66.48	0.000982
27.85	0.001175	67.8	0.00108
28.72	0.001158	69.07	0.001088
31.03	0.001183	70.32	0.001124
32.32	0.001325	71.58	0.00115
33.62	0.001283	72.88	0.001177
34.9	0.001283	74.15	0.001204
36.17	0.001208	75.43	0.00123

TABLE XV (Continued)

Time (hr)	Chloride (C/Co)	Time (hr)	Sodium (C/Co)
37.47	0.001367	52.72	0.001292
38.73	0.00125	81	0.001584
41.28	0.001433	82.25	0.001575
42.58	0.001425	83.55	0.001717
43.85	0.001208	84.82	0.00169
45.12	0.001092	86.1	0.001814
46.4	0.001117	87.38	0.00192
47.68	0.000967	88.67	0.001991
48.97	0.001017	89.93	0.002035
50.25	0.000933	91.2	0.002071
52.8	0.00095	92.47	0.00215
56.2	0.001008	93.75	0.002283
57.48	0.000975	95.02	0.002372
58.75	0.001008	96.28	0.002434
60.02	0.001058	97.57	0.002566
61.3	0.00115	98.85	0.002681
62.62	0.001233	100.12	0.002735
63.92	0.001183	101.38	0.002876
65.18	0.001067	104.68	0.003921
66.47	0.00105	105.95	0.004356
67.73	0.001425	107.23	0.004688
69	0.000983	108.5	0.004843
70.28	0.001125	109.78	0.005168
72.87	0.001108	111.05	0.005478
74.13	0.001117	112.33	0.005881
75.42	0.001083	113.62	0.006233
79.67	0.001067	114.88	0.006662
80.97	0.001058	116.15	0.007225
82.23	0.000942	117.42	0.007624
83.53	0.001033	118.7	0.008067
84.8	0.000917	119.97	0.008484
86.08	0.000975	121.23	0.008938
87.35	0.000975	123.13	0.009637
88.63	0.000958	124.38	0.009726
89.9	0.000958	125.63	0.010133
91.17	0.000942	128.8	0.011655
92.45	0.000933	130.07	0.012319
93.73	0.000992	131.32	0.013239
94.98	0.000942	132.58	0.013858
96.27	0.000958	133.85	0.014708

TABLE XV (Continued)

Time (hr)	Chloride (C/Co)	Time (hr)	Sodium (C/Co)
97.53	0.000917	135.12	0.015788
98.82	0.000983	136.38	0.016602
100.08	0.000883	137.63	0.017965
101.37	0.0009	138.9	0.019257
103.38	0.001133	140.17	0.019637
104.65	0.001183	141.43	0.02085
105.93	0.001192	142.68	0.021947
107.2	0.001167	143.95	0.022867
108.48	0.00125	145.22	0.023611
109.75	0.001217	146.48	0.024717
111.02	0.001208	147.75	0.026115
112.3	0.001242	149.55	0.027044
113.58	0.001225	150.78	0.028416
114.87	0.0012	152.05	0.030982
116.13	0.00115	153.32	0.034894
117.4	0.0012	154.58	0.036912
118.68	0.00115	155.85	0.039292
119.95	0.001208	157.12	0.041027
121.22	0.001217	158.38	0.042044
122.93	0.001258	159.65	0.044354
124.22	0.001283	160.92	0.047708
125.48	0.001333	162.18	0.050611
125.95	0.001133	163.5	0.052566
128.78	0.001358	164.75	0.054619
130.03	0.001333	166.03	0.058673
131.3	0.001367	167.32	0.061221
132.57	0.0014	168.62	0.064938
133.83	0.00145	169.9	0.067796
135.08	0.001483	171.17	0.072602
136.35	0.001458	172.43	0.07831
137.62	0.0015	173.72	0.082009
138.88	0.001525	174.87	0.08477
140.15	0.00155	176.13	0.090973
141.4	0.001625	177.43	0.098319
142.67	0.001733	178.7	0.105664
143.93	0.001875	179.97	0.111239
145.2	0.002	181.25	0.117788
146.45	0.002133	182.52	0.125929
147.72	0.002317	183.78	0.134867
149.75	0.002442	185.07	0.143628

TABLE XV (Continued)

Time (hr)	Chloride (C/Co)	Time (hr)	Sodium (C/Co)
150.77	0.00275	186.37	0.150708
152.03	0.002817	187.65	0.162655
153.3	0.003167	188.72	0.170885
154.57	0.003542	189.98	0.177876
155.83	0.004417	191.25	0.192212
157.1	0.005417	192.52	0.205487
158.37	0.006	193.78	0.213628
159.63	0.0065	195.05	0.228761
160.88	0.007142	196.35	0.243097
162.15	0.008417	197.3	0.250708
163.47	0.009667	198.57	0.271858
164.73	0.0115	212.55	0.465221
166	0.013083	213.88	0.497965
167.28	0.015167	215.7	0.516991
168.58	0.0175	217.58	0.537257
169.87	0.020333	218.85	0.556283
171.15	0.023167	220.12	0.574513
172.42	0.026667	221.4	0.590354
173.68	0.0305	222.82	0.59531
176.12	0.039417	225.12	0.62177
177.4	0.04475	227.47	0.641947
178.68	0.049	229.55	0.674071
179.95	0.056417	230.82	0.682124
181.22	0.06575	232.1	0.695398
182.48	0.071333	233.37	0.712566
183.75	0.082667	234.65	0.736726
185.03	0.091667	235.92	0.750354
186.33	0.100833	237.18	0.75646
187.63	0.116667	238.45	0.776549
189.97	0.138333	239.72	0.791327
191.22	0.148333	241	0.812743
192.48	0.173333	242.27	0.81823
195.02	0.231667		
196.3	0.284167		
198.55	0.343333		
199.82	0.381667		
201.13	0.419167		
202.42	0.496667		
203.7	0.5475		
204.97	0.55		

TABLE XV (Continued)

Time (hr)	Chloride (C/Co)	Time (hr)	Sodium (C/Co)
206.23	0.566667		
207.57	0.675		
214.08	0.808333		
217.78	0.858333		
221.6	0.941667		
232.08	0.983333		
233.35	0.991667		
234.62	1		
235.88	0.991667		
237.15	0.991667		
238.42	0.991667		
239.7	0.991667		
240.97	0.983333		
242.23	0.983333		

Run R503 (Two Peaks in Feed Concentration)

0.83	0.002033	2.12	0.001278
2.1	0.002167	3.38	0.001171
3.37	0.001692	4.65	0.001303
4.63	0.001825	5.92	0.00134
5.9	0.001875	7.18	0.001301
7.17	0.0022	8.45	0.001381
9.68	0.001942	9.72	0.001434
10.95	0.002025	10.98	0.001451
12.22	0.0018	12.23	0.001496
13.48	0.001992	13.5	0.001584
14.75	0.001833	14.77	0.001565
16	0.00175	16.03	0.001504
17.27	0.001425	17.3	0.001504
18.53	0.0016	18.55	0.001531
19.8	0.001708	19.82	0.001597
21.07	0.001758	21.08	0.001531
22.33	0.001892	22.35	0.001688
23.6	0.002117	23.62	0.001642
24.12	0.001925	24.13	0.001633
25.4	0.001742	25.43	0.010699

TABLE XV (Continued)

Time (hr)	Chloride (C/Co)	Time (hr)	Sodium (C/Co)
26.67	0.001775	26.68	0.01554
27.93	0.0017	27.97	0.022575
29.2	0.001817	29.23	0.012283
30.5	0.00135	30.52	0.00481
31.77	0.00195	31.78	0.005094
33.03	0.0017	33.07	0.005315
34.32	0.001558	34.33	0.005566
35.62	0.001617	35.63	0.005873
36.88	0.001583	36.9	0.005932
38.17	0.001508	38.2	0.006015
39.47	0.001567	39.48	0.006154
40.73	0.001517	40.77	0.006224
42.02	0.001542	42.05	0.006464
43.28	0.001692	43.32	0.006717
44.57	0.001642	44.6	0.006778
45.83	0.001742	45.87	0.006735
47.1	0.002	47.13	0.027894
48.38	0.001692	48.42	0.037
49.65	0.00165	49.68	0.045885
50.93	0.002075	50.95	0.023327
51.35	0.001783	51.38	0.016549
52.62	0.001675	52.65	0.015549
53.9	0.001758	53.92	0.015885
55.17	0.001758	55.18	0.017035
56.43	0.001867	56.47	0.017522
57.72	0.001833	57.75	0.018575
59	0.0015	59.03	0.019372
60.28	0.001575	60.32	0.020248
61.57	0.001858	61.6	0.020204
62.83	0.001625	62.87	0.022389
64.12	0.001708	64.15	0.023097
65.42	0.002083	65.43	0.024088
66.72	0.001583	66.75	0.025584
67.98	0.00165	68.02	0.026469
69.27	0.001758	69.3	0.027708
70.53	0.001683	70.55	0.027628
71.8	0.0016	71.83	0.029425
72.73	0.001692	72.87	0.02969
74	0.0015	74.12	0.032142
75.27	0.0031	75.38	0.033743

TABLE XV (Continued)

Time (hr)	Chloride (C/Co)	Time (hr)	Sodium (C/Co)
76.55	0.002692	76.65	0.036442
77.83	0.00285	77.92	0.038265
79.1	0.002692	79.17	0.040336
80.37	0.002967	80.43	0.042796
81.63	0.003108	81.72	0.04554
82.92	0.003292	84.23	0.051894
84.18	0.003433	85.5	0.054204
85.47	0.003775	86.75	0.057301
86.73	0.004308	88.03	0.059788
88	0.004533	89.32	0.062664
89.28	0.005775	90.58	0.066257
90.55	0.006208	91.87	0.070469
91.85	0.0066	93.28	0.074814
95.35	0.007933	95.53	0.078991
96.72	0.00795	96.8	0.083265
97.15	0.009667	97.18	0.08392
98.42	0.009833	98.45	0.088496
99.7	0.010833	99.73	0.093097
101.07	0.012417	101.1	0.100442
102.38	0.016	102.42	0.105487
103.68	0.017583	103.72	0.116372
105.08	0.020083	105.12	0.124248
106.45	0.025083	106.48	0.133097
107.8	0.028583	107.83	0.139735
109.15	0.0305	109.17	0.145575
110.52	0.03575	110.53	0.152389
111.78	0.037667	111.82	0.160265
113.2	0.0445	113.23	0.170619
114.58	0.0485	114.62	0.178142
115.97	0.05625	116	0.188584
117.38	0.065083	117.4	0.198053
120.58	0.096667	120.62	0.210442
121.9	0.100833	122.18	0.224159
123.25	0.103333	123.45	0.236814
124.58	0.135833	124.7	0.248673
125.9	0.155833	125.97	0.25885
127.23	0.171667	127.27	0.276814
128.55	0.216667	128.58	0.292035
129.88	0.239167	129.92	0.310265
131.27	0.28	131.28	0.325487

TABLE XV (Continued)

Time (hr)	Chloride (C/Co)	Time (hr)	Sodium (C/Co)
132.57	0.316667	132.6	0.34
133.9	0.358333	133.93	0.349558
135.25	0.4075	135.28	0.368761
136.6	0.445833	136.63	0.377788
137.95	0.505	137.98	0.393274
139.22	0.531667	139.25	0.413274
140.5	0.5975	140.53	0.423451
141.78	0.635833	141.82	0.443628
143.07	0.673333	143.1	0.45469
		144.37	0.466018
		145.37	0.476372
		146.63	0.490354
		147.88	0.509912
		149.15	0.522389
		150.4	0.533628
		151.67	0.542566
		152.92	0.556637
		154.18	0.569027
		155.45	0.578761
		156.98	0.597345
		158.25	0.60708
		159.52	0.618584
		160.8	0.630973
		162.08	0.640708
		163.35	0.651327
		164.62	0.668142

TABLE XVI
 NUMERICAL DATA OF INCOMPLETE MIXING
 OF RESINS EXPERIMENTS

Time (hr)	Chloride (C/Co)	Sodium (C/Co)
Run R1201 (Complete Mixing)		
0.37	0.39002	
0.88	0.402741	0.562616
1.47	0.422651	0.566681
2.23	0.45841	0.572271
2.7	0.496748	0.58885
3.22	0.651336	0.591653
3.82	0.71879	0.595174
4.52	0.830461	0.628821
5.13	0.903547	0.657859
5.73	0.935206	0.669473
6.25	0.982693	0.674477
6.88	1.0	0.682031
7.55	1.0	0.690835
8.1	1.0	0.690018
8.63	1.0	0.699718
9.13		0.719286
9.95		0.722179
10.63		0.74092
11.23		0.752476
11.8		0.757639
12.33		0.759575

Run R107 (Incomplete Mixing)

0.4	0.408448	0.541044
1.15	0.417047	0.548505
1.72	0.447703	0.554244
2.42	0.496048	0.565721
2.95	0.580484	0.576051
3.47	0.621382	0.585807
4.03	0.743327	0.592694

TABLE XVI (Continued)

Time (hr)	Chloride (C/Co)	Sodium (C/Co)
4.62	0.865272	0.638604
5.12	0.921555	0.661559
5.7	0.968456	0.670089
6.27	0.996855	0.671007
6.82	1.00598	0.680238
7.53	1.00598	0.709523
8.03	0.996855	0.704368
8.47	1.00598	0.70747
9.05	0.996855	0.713209
9.63	0.996855	0.718947
10.33	1.00598	0.7226
10.95	0.996855	0.733563
11.58	1.00598	0.741096
12.1	0.996855	0.743496

R116 (Complete Mixing)

0.32	0.390	0.553
0.98	0.392	0.562
1.62	0.428	0.556
2.05	0.447	0.570
2.55	0.475	0.581
3.08	0.574	0.586
3.57	0.704	0.591
4.12	0.796	0.598
4.63	0.843	0.625
5.28	0.896	0.659
5.72	0.929	0.679
6.22	0.985	0.681
6.70	1.001	0.688
7.33	1.000	0.692
7.87	1.000	0.701
8.40	1.000	0.710
8.88		0.719
9.52		0.725
10.05		0.735
10.73		0.750
11.37		0.765
11.90		0.769
12.53		0.771

TABLE XVI (Continued)

Time (hr)	Chloride (C/Co)	Sodium (C/Co)
-----------	--------------------	------------------

Run R0213 (Complete Mixing)

0.33	0.469764	0.495095
0.93	0.481772	0.500756
1.57	0.505787	0.507065
2.12	0.529803	0.514635
2.83	0.576634	0.522584
3.35	0.702716	0.530722
3.85	0.801781	0.559425
4.38	0.92186	0.57425
4.97	0.963887	0.581505
5.43	0.996308	0.596898
5.92	1.004113	0.605288
6.43	1.016121	0.622636
6.92	1.022125	0.628188
7.48	1.004113	0.633361
8.15	1.016121	0.64112
8.63	1.003513	0.651088
9.17	1.005314	0.659099
9.65	1.016121	0.669193
10.3	1.016121	0.679917
11.1	1.005314	0.688749
11.65	1.004113	0.695689
12.13	1.000511	0.70471

Run R0216 (Incomplete Mixing)

0.33	0.469764	0.495095
0.93	0.481772	0.500756
1.57	0.505787	0.507065
2.12	0.529803	0.514635
2.83	0.576634	0.522584
3.35	0.702716	0.530722
3.85	0.801781	0.559425
4.38	0.92186	0.57425
4.97	0.963887	0.581505
5.43	0.996308	0.596898

TABLE XVI (Continued)

Time (hr)	Chloride (C/Co)	Sodium (C/Co)
5.92	1.004113	0.605288
6.43	1.016121	0.622636
6.92	1.022125	0.628188
7.48	1.004113	0.633361
8.15	1.016121	0.64112
8.63	1.003513	0.651088
9.17	1.005314	0.659099
9.65	1.016121	0.669193
10.3	1.016121	0.679917
11.1	1.005314	0.688749
11.65	1.004113	0.695689
12.13	1.000511	0.70471

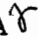
TABLE XVII

pH DATA

Time (hr)	pH	Time (hr)	pH
Run R1201 (Complete Mixing)		Run R107 (Incomplete Mixing)	
0.18	8.225199	0.07	7.7733
0.68	8.121165	0.57	7.724534
1.18	8.026884	1.07	7.415682
1.68	7.89359	1.57	7.415682
2.18	7.646508	2.07	6.027475
2.68	6.209535	2.57	5.565822
3.18	5.669857	3.07	5.256971
3.68	5.393516	3.57	5.081413
4.18	5.263473	4.07	5.091166
4.68	5.279728	4.57	4.987132
5.17	5.250468	5.07	5.0424
5.67	5.279728	5.57	5.052153
6.17	5.178945	6.07	5.07491
6.23	5.400018	6.57	5.097668
6.73	5.328494	7.07	5.081413
7.23	5.234213	7.57	5.097668
7.73	5.201702	8.07	5.091166
8.23	5.240715	8.48	5.361005
8.59	5.393516	8.98	5.146434
9.09	5.146434	9.48	5.146434
9.59	5.217958	9.98	5.178945
10.09	5.162689	10.48	5.091166
10.59	5.201702	10.98	5.152936
11.09	5.169192	11.48	5.097668
11.59	5.162689	11.98	5.097668
12.09	5.113923		
Run R0213 (Complete Mixing)		Run R0216 (Incomplete Mixing)	
0.06	5.829159	0.07	5.933193
0.56	5.653601	0.57	5.874674
1.56	5.487797	1.07	5.74138
2.06	5.334996	1.57	5.647099
2.56	5.217958	2.07	5.494299
3.06	5.120425	2.57	5.305737

TABLE XVII (Continued)

Time (hr)	pH	Time (hr)	pH
3.56	5.130179	3.07	5.113923
4.06	5.081413	3.57	5.019642
4.56	5.081413	4.07	5.07491
5.06	5.058655	4.57	5.052153
5.56	5.058655	5.07	5.081413
6.06	5.081413	5.57	5.07491
6.56	5.081413	6.07	5.081413
7.06	5.107421	6.57	5.107421
7.56	5.052153	7.07	5.058655
8.06	5.120425	7.57	5.052153
8.56	5.058655	8.07	5.052153
9.06	5.081413	8.57	5.091166
9.56	5.07491	9.07	5.097668
10.06	5.097668	9.57	5.120425
10.56	5.097668	10.07	5.097668
11.06	5.052153	10.57	5.146434
11.56	5.058655	11.07	5.130179
12.06	5.058655	11.57	5.178945
		12.07	5.107421

VITA 

Byeong Il Noh

Candidate for the Degree of
Doctor of Philosophy

Thesis: EFFECTS OF STEP CHANGES IN FEED CONCENTRATION AND
INCOMPLETE MIXING OF ANION AND CATION RESIN ON
THE PERFORMANCE OF MIXED-BED ION EXCHANGE

Major Field: Chemical Engineering

Biographical:

Personal Data: Born in Kyungbuk, Korea, October 18,
1961, the son of Bum Ku and Chang Seon Noh.

Education: Educated from the Elementary School to
the University at Seoul in Korea; received
Bachelor of Science and Master of Science in
Chemical Engineering from Hanyang University in
February, 1984 and Oklahoma State University in
December, 1988, respectively; completed
requirements for the Doctor of Philosophy Degree
at Oklahoma State University in July, 1992.

Professional Experience: Research Engineer in Daehan
Electric Wire Ltd. (Seoul) in 1986; Graduate
Teaching and Research Assistant at the school of
Chemical Engineering, Oklahoma State University,
Jan., 1987, to May, 1992.

Professional Societies: The Korean Scientists and
Engineers Association in America.